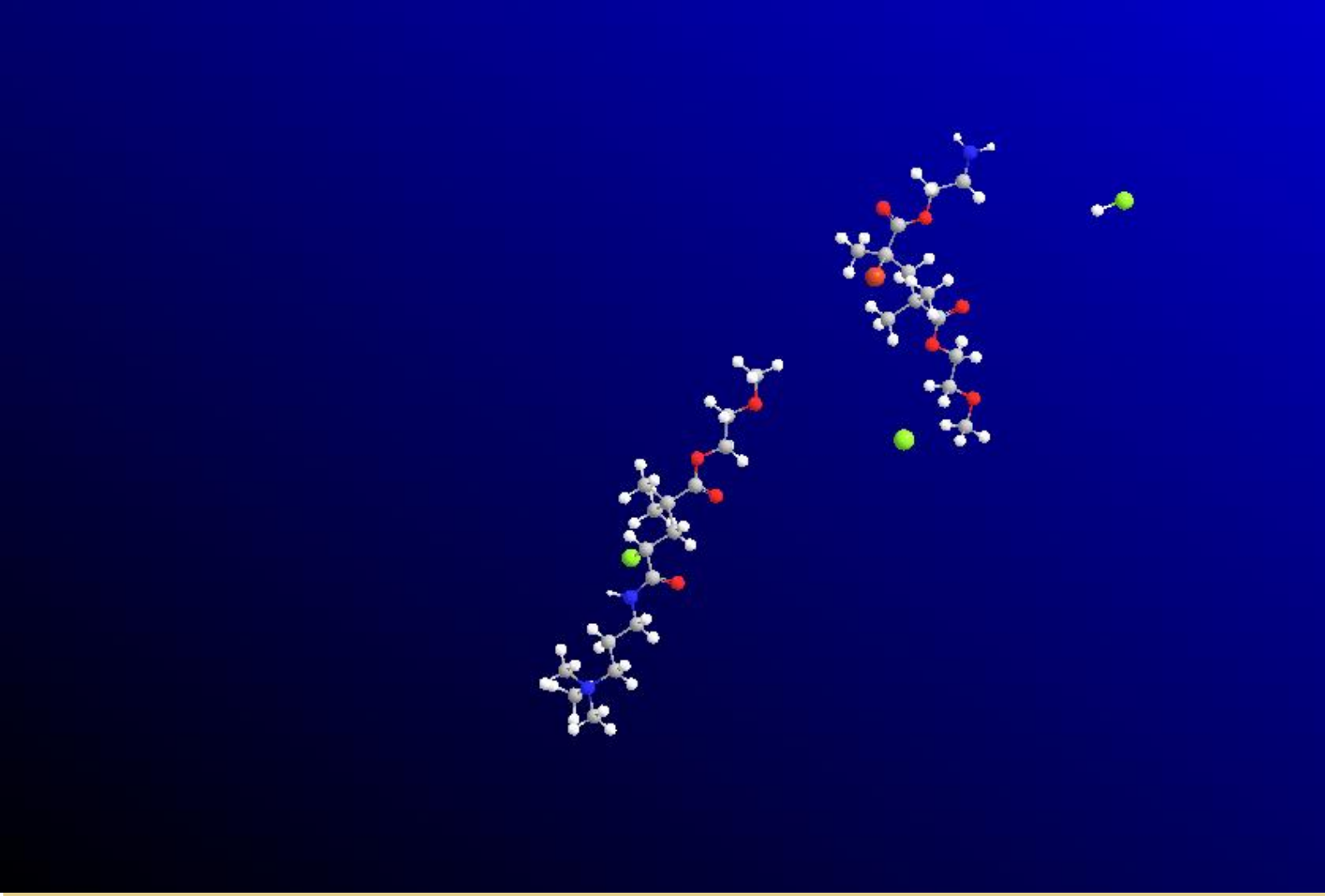

Mafalda Silva de Lima

Synthesis of cationic block copolymers by reversible deactivation radical polymerization for gene delivery

Dissertation guided by Jorge F.J. Coelho, PhD, and Patrícia V. Mendonça, PhD, and presented to the Faculty of Sciences and Technology of University of Coimbra to obtain a Master's degree in Biomedical Engineering

September 2016

· U C ·

UNIVERSIDADE DE COIMBRA

FCTUC FACULDADE DE CIÊNCIAS
E TECNOLOGIA
UNIVERSIDADE DE COIMBRA

Mafalda Silva de Lima

Synthesis of cationic block copolymers by reversible deactivation radical polymerization for gene delivery

Dissertation submitted to University of Coimbra in order to fulfill the necessary requirements to obtain the Masters in Biomedical Engineering degree.

Dissertação apresentada à Universidade de Coimbra para cumprimento dos requisitos necessários à obtenção do grau de Mestre em Engenharia Biomédica

Advisors:

Dr. Jorge F. J. Coelho (CEMUC, Department of Chemical Engineering, University of Coimbra, 3030-790 Coimbra, Portugal)

Dr. Arménio C. Serra (CEMUC, Department of Chemical Engineering, University of Coimbra, 3030-790 Coimbra, Portugal)

Coimbra, 2016

This work was developed in collaboration with:

Chemical Engineering Department, Faculty of Science and Technology, University of Coimbra

CNC - Center for Neuroscience and Cell Biology, University of Coimbra, Portugal

ACKNOWLEDGMENTS/AGRADECIMENTOS

Sempre tive a sorte de estar rodeada de pessoas quem me fazem bem e que querem o melhor para mim. Quero agradecer a todos os que, de uma forma ou de outra, ajudaram a que estes últimos cinco anos fossem tão especiais.

Quero agradecer ao professor Jorge Coelho pela oportunidade de poder escolher um dos projetos do grupo e me debruçar sobre ele.

Quero agradecer à incansável Patrícia Mendonça pela disponibilidade, carinho e paciência para me ensinar e guiar nesta jornada.

A todo o grupo de investigação, em especial aos companheiros do B37, ao João Costa, ao Pedro Maximiniano, à Joana Góis e à Joana Mendonça pelo acolhimento, boa disposição e pelas ajudas imprescindíveis.

A todos os meus amigos, quer no *xis*, quer nos *Lobos* quero agradecer-vos pelas indispensáveis horas de ociosidade e procrastinação bem passadas e pela ajuda quando os semestres começavam a complicar. Espero ter conseguido retribuir todo o apoio e carinho. Quero ainda deixar um agradecimento especial ao André Matos por ter sido um amigo insubstituível ao longo desta jornada.

Tenho uma família pequena, mas que sempre me apoiou incondicionalmente e de braços abertos, como uma maravilhosa rede de segurança e, ao mesmo tempo, uma pista de lançamento a dar-me forças. Agradeço-vos a todos pela ajuda, pelo apoio e pelo carinho constantes. Obrigada por me desafiarem a querer sempre o melhor que a vida tem para oferecer.

Aos meus pais, especialmente, quero aqui deixar um enorme obrigada por todo o esforço que fizeram, sempre com um sorriso, por toda a dedicação e por todo o apoio absoluto e irrestrito.

Às minhas irmãs quero deixar um beijinho enorme. A ti, Mariana, um especial obrigada por estares sempre lá para partilhar o bom e o mau no final de cada dia, principalmente nestes últimos quatro anos. A ti, Matilde, que me mostras como ter força para correr atrás do que nos faz felizes.

A ti, João Silva, quero agradecer-te por teres sido o meu porto seguro, por me trazeres para o presente e por me ensinares a valorizar o infinito que um momento encerra.

Obrigada! Muito obrigada a todos!

Mafalda Lima

ABSTRACT

The aim of this work was to synthesize and characterize well-defined cationic copolymers for gene delivery applications via reversible deactivation radical polymerization (RDRP) techniques. It was also a goal of this study to evaluate the differences in the reaction rate and control over the polymerization of methyl acrylate (MA) by supplemental activator and reducing agent atom transfer radical polymerization (SARA ATRP), when using tetrahydrofuran (THF), 2-methyltetrahydrofuran (2-MeTHF) or cyclopentyl methyl ether (CPME).

Two main sets of well-defined block copolymers for gene delivery assays were synthesized: poly((3-acrylamidopropyl)trimethylammonium chloride)-based (PAMPTMA-based) copolymers, with emphasis on poly(ethylene glycol)$_{45}$-*b*-PAMPTMA$_n$ (PEG$_{45}$-*b*-PAMPTMA$_n$), via SARA ATRP, and poly(2-aminoethyl methacrylate hydrochloride)-based (PAMA-based) polymers, with emphasis on PEG$_{45}$-*b*-PAMA$_n$ block copolymers, via activators regenerated by electron transfer (ARGET) ATRP with slow feeding of ascorbic acid (AscA) as the reducing agent. The different copolymers were tested in COS-7 cell line. All PAMPTMA-based copolymers showed no transfection efficiency. It was postulated that these unexpected results could be due to different reasons: (i) the inability of the polyplex to enter in the cell; (ii) the unsuccessful unpackaging of the polyplex; (iii) the possible cytotoxicity of the polymer. In contrast, the PEG$_{45}$-*b*-PAMA$_n$ samples showed promising results, having high transfection efficiencies, especially in the presence of serum. Moreover, for PAMA-based samples, it was possible to establish important correlations involving the advantages using of PEG in the polyplex composition.

In order to fulfill the second purpose of this project, the activity of the metallic catalytic system [CuBr$_2$]$_0$/[Me$_6$TREN]$_0$/Cu(0) was evaluated for the polymerization of MA at 30 °C, using solvents that belong to the same family but have different polarities, namely THF, 2-MeTHF or CPME. The kinetic results showed no significant differences between the reaction rates, regardless of the solvent mixture used, as well as a close agreement between the experimental and theoretical molecular weights. However, the evident loss of control observed for high monomer conversions raised concerns over the stability of the system. Further investigation was done through chain-extension

experiments, where the presence of dead chains was confirmed by the existence of a macroinitiator shoulder in each SEC trace of the extended PMA-Br samples. Nevertheless, the percentage of dead chains was in the range expected for a SARA ATRP system. Further studies were performed by UV spectroscopy aiming to observe eventual differences in the reduction of $CuBr_2$ between the different solvent mixtures investigated for the SARA ATRP of MA. However, for all the systems studied, an unexpected increase in the maximum absorbance peak and a successive shift to smaller wavelengths was evident during the reaction time. Further studies are required in order to establish a better understanding of the data obtained.

RESUMO

O objetivo deste trabalho foi sintetizar e caracterizar copolímeros catiónicos bem-definidos para aplicações de entrega de material genético através de técnicas de RDRP. Foi também um objetivo deste estudo a avaliação de diferenças na velocidade de reação e controlo sobre a polimerização de MA por SARA ATRP, quando se utiliza THF, 2-MeTHF ou CPME.

Dois conjuntos principais de copolímeros em bloco bem-definidos foram sintetizados para os ensaios de entrega de genes: copolímeros de base PAMPTMA, com ênfase nos copolímeros em bloco PEG_{45}-*b*-$PAMPTMA_n$, via SARA ATRP, e polímeros de base PAMA, com ênfase nos copolímeros em bloco PEG_{45}-*b*-$PAMA_n$, via ARGET ATRP com adição lenta de AscA como agente redutor. Os diferentes copolímeros foram testados na linha celular COS-7. Todos os copolímeros de base PAMPTMA não mostraram qualquer eficiência de transfeção. Teoriza-se que estes inesperados resultados possam ser devidos a diferentes motivos: (i) à incapacidade do poliplexo entrar na célula; (ii) à descarga sem êxito do poliplexo; (iii) à eventual citoxicidade do polímero. Contudo, as amostras de PEG_{45}-*b*-$PAMA_n$ evidenciaram resultados promissores, tendo elevadas eficiências de transfeção, especialmente na presença de sérum. Mais ainda, com as amostras de base PAMA foi possível estabelecer correlações importantes relativas às vantagens da utilização de PEG na composição do poliplexo.

De modo a cumprir o segundo propósito deste trabalho, a atividade do sistema catalítico metálico $[CuBr_2]_0/[Me_6TREN]_0$/Cu(0) foi avaliada para a polimerização de MA a 30 °C, usando solventes que pertencem à mesma família, mas que têm polaridades diferentes, nomeadamente THF, 2-MeTHF ou CPME. Os resultados cinéticos não apresentaram diferenças significativas entre as velocidades de reação, independentemente da mistura de solventes usada, havendo uma grande proximidade entre os pesos moleculares teóricos e experimentais. Contudo, a perda evidente de controlo observada a altas conversões de monómero levantou dúvidas sobre a estabilidade do sistema. Outras investigações foram feitas através de extensões de cadeia, onde a presença de cadeias mortas foi confirmada pela existência de um ombro de macroiniciador em cada traço de SEC das amostras estendidas de PMA-Br. Todavia, a percentagem de cadeias mortas estava dentro do espectável, para um sistema SARA

ATRP. Estudos posteriores foram feitos com espectroscopia UV com o objetivo de observar eventuais diferenças na redução de $CuBr_2$ entre as misturas de solventes investigadas para o SARA ATRP do MA. Porém, para todos os sistemas estudados, verificou-se uma inesperada subida do pico de máxima absorvância, assim como um desvio sucessivo deste para comprimentos de onda menores, durante o tempo de reação. De modo a melhor compreender os dados obtidos, estudos posteriores serão necessários.

LIST OF ACRONYMS

ADA	Adenosine deaminase
AIBN	Azobisisobutyronitrile
AMA	2-Aminoethyl methacrylate hydrochloride
AMPTMA	(3-Acrylamidopropyl)trimethylammonium chloride
ARGET	Activators regenerated by electron transfer
AscA	Ascorbic acid
ATRP	Atom transfer radical polymerization
BBiB	2-Bromoisobutyryl bromide
CLRP	Controlled/living radical polymerization
CPME	Cyclopentyl methyl ether
DCM	Dichloromethane
DMAP	1,2-Diaminoethane
DMAEMA	(2-Dimethylamino)ethylmethacrylate
DMF	Dimethyl formamide
DMSO	Dimethyl sulfoxide
DNA	Deoxyribonucleic acid
DOTAP	1,2-Dioleoyl-3-methylammonium-propane
DP	Degree of polymerization
DPA	2-(Diisopropylamino)ethyl methacrylate
eATRP	Electrochemically mediated atom transfer radical polymerization
EBiB	Ethyl α-bromoisobutyrate
EBPA	Ethyl α-bromophenylacetate
ECP	Ethyl 2-chloropropionate
EtBr	Ethidium bromide
EtOH	Ethanol
FRP	Free radical polymerization
FTIR-ATR	Fourier transform infrared attenuated total reflection
GMA	Glycidyl methacrylate
HPLC	High performance liquid chromatography

ICAR	Initiators for continuous activator regeneration
IPA	Isopropanol
LCST	Lower critical solution temperature
MA	Methyl acrylate
MeOH	Methanol
2-MeTHF	2-Methyltetrahydrofuran
Me_6TREN	Tris[2-(dimethylamino)ethyl]amine
NIPAAM	N-isopropylacrylamide
NMR	Nuclear magnetic resonance
ODNs	Oligonucleotids
PAA	Poly(amidoamine)
PAMA	Poly(2-aminoethyl methacrylate hydrochloride)
PAMPTMA	Poly((3-acrylamidopropyl)trimethylammonium chloride)
PβAE	Poly(β-amino ester)
PDMAEMA	Poly((2-dimethylamino)ethylmethacrylate)
PDPA	Poly(2-(diisopropylamino)ethyl methacrylate)
PEG	Poly(ethylene glycol)
PEI	Polyethylene imine
PEO	Polyethylene oxide
PLL	Poly-l-lysine
PMA	Poly(methyl acrylate)
PNIPAAM	Poly(N-isopropylacrylamide)
PPAA	Poly(2-propylacrylic acid)
ppm	Parts per million
PRE	Persistent radical effect
PTFE	Polytetrafluoroethylene
RAFT	Reversible addition-fragmentation chain transfer
RDRP	Reversible deactivation radical polymerization
RI	Refractive index
rpm	Rotations per minute
r.t.	Room temperature

SARA	Supplemental activator and reducing agent
SCID	Severe combined immunodeficiency
SEC	Size exclusion chromatography
siRNA	Small interfering ribonucleic acid
Sty	Styrene
TEA	Triethylamine
THF	Tetrahydrofuran
TPMA	Tris(pyridin-2-ylmethyl)amine
UV-Vis	Ultraviolet-visible
VC	Vinyl chloride

NOMENCLATURE

α	Degree of protonation
$Đ$	Dispersity
M_n^{NMR}	Number-average molecular mass determined by NMR spectroscopy
M_n^{SEC}	Number-average molecular mass determined by SEC
M_n^{th}	Theoretical number-average molecular mass
M_w	Theoretical mass-average molecular mass
k_p^{app}	Apparent rate constant of propagation
k_a	Activation rate constant
k_d	Deactivation rate constant
k_{disp}	Disproportionation rate constant
k_{comp}	Comproportionation rate constant
k_p	Propagation rate constant
k_t	Termination rate constant
T	Temperature

CONTENTS

Acknowledgments/Agradecimentos VII
Abstract IX
Resumo XI
List of acronyms XIII
Nomenclature XVII
Contents XIX
List of figures XXI
List of tables XXV
List of schemes XXVII
Goals, motivation and research impact XXIX
Chapter 1: Literature review ..... - 1 -
1 Literature review ..... - 3 -
1.1 Gene delivery systems ..... - 3 -
1.1.1 Cationic polymers as non-viral gene delivery vectors ..... - 5 -
1.2 Reversible Deactivation Radical Polymerization (RDRP) ..... - 12 -
1.2.1 Atom transfer radical polymerization ..... - 13 -
Chapter 2: Cationic copolymers for gene delivery ..... - 19 -
2 Cationic copolymers for gene delivery ..... - 21 -
2.1 Abstract ..... - 21 -
2.2 Introduction ..... - 21 -
2.3 Experimental ..... - 22 -
2.3.1 Materials ..... - 22 -
2.3.2 Techniques ..... - 23 -
2.3.3 Procedures ..... - 24 -
2.4 Results and discussion ..... - 28 -
2.4.1 PEG_{45}-*b*-PAMPTMA and PAMPTMA-*b*-PEG_{72}-*b*-PAMPTMA block copolymers ..... - 28 -
2.4.2 PAMPTMA-based random copolymers ..... - 31 -
2.4.3 PEG_{45}-*b*-$PAMA_n$ block copolymers ..... - 37 -
2.4.4 Gene delivery results from PAMA-based polymers ..... - 41 -
2.5 Conclusions and future work ..... - 44 -

Chapter 3: Influence of different “THF-like” solvents on the PMA synthesis by SARA ATRP - 21 -
3 Influence of different “THF-like” solvents on the PMA synthesis by SARA ATRP - 49 -
3.1 Abstract - 49 -
3.2 Introduction - 49 -
3.3 Experimental - 51 -
3.3.1 Materials - 51 -
3.3.2 Techniques - 52 -
3.3.3 Procedures - 53 -
3.4 Results and discussion - 55 -
3.5 Conclusions and future work - 63 -
References - 65 -
Appendices - 71 -
Appendix A. Supporting information for the synthesized macroinitiators and ligands and for the procedures used in Chapter 2 A1
Appendix B. Supporting information for Chapter 2, Section 2.4.1 B1
Appendix C. Supporting information for Chapter 2, Section 2.4.3 C1
Appendix D. Supporting information for Chapter 2, Section 2.4.4 D1
Appendix E. Supporting information for Chapter 3 E1

LIST OF FIGURES

Figure 1 - Schematic representation of the strategy followed in this work. XXIX
Figure 2 - Schematic representation of the formation of a polyplex. ..... - 6 -
Figure 3 – Chemical structure of PLL and PEI. ..... - 7 -
Figure 4 - PDMAEMA chemical structure. ..... - 9 -
Figure 5 – Examples of different polymer structures that can be produced using RDRP techniques: **(a)** copolymer composition; **(b)** architecture. ..... - 13 -
Figure 6 - Typical synthesis of PEG_{45}-*b*-$PAMPTMA_n$ via SARA ATRP. ..... - 28 -
Figure 7 - **(a)** Kinetic plot of $\ln[M]_0/[M]$ *vs.* time (min) and **(b)** plot of number-average molecular weight (M_n^{SEC}) and $Đ$ (M_w/M_n) *vs.* monomer conversion (the dashed line represents theoretical molecular weight at a given conversion) for the SARA ATRP of AMPTMA initiated by PEG_{45}-Br in water at 25°C. Reaction conditions: $[AMPTMA]_0/[PEG_{45}\text{-}Br]_0/[CuCl_2]_0/[Me_6TREN]_0$/Cu(0) wire = 57/1/0.5/1/Cu(0) wire: *l* = 10 cm; *d* = 1 mm; $V_{solvent}$ = 3.2 mL ..... - 29 -
Figure 8 - 400 MHz ^{1}H NMR spectrum, in D_2O, of a pure PEG_{45}-*b*-$PAMPTMA_{47}$ sample (M_n^{SEC} = 15.9 x10^3; $Đ$ = 1.10) obtained by SARA ATRP. Reaction conditions: $[AMPTMA]_0/[PEG_{45}\text{-}Br]_0/[CuCl_2]_0/[Me_6TREN]_0$/Cu(0) wire = 40/1/0.5/1/Cu(0) wire: *l* = 10 cm; *d* = 1 mm; $V_{solvent}$ = 3.2 mL ..... - 30 -
Figure 9 - Typical synthesis of $PAMPTMA_n$-*co*-$PNIPAAM_m$ by SARA ATRP. ..... - 32 -
Figure 10 - Typical Synthesis of $PAMPTMA_n$-*co*-$PDPA_m$ by SARA ATRP. ..... - 32 -
Figure 11 - Typical synthesis of $PAMPTMA_n$-*co*-PMA_m by SARA ATRP. ..... - 33 -
Figure 12 - 400 MHz ^{1}H NMR spectrum, in D_2O, of a pure $PAMPTMA_{11}$-*co*-$PNIPAAM_{101}$ sample (M_n^{th} = 1.9 x 10^3) obtained by SARA ATRP. Reaction conditions: $[AMPTMA]_0/[NIPAAM]_0/[ECP]_0/[CuCl_2]_0/[Me_6TREN]_0$/Cu(0) wire = 10/100/1/0.5/1/Cu(0) wire: *l* = 10 cm; *d* = 1 mm; $V_{solvent}$ = 3.2 mL ..... - 34 -
Figure 13 - 400 MHz ^{1}H NMR spectrum, in D_2O, of a pure $PAMPTMA_n$-*co*-$PDPA_m$ sample (M_n^{SEC} = 28.9 x 10^3, $Đ$ = 1.19) obtained by SARA ATRP. Reaction conditions: $[AMPTMA]_0/[DPA]_0/[EBiB]_0/[CuBr_2]_0/[Me6TREN]_0$/Cu(0) wire = 10/100/1/0.5/1/Cu(0) wire: *l* = 10 cm; *d* = 1 mm; H_2O/IPA = 10/90 (v/v) with DPA/solvent = 1. ..... - 35 -

Figure 14 - 400 MHz ^{1}H NMR spectrum in 80/20 EtOD/D_2O of a pure PAMPTMA$_n$-*co*-PMA$_m$ sample (M_n^{th} = 6.7 x 10^3) obtained by SARA ATRP. Reaction conditions: $[AMPTMA]_0/[MA]_0/[EBiB]_0/[CuBr_2]_0/[Me6TREN]_0$/Cu(0) wire = 10/100/1/0.5/1/Cu(0) wire: *l* = 10 cm; *d* = 1 mm; H_2O/EtOH = 20/80 (v/v) with MA/solvent = 0.5 ..... - 36 -
Figure 15 – FTIR spectra of PAMPTMA-*co*-PMA, PAMPTMA and PMA..... - 36 -
Figure 16 - Typical synthesis of **(a)** PEG$_{45}$-*b*-PAMA$_n$ and **(b)** of PAMA$_n$ by ARGET ATRP. .. - 38 -
Figure 17 - 400 MHz ^{1}H NMR spectrum, in D_2O, of a pure PEG$_{45}$-*b*-PAMA$_{111}$ sample (M_n^{NMR} = 20.4 x 10^3; M_n^{SEC} = 20.6 x 10^3, Đ = 1.09) obtained by ARGET ATRP. Reaction conditions: $[AMA]_0/[PEG_{45}\text{-}Br]_0/[CuBr_2]_0/[TPMA]_0$ = 100/1/0.5/1/2; FR_{AscA} = 43 nmol/min; $V_{solvent}$ = 1.43 mL; T = 35°C..... - 39 -
Figure 18 - **(a)** Titration curves of the PAMA-based samples tested; **(b)** same titration curves as in **(a)** with the x-axis expressed in terms of the average degree of protonation, α. ..... - 40 -
Figure 19 - Effect of the N/P ratio and composition of polyplexes on the viability of COS-7 cells using **(a)** PAMA$_{103}$ and **(b)** PEG$_{45}$-*b*-PAMA$_{111}$. ..... - 42 -
Figure 20 - Effect of the N/P ratio and composition of polyplexes on their transfection activity COS-7 cell lines using **(a)** PAMA$_{103}$ and **(b)** PEG$_{45}$-*b*-PAMA$_{111}$..... - 42 -
Figure 21 - Accessibility of ethidium bromide to DNA of the different polyplexes prepared at different N/P ratios..... - 43 -
Figure 22 - Chemical structure of the "THF-like" solvents used in this work: THF, CPME and 2-MeTHF. ..... - 50 -
Figure 23 – **(a)** Kinetic plots of conversion and $\ln[M]_0/[M]$ *vs.* time (h) and **(b)** plot of number-average molecular weights (M_n^{SEC}) and *Đ vs.* monomer conversion (the dashed lines represent theoretical molecular weight at a given conversion) for the SARA ATRP of MA in CPME/EtOH/H_2O = 70/28/2 (v/v/v) (red), THF/EtOH/H_2O = 70/28/2 (v/v/v) (black) and 2-MeTHF/EtOH/H_2O = 70/28/2 (v/v/v) (blue) at 30°C. Reaction conditions: $[MA]_0/[EBiB]_0/[CuBr_2]_0/[Me_6TREN]_0$/Cu(0) wire = 222/1/0.1/1.1/Cu(0) wire: *l* = 5 cm; *d* = 1 mm; $V_{solvent}$ = 2 mL..... - 55 -
Figure 24 - 400 MHz ^{1}H NMR spectrum, in $CDCl_3$, of a purified PMA$_{65}$ sample (M_n^{RMN} = 5.8 x 10^3; M_n^{sec} = 6.6 x 10^3; Đ = 1.09, monomer conversion = 84 %) obtained by SARA ATRP. Reaction conditions: $[MA]_0$/[solvent] = 2/1 (v/v); CPME/EtOH/H_2O = 70/28/2

(v/v/v); $[MA]_0/[EBiB]_0/[CuBr_2]_0/[Me_6TREN]_0$/Cu(0) wire = 70/1/0.1/1.1/Cu(0) wire: *l* = 5 cm; *d* = 1 mm; $V_{solvent}$ = 2 mL; T = 30 °C. ..... - 56 -
Figure 25 - SEC traces of PMA-Br before and after chain extension with MA: macroinitiator obtained at 84% of monomer conversion (green line) and extended polymer at 75% monomer conversion (blue line); macroinitiator - $[MA]_0$/[solvent] = 2/1 (v/v) in CPME/EtOH/H_2O = 70/28/2 (v/v/v), with $[MA]_0/[EBiB]_0/[CuBr_2]_0/[Me_6TREN]_0$/Cu(0) wire = 70/1/0.1/1.1/Cu(0) wire: *l* = 5 cm; *d* = 1 mm at 30 °C; chain extension by SARA ATRP in DMSO with $[MA]_0$/[solvent] = 2/1 (v/v), $[MA]_0/[PMA\text{-}Br]_0/[CuBr_2]_0/[Me_6TREN]_0$/Cu(0) wire = 500/1/0.1/1.1/Cu(0) wire: *l* = 5 cm; *d* = 1 mm at 30 °C, $V_{solvent}$ = 1.25 mL..... - 58 -
Figure 26 - Comproportionation of $CuBr_2$/Me_6TREN with Cu(0) in CPME/EtOH/H_2O = 70/28/2 (v/v/v) in the presence of ligand excess, $[CuBr_2]_0/[Me_6TREN]_0$/Cu(0) wire = 0.1/1.1/Cu(0) wire: *l* = 5 cm; *d* = 1 mm, with $[CuBr_2]$ = 0.005 mmol/mL, at 30°C..... - 60 -
Figure 27 - Comproportionation of $CuBr_2$/Me_6TREN with Cu(0) in **(a)** THF/EtOH/H_2O = 70/28/2 (v/v/v) and **(b)** 2-MeTHF/EtOH/H_2O = 70/28/2 (v/v/v) in the presence of ligand excess, $[CuBr_2]_0/[Me_6TREN]_0$/Cu(0) wire = 0.1/1.1/Cu(0) wire: *l* = 5 cm; *d* = 1 mm, with $[CuBr_2]$ = 0.005 mmol/mL, at 30°C. ..... - 62 -
Figure 28 - Comproportionation of $CuBr_2$/Me_6TREN with Cu(0) in CPME/EtOH/H_2O = 70/28/2 (v/v/v) in the presence of ligand excess, reaction conditions: $[MA]_0$/[solvent] = 2/1 (v/v); CPME/EtOH/H_2O = 70/28/2 (v/v/v); $[MA]_0/[EBiB]_0/[CuBr_2]_0/[Me_6TREN]_0$/Cu(0) wire = 222/1/0.1/1.1/Cu(0) wire: *l* = 5 cm; *d* = 1 mm; $V_{solvent}$ = 1.25 mL, with $[CuBr_2]$ = 0.005 mmol/mL, at 30°C..... - 63 -

LIST OF TABLES

Table 1 - General properties of the PEG_{45}-*b*-$PAMPTMA_n$ block copolymers. ..... - 30 -
Table 2 - General properties at 40 minutes of $PAMPTMA_n$-*b*-PEG_{72}-*b*-$PAMPTMA_n$ SARA ATRP reaction time. ..... - 31 -
Table 3 - Summary of $PAMPTMA_m$-*co*-$PNIPAAM_n$ (GD24), $PAMPTMA_m$-*co*-$PDPA_n$ (GD25) and $PAMPTMA_m$-*co*-PMA_n (GD26) general properties. ..... - 33 -
Table 4 - General properties of the PAMA-based samples synthesized. ..... - 38 -
Table 5 – Some general physical properties of the organic solvents: THF, 2-MeTHF and CPME ..... - 50 -
Table 6 - General properties of the PMA_n-Br polymers used as macroinitiators in the chain extensions. ..... - 57 -
Table 7 – General properties of the PMA-Br extended polymers. ..... - 59 -

LIST OF SCHEMES

Scheme 1 - General RDRP equilibrium between active and dormant species. ..... - 12 -
Scheme 2 - General scheme of the ATRP equilibrium. ..... - 14 -
Scheme 3 - General mechanism of the SARA ATRP mediated by Cu(0) and Cu(II)X_2. - 16 -
Scheme 4 - General mechanism of the ARGET ATRP. ..... - 17 -

GOALS, MOTIVATION AND RESEARCH IMPACT

Reversible deactivation radical polymerization (RDRP) methods have emerged as excellent tools for macromolecular engineering, since they allow a precise control over the polymer features (e.g., molecular weight, composition, topology and architecture) [1]. Atom transfer radical polymerization (ATRP), which uses a metal/ligand catalytic complex to mediate the polymerization, is one of the most robust and versatile RDRP methods [2]. Recently, eco-friendly conditions were developed for the polymerization of two promising cationic monomers by ATRP related chemistries: (3-acrylamidopropyl) trimethylammonium chloride (AMPTMA), by supplemental activator and reducing agent atom transfer radical polymerization (SARA ATRP) [3] and 2-aminoethyl methacrylate hydrochloride (AMA), by activators regeneration by electron transfer (ARGET) ATRP [4]. Aqueous medium and low catalyst loading are attractive features of these systems, considering the preparation of polymers for biomedical applications. Therefore, the aim of this work is to use the eco-friendly ATRP systems reported in the literature for the polymerization of both AMPTMA and AMA to design new well-defined copolymers that can be used as non-viral vectors for gene delivery applications (Figure 1).

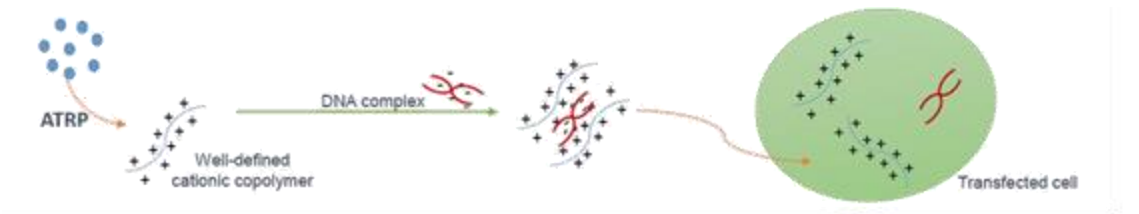

Figure 1 - Schematic representation of the strategy followed in this work.

Under the light of "Green Chemistry", there has been a tendency to develop efficient systems that produce a lesser CO_2 footprint, when compared to conventional systems. Since solvents tend to produce the biggest waste in chemical processes [5], the search for greener options is a key aspect to reduce the footprint produced by chemical processes. Tetrahydrofuran (THF) is a well-known, widely used and toxic organic solvent. Cyclopentyl methyl ether (CPME) and 2-methyltetrahydrofuran (2-MeTHF) are two greener candidates that could replace THF in some reaction systems. Previous work has demonstrated the advantage of using a CPME/ethanol(EtOH)/H_2O = 70/28/2 (v/v/v)

solvent mixture for the SARA ATRP of methyl acrylate (MA) [6]. Based on this knowledge, in this work, the differences between the use of THF, CPME and 2-MeTHF as co-solvents were also studied in the synthesis of poly(MA) (PMA) via SARA ATRP.

This work is expected to have an important impact on two different areas: the design of new polymers for polyplexes that are used in one of the most promising therapeutics strategies, gene delivery, and the development of new reaction systems that are greener by eliminating the need for use of toxic solvents as THF.

CHAPTER 1: LITERATURE REVIEW

1 LITERATURE REVIEW

1.1 GENE DELIVERY SYSTEMS

For a vast array of diseases, gene therapy aims to offer medical treatments, or preventions, by gene transfer into specific cells of the patient [7]. The proper identification of the genetic roots of specific diseases has been the subject of intensive research, as the identification of the gene causing the disease turns the prevention and/or treatment easier. While standard treatments are merely capable of acting on the symptoms, gene therapy aims to act directly on the source of the problem, not only treating symptoms, but also potentially eliminating the cause of the disease [7, 8]. In some cases, such as cancer therapies, the treatment only requires a short-term gene expression. However, for most genetic diseases (acquired or inherited) a long-term gene expression is vital in order for the treatment to be effective [9]. As an example, the first clinical studies involving gene transfer began in 1990 for the treatment of the adenosine deaminase (ADA) gene for patients with Severe Combined Immunodeficiency due to Adenosine Deaminase Deficiency (SCID) [10]. After years of research, on May 2016 it was announced that the European Commission has approved GSK's Strimvelis™, as the first *ex-vivo* stem cell gene therapy to treat patients with ADA-SCID [11]. From this example, it is clear that gene therapy is one among the greatest medical revolutions of this century.

Throughout the years, extensive research has been done in order to develop viable gene delivery systems, known as vectors. Important efforts have been made in order to find an efficient, tunable/controllable, non-toxic and with a favorable immune response, delivery vector [8]. There are different types of gene delivery vectors for somatic cells, either viral or non-viral. In spite of the numerous systems available, the success of the gene therapy application ultimately depends on the delivery of the genetic material through the cell membrane into the cell nucleus [12].

Viral vectors

The main activity of a virus is to self-replicate. In order to do this, it carries its genome from one host cell to another, entering the new target cell nucleus and initiating the expression of its genome [8]. Viral gene-transfer systems are based on adapted-

viruses, where part of the virus genome is replaced with a therapeutic gene and some areas are removed in order to derange its replication and make the viral vector safer [7, 8, 12]. Despite the fact that the viral approach has been known to provide the most efficient transfection rates [7] and successful gene therapy systems [12], there are several safety concerns. In short, viral vectors have high immunogenicity and the potential to generate a replication-competent virus during manufacturing or after administration to patients, despite all possible safety measures. Moreover, viral vectors have an inherit transgenic[1] capacity size and, since they require a genome modification, they are also difficult to manufacture [7, 8, 12]. As an example, retroviral vectors are one of the most frequently employed systems in gene therapy [12]. Relevant information on viral vectors can be found in some dedicated reviews [9, 12, 13].

Non-viral vectors

Non-viral gene-transfer system is the generic designation of all the physical and chemical systems that are not virus-based [12]. The major advantage of non-viral systems is that they can be accurately designed to have specific physicochemical properties, which can potentially improve their biological interaction, especially with the development of advanced polymerization methods (e.g., RDRP) [14]. Moreover, non-viral vectors have no insert-size limitation, have high availability, are easier to manufacture and are much less immunogenic than viral vectors [12]. In short, these systems are more flexible than their viral counterparts, in spite of their possible cytotoxicity and low transfection efficiency [8].

To facilitate the entrance of the genetic material into the cell, several physical methods could be used (e.g., naked DNA, electroporation or DNA particle bombardment by gene gun). In non-viral physical gene delivery systems, the genetic material is delivered due to a momentary penetration into the cell membrane caused by the use of either mechanical, electrical, ultrasonic, hydrodynamic or laser-based energy [12].

Chemical non-viral vectors are usually nanosized complexes that result from the complexation of the negatively charged nucleic acid with cationic polymer. This polycation may be a cationic liposome/micelle or a cationic polymer, forming lipoplexes

[1] **Transgene –** the gene delivered by the vector.

or polyplexes, respectively, when bound to the genetic material [12]. Compared to liposomes, most cationic polymer gene delivery vectors possess lower transfection efficiencies. Nonetheless, polymers form complexes with a narrow particle size distribution, are more stable against the action of nuclease and their hydrophilicity can be easily tuned by copolymerization [15].

When designing gene delivery vectors, it is relevant to understand the different barriers preventing a successful gene delivery [16]. Unlike a virus, which has naturally evolved functions to surpass each obstacle, non-viral vectors must be designed accounting for all the different extracellular and intracellular obstacles [8]. The difficulty in improving the efficacy of non-viral polymeric vectors remains associated to the scarce understanding of how polymeric vectors could overcome each intracellular obstacle. In addition, there is still much to learn in regards to the actual contribution of the physicochemical properties to an efficient intracellular transfection [17]. Besides the need to synthesize a safe, stable, non-toxic, non-immunogenic and non-pathogenic non-viral vector, a few design criteria must be considered when designing synthetic vectors. These include: DNA protection, the ability to pack large DNA plasmids, ease of administration and fabrication, serum stability, targetability to specific cell-types, cost-effective synthesis, easy purification, efficient cellular internalization, endolysosomal escape, nuclear transport, efficient unpackaging and infection of non-dividing cells [8]. Typically, a vector is designed to overcome one or more specific barriers (e.g., aggregation when in circulation, protein binding, etc.) [17].

The subject of this study is non-viral synthetic gene delivery vectors, which will be further explored in the following section.

1.1.1 Cationic polymers as non-viral gene delivery vectors

Due to their physicochemical properties, cationic polymers have attracted increasing attention as potential candidates for biomedical applications. This is especially relevant considering gene delivery, since the positive charges of cationic polymers allow electrostatic interactions between the nucleic acid (anionic – phosphates along the nucleic acid backbone) and the polymer, forming the so-called polyplexes [18-20] (Figure 2). Each polyplex particle is often formed by several nucleic

acid molecules and polymer chains (Figure 2). Additionally, the positive charges on the particle surface provide nucleic acid protection ensuring the stability of the polyplex [8]; however, an excess of cationic charges on the polyplex surface could contribute to the cytotoxicity of the system [16].

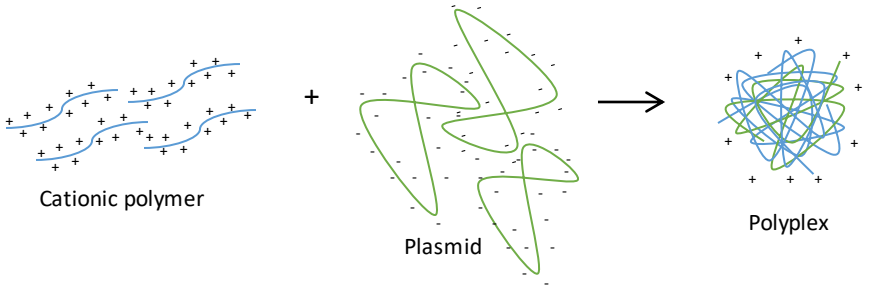

Figure 1 - Schematic representation of the formation of a polyplex.

Recently, Yanan Yue and Chi Wu [17] have examined four critical and underrated points for the success of the intracellular processing of the polyplex. One of those topics is that free cationic polymer chains in a solution mixture of DNA and polymer seem to be responsible for gene transfection, while the polycationic chains forming the polyplexes only act as the protectors of the genetic material. Another debated parameter is whether the "proton sponge" [2] could legitimately explain the high transfection ratings of some pH-responsive polymers (e.g., polyethylene imine - PEI).

The relationship between the cationic polymer characteristics (e.g. structure, etc.) and the biophysical properties of the polyplex formed have been subject of intense research [8, 12, 17, 21]. Factors like charge density, length of the side chain, charge type, molecular weight, charge spacing along the side chain or hydrophobicity could affect the interaction of the polycation with the plasmid, with direct consequences on their biophysical properties [16, 21]. For example, the increase of the polymer's molecular weight, leads to the increase of the net positive charge density, allowing a tighter DNA binding and the formation of a more stable complex [12]. Nevertheless, the strong binding and efficient DNA condensation are not enough for an efficient transfection,

[2] "Proton sponge" - designation for the effect of an increase of osmotic pressure inside an endolysosome caused by the continuous protonation of amines on polymer chains, an influx of counter ions and ultimately the burst of the endolysosome.

since tight binding can difficult the unpackaging and, therefore, an efficient delivery of the gene and transfection [8]. Moreover, long polycationic chains tend to have higher cytotoxicity [17]. It is, therefore, necessary to find a proper balance between the properties of the cationic polymer and the features necessary for the application. More detailed information on this topic can be found in the literature [21].

As previously mentioned, for gene therapy applications it is vital to maximize transfection efficiency and minimize cytotoxicity. To this end, since the first gene transfection reporting the use a polycation vector [22], the systematic study of new cationic polymers with different physical/chemical characteristics has been overwhelming and ever-growing [23]. In the scope of this work, only a few relevant examples will be discussed. More in depth information can be found in [23] and [16].

Off-the-shelf polymers like PEI [24] and poly-l-lysine (PLL) (Figure 3) are amongst the most extensively studied polymers, having been known to produce some of the most promising transfection results [25]. Cationic polysaccharides, mainly chitosan derivatives and cationic polymers based on dextran-spermine, have also been studied in gene delivery applications. Chitosan, for example, has excelled in drug delivery essays, and has been shown promising results in gene delivery [25].

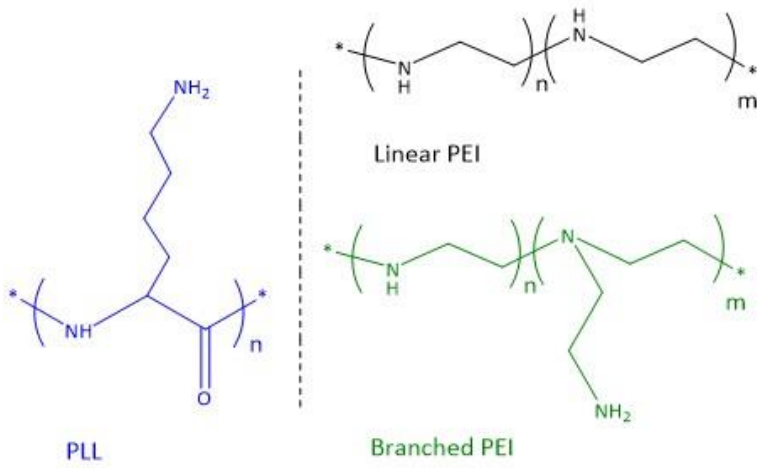

Figure 3 – Chemical structure of PLL and PEI.

PEI is a cationic polyamine with a high pH-buffering capacity [26] that is commercially available in two main architectures: linear and branched (Figure 3). PEI-based structures have been widely studied since their first report in 1995 [27]. In spite of the proven high transfection efficiency [28], likely related to its "proton sponge"

effect [26], PEI also presents a high cytotoxicity (highly influenced by the chain length and the topology [17]). Furthermore, this polymer has poor *in vivo* stability due to a short circulation time and high aggregation, since PEI easily interacts with blood cells and serum proteins [25]. Another disadvantage of using PEI for gene delivery applications is that commercially available PEIs are typically polydisperse and have a poorly-defined composition, requiring further modifications, if a more controlled structure is required [14].

PLL (Figure 3) was one of the first cationic polymers to be reported for gene delivery applications [22]. With lysine repeating units that provide a biodegradable character [25], PLL is a positively charged linear polypeptide [29]. The main disadvantage of the usage of PLL is that its polyplexes are rapidly bound to plasma proteins and easily cleared from circulation, diminishing the transfection efficiency [25]. The relationships between the structure of PLL and the transfection activity were studied in detail [29].

Poly((2-dimethylamino)ethylmethacrylate) (PDMAEMA, Figure 4) based polymers have been described to have excellent transfection efficiency [30], probably due to their endossomal destabilization property and the ability to dissociate from DNA in the cytosol [31]. At physiological pH (7.4 in the cytosol [32]), PDMAEMA its slightly protonated since it has an average pK_a of 7.5, behaving as a proton sponge [31]. However, even though it is a promising non-viral gene delivery vector, cytotoxicity issues [33] prevent PDMAEMA to be an optimal solution. Although PDMAEMA has typically a less transfection efficiency than PEI, the synthesis and characterization of well-defined PDMAEMA is well described in the literature, which allows PDMAEMA to be a model for the assessment of the connections between the chain structure and function in gene delivery applications [17]. On this matter, the synthesis of linear, 3-arm and 5-arm star-shaped PDMAEMA via ATRP was reported [34]. Recently, the synthesis of a well-defined PDMAEMA via SARA ATRP under mild condition was reported [35]. The same group also reported a novel triblock copolymer of PDMAEMA-*b*-poly(β-amino ester)-*b*-PDMAEMA to be a promising polymeric non-viral vector [19].

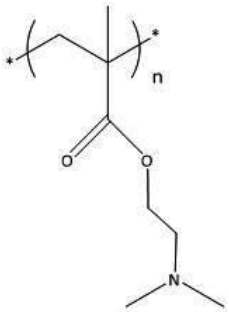

Figure 4 - PDMAEMA chemical structure.

An attachment of poly(ethylene glycol) (PEG) to the polymer (PEGylation), for example, has been used as a solution to prevent plasma protein binding and to increase half-life circulation of the complex. Hence, PEGylation decreases cytotoxicity, increases transfection efficiency [12] and improves the *in vivo* stability of the polyplex [36]. Moreover, it has been known to protect the therapeutic payload from proteins [37].

Studies were made with copolymers with a tertiary amine methacrylate and with PEG, where PEG produced a proven beneficial effect on the ability to the copolymers to bind with DNA and to produce stable and compact polyplexes [38]. Interesting results in these studies were that: a PDMAEMA homopolymer produced better transfection than the control PLL; PEG-based copolymers, while increasing the hydrophilicity of the polyplex, had poorer transfection rates due to a loss in the ability of the polyplex to penetrate into the cells, likely related to the steric stabilization effect of a PEG corona [38]. More recently, another group also reported PEGylated PDMAEMA well-defined copolymers via reversible addition-fragmentation chain transfer (RAFT) polymerization [36]. The main purpose was to evaluate the effect of PEG architecture and molecular weight on the cytotoxicity and gene delivery efficacy. The ability of the polymers tested to complex and release DNA were not significantly affected by changes in the PEG topology, as opposed to the relevant effect that the PEG architecture had on the polyplexes size and zeta potential [36].

Another relevant group of non-viral polymeric vectors are the pH-sensitive, membrane-disruptive polymers [17, 32]. Acid-responsive membrane disruptive polymers, like poly(2-propylacrylic acid) (PPAA), have been designed aiming for an endosomal release that mimics the one of viruses [17]. PPAA has been used, with remarkable results, alongside a cationic DNA/(1,2-dioleoyl-3-methylammonium-

propane) (DOTAP) lipoplexes [39]. Alternatively, pH-responsive polymers, like poly(amidoamine) (PAA), could also be potentially interesting for gene delivery applications [23].

In stimuli-responsive polymers (e.g., PEI, PPAA, etc.) the interaction with the nucleic acids could be changed as a response to small variations in the external environment (e.g., temperature, pH), making them potentially interesting to gene delivery applications [32]. This ability to alter the interaction with the nucleic acid could be the key to improve transfection efficiency, since the introduction of a stimuli-responsive segment in the vector could improve release at target site, while maintaining a strong/protective binding during transport [32]. In this work, two stimuli-responsive monomers were used, 2-(diisopropylamino)ethyl methacrylate (DPA, pH-responsive) and N-isopropylacrylamide (NIPAAM, temperature-responsive), to synthesize copolymers of PAMPTMA$_n$-*co*-PDPA$_n$ and PAMPTMA$_n$-*co*-PNIPAAM$_n$.

Poly(2-(diisopropylamino)ethyl methacrylate) (PDPA) is a pH-responsive polymer with a pK_a of 6.2 [40]. As other pH-responsive polymers, DPA-based polymers have attracted increasing attention for gene delivery applications [41].

N-isopropylacrylamide (NIPAAM) is a temperature-responsive monomer. When in solution, poly-NIPAAM (PNIPAAM) is hydrophilic at temperatures below its lower critical solution temperature (LCST) and endures an entropy-driven transition to a hydrophobic structure at temperatures above its LCST resulting in an insoluble aggregate. [42] LCST for PNIPAAM has been reported to be in range of 30-35°C [42], yet it is frequently described to be at 32°C in pure water [32]. The closeness of the LCST of PNIPAAM to the normal body temperature as well as the possible fine tuning of this value, are the two main reasons that justify the broad interest on this polymer during the past decades [43]. Changing the solvent mixture is probably the simplest way to change the thermal response of PNIPAAM. Other ways include salt addition, copolymerization with other monomers or variation of the solution pH. [42] Nevertheless, adding an organic solvent, for example, is not the ideal solution for biomedical applications due to toxicity issues. It has been reported that LCST increases as the molecular weight and polymer concentration decreases [44], meaning that the LCST can be tuned to a temperature closer to the human body temperature by simply decreasing the molecular weight of the polymer or controlling the polymer concentration. The addition of either more

hydrophilic or hydrophobic co-monomers is a another approach to tune the LCST of PNIPAAM-based copolymers [32]. Moreover, a PNIPAAM-based copolymer could potentially be interesting for gene delivery applications since it reduces the need of cationic charges in the polyplex [32].

The two cationic monomers used in this work were (3--acrylamidopropyl)trimethylammonium chloride (AMPTMA) and 2-aminoethyl methacrylate hydrochloride (AMA). PEG_{45}-Br was used as macroinitiator for several PEG_{45}-*b*-$PAMPTMA_n$ and PEG_{45}-*b*-$PAMA_n$ block copolymers.

AMPTMA is a quaternary ammonium salt [45]. As a cationic hydrophilic monomer, AMPTMA has been used in combination with NIPAAM [43, 46, 47], exhibiting potential to be used as drug delivery systems [48], microcarriers for cell proliferation [49] and as gene delivery vectors [43]. To the extent of the research made, AMPTMA has only been used in gene delivery applications in combination with NIPAAM for the synthesis of PNIPAAM-*b*-PAMPTMA block copolymers intended for the delivery of siRNA. The highest transfection efficiencies were obtained for shorter charged blocks [43].

AMA is a pH-responsive monomer with a pK_a of 8.8, significantly higher than the pK_a of the poly(AMA) homopolymer ($pK_a \approx 7.6$), being both unstable under basic conditions (pH > 9) [50]. Chemical degradation of PAMA occurs under basic conditions (pH > 9) [50]. Due to the presence of primary amino groups, PAMA has a cationic behavior at physiological pH, being able to bind to negatively charged nucleic acids [51]. PAMA homopolymers synthesized via ATRP have been used as potential DNA vaccine to dendritic cells, pointing to the low cytotoxicity of the PAMA homopolymers and good transfection efficiency either with or without serum [52]. PEGylated PAMA block copolymers synthesized via ATRP have been previously employed for the delivery of heparin [53], oligonucleotids [54], DNA in dendritic cells [51] and small interfering RNA (siRNA) [55], exhibiting promising results. Tang *et al* [51] showed that there is a clear correlation between the length of the PAMA block and both the physicochemical properties of the polyplex and the interaction with dendritic cells. Recently, the synthesis of PAMA via ARGET ATRP under mild conditions was reported [4]. To the extent of the research made, PAMA-based copolymers have never been reported for DNA delivery in COS-7 cells.

1.2 REVERSIBLE DEACTIVATION RADICAL POLYMERIZATION (RDRP)

In order to prepare reliable and effective therapeutic products, it is vital to ensure that the synthesized materials have homogeneous properties with well-controlled architectures and narrow molecular weight distribution [16].

Common polymerization methods, namely free radical polymerization (FRP), feature a lack of control over the polymers structure and molecular weight [56] and by using them it is almost impossible to perform a proper functionalization of the synthesized polymers. FRP is commonly employed in large-scale production of polymers. It is a versatile technique that allows the polymerization of a vast array of monomers under mild reactions conditions. Despite the advantages, the polymer chain growth is extremely fast (~1s) in FRP systems, which difficult any control over the polymer structure [56]. The control over the molecular weight is not possible due to termination and chain transfer reactions occurring throughout the polymerization, which causes a broad molecular weight distribution [56].

During the past two decades, new polymerization techniques have been developed, namely RDRP (formerly known as "controlled/living" radical polymerization, CLRP), allowing good control over the polymers properties (structure, architecture, topology, composition and molecular weight) [1], while using mild experimental conditions. The basic principle of this type of polymerization techniques is to maintain the concentration of radicals extremely low during the polymerization. At low concentration of active radicals, the termination reactions would be neglected and the resulting polymers would have high chain-end functionality. This is achieved through an equilibrium between active (propagating radicals) and dormant species (Scheme 1), which is characteristic of all RDRP polymerization systems, along with an extremely fast initiation allowing a simultaneous start of all the polymer chains [1].

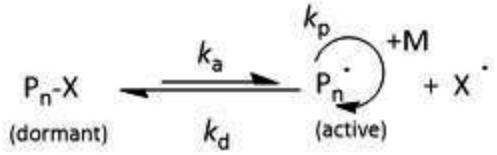

Scheme 1 - General RDRP equilibrium between active and dormant species.

There are different RDRP techniques, being the main difference between them the way that the dynamic equilibrium is regulated. Typically, there is an agent (X in Scheme 1) that rapidly exchanges between active and dormant species to afford the controlled growth (with propagation rate constant, k_p) of the polymer chains. This equilibrium is regulated by activation and deactivation rate constants, respectively k_a and k_d [1, 2].

RDRP can be applied to a wide range of monomers with diverse functionalities, offering the possibility to prepare controlled ($1.01 < Đ = M_w/M_n < 1.50$) and complex polymeric structures [1] (Figure 5) for different applications. Moreover, polymers synthesized through RDRP can be easily functionalized with different pendant groups, that could be further modified, allowing the preparation of block copolymers with controlled compositions (Figure 5) [57]. Note that the polymer structures also include homopolymers, which can also have different architectures.

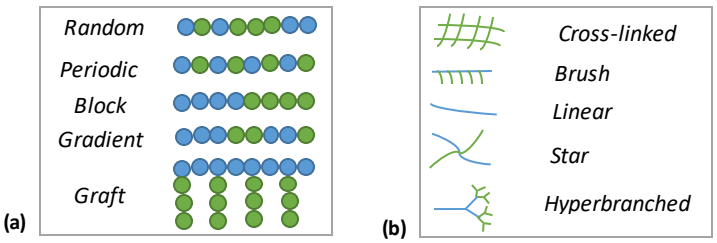

Figure 5 – Examples of different polymer structures that can be produced using RDRP techniques: **(a)** copolymer composition; **(b)** architecture.

One of the most used RDRP techniques for the synthesis of these complex structures is the ATRP [2]. In this work, two variations of ATRP were used: the supplemental activator and reducing agent (SARA ATRP) and the activators regenerated by electron transfer (ARGET ATRP).

1.2.1 Atom transfer radical polymerization

As previously mentioned, ATRP is on the most used RDRPs technique that allows the preparation of polymers with controlled molecular weight, low molar mass dispersity ($Đ = M_w/M_n$), complex architectures and high chain-end functionality [1, 2]. The control of the polymerization is achieved by reversible cycles of activation/deactivation of alkyl halide polymer chains, caused by a metal/ligand catalytic

complex (Scheme 2). A transition metal species (M_t^n) able to increase its oxidation state, a ligand (L) and a halogen counterion able to form a covalent or ionic bond with the metal center are the core of any successful ATRP catalytic system. An alkyl halogen bond (P_n-X) is homolytically cleaved (at a rate constant k_a) by the metal catalyst/ligand complex in the lower oxidation state (M_t^n/L), resulting in a higher oxidation state metal halide complex ($M_t^{n+1}X_m$/L) and a radical ($P_n^\bullet$). The radical $P_n^\bullet$ is then able to propagate (at rate constant k_p), to terminate by either coupling or disproportionating (at rate constant k_t) or to be reversibly deactivated (at rate constant k_d). Even though termination reactions are possible, they are minimized due a shift of the equilibrium towards the dormant species caused by the accumulation of the higher oxidation state metal halide complex, in the beginning of the polymerization (persistent radical effect – PRE) [1, 2].

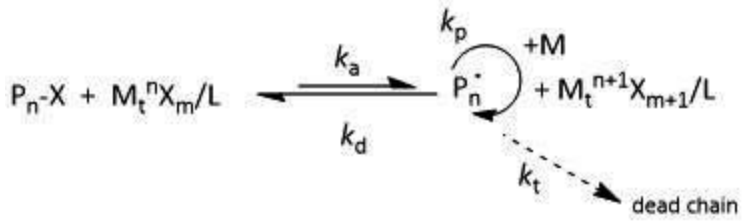

Scheme 2 - General scheme of the ATRP equilibrium.

ATRP has been successfully mediated by a variety of metal catalysts, however complexes of copper with nitrogen-based ligand, for example, are possibly the most efficient catalytic systems for a broad range of monomers. The main advantages of the ATRP technique over other RDRP systems are the commercial availability of the necessary reagents and simplicity of the procedures. [1] Styrenes, (meth)acrylates, (meth)acrylamides and acrylonitrile are typical monomers successfully polymerized using ATRP [2]. Another advantage of these systems is that the absolute amount of metal catalyst can be decreased without affecting the rate of polymerization, but not indefinitely since the equilibrium could be disrupted [1].

In order to minimize the cytotoxicity of the polymer, it is necessary to use systems inherently as non-toxic as possible and have an adequate purification process. Throughout the years, ATRP has been evolving in order to minimize the metal concentration, aiming for “greener” polymerization systems [56]. Minimizing the copper

content, while maintaining a good control over the polymerization, can be achieved by the continuous *in situ* regeneration of the activator complex [58]. Extensive research has been done in order to develop polymerization systems that use low amounts of metal catalyst and that provide mild reaction conditions, while maintaining a precise control over the polymers dispersity. On this matter, different ATRP variations have been proposed: ARGET ATRP [59, 60], SARA ATRP [61, 62], initiators for continuous activator regeneration (ICAR) ATRP [59] and electrochemically mediated ATRP (eATRP) [63, 64]. Recently, a metal-free ATRP system was also reported [65, 66].

ATRP can be carried out either in bulk, in solution or in a heterogeneous system (ex.: emulsion, suspension). The need of a solvent is especially relevant in cases where the polymer is insoluble in its monomer. For a library of monomers ATRP has been carried out in solvents like diphenyl ether [67], dimethyl formamide (DMF) [68] and dimethyl sulfoxide (DMSO) [69]. Studies were even performed comparing the influence of several solvents in the performance of the polymerization system (e.g., pure H_2O, DMF, acetone, THF, EtOH in the ATRP of NIPAAM) [70]. Solvent choice is dependent upon chain transfer to solvent and interactions between the solvent and the catalytic system, that should be minimal. The polarity of the selected solvent must be also considered, since polar solvents tend to provide faster and less controlled polymerizations [2]. A tendency to search for ATRP systems using "greener" solvents has increased, with more frequent reports of aqueous solvent mixtures (or pure aqueous systems [71-73]) or even isomers of known organic solvents, like THF [3, 4, 6, 71]. In this work, the influence of the solvent mixture on the polymerization features was studied trough SARA ATRP of MA using "THF-like" solvents.

The following sections present more detailed information on the polymerization techniques used in this work (SARA and ARGET ATRP) for the preparation of the gene delivery block copolymer.

Supplemental activator and reducing agent ATRP

The mechanism of RDRP in the presence of zero valent metals, namely Cu(0), has been known as SARA ATRP (Scheme 3) and it has been well-described by the Matyaszewki's group [58].

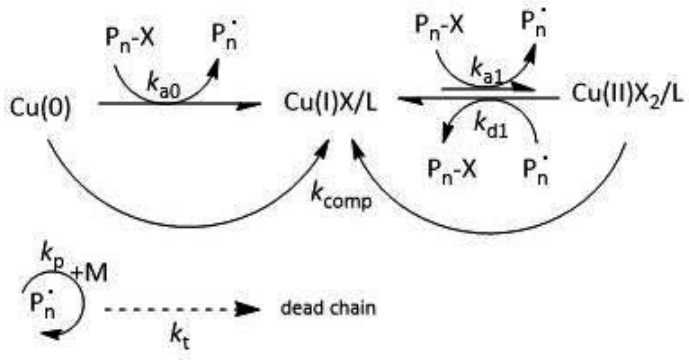

Scheme 3 - General mechanism of the SARA ATRP mediated by Cu(0) and Cu(II)X_2.

In the SARA ATRP mechanism, as it can be seen on Scheme 3, zero-valent metals [62] (e.g., Cu(0) [3], Fe(0) [74]) or inorganic sulfites (e.g. $Na_2S_2O_4$) [75], are used as both reducing agents and supplemental activators. When Cu(0) is used as a SARA agent, there is a *in situ* slow regeneration of the Cu(I)X species by the reduction of Cu(II)X_2, [76]. In addition, the SARA agent is also able to directly activate alkyl halide chains. However, this activation is a contributing reaction (being the main activator the Cu(I)X) as occurs in the normal ATRP process [58]. SARA ATRP has already been used for the polymerization of several monomers in different solvent mixtures, including water [72, 74].

Previous work demonstrated that the SARA ATRP technique, in mild reaction conditions, was able to offer a good control in the polymerization of AMPTMA. The system used as a solvent was either water or ethanol/water mixtures at room temperature (25 °C) with a catalytic system composed of Cu(0) wire, small amounts of $CuCl_2$ and Me_6TREN in excess [3].

Activators regenerated by electron transfer ATRP

The ARGET ATRP could be advantageous over other ATRP systems when considering biomedical applications (or industrialization) since it allows the use of lower amounts of metal catalyst (concentration of catalyst in comparison to the concentration of monomer) to achieve control over the polymerization [59, 71]. In this ATRP variation, a reducing agent (e.g., ascorbic acid, AscA) is used in excess for the continuous (re)generation of the activator species (Cu(I)) (Scheme 4) [1]. Unlike SARA ATRP, in ARGET ATRP the reducing agent does not activate alkyl halides.

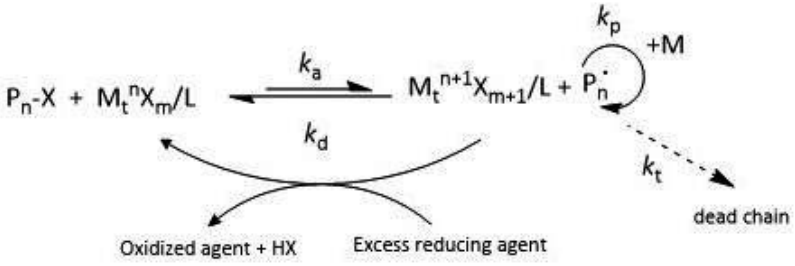

Scheme 4 - General mechanism of the ARGET ATRP.

ARGET ATRP has been successfully implemented in aqueous medium [71], and, as an example, has provided good control over acrylates and styrene polymerization using only 50 ppm and 10 ppm of Cu catalyst [77], respectively, as well as well-defined block copolymers [1]. Recently, a straightforward ARGET ATRP system was described for the polymerization of AMA under mild reaction conditions, using a slow feeding of AscA [4]. The reaction could be done in alcohol/water mixtures or even pure aqueous system, which would be favorable considering biomedical applications. Therefore, this knowledge was used for the preparation of PEG-*b*-PAMA block copolymers, in this work.

CHAPTER 2: CATIONIC COPOLYMERS FOR GENE DELIVERY

2 CATIONIC COPOLYMERS FOR GENE DELIVERY

2.1 ABSTRACT

The aim of this work was to design well-defined cationic copolymers for gene delivery applications via RDRP techniques. PAMPTMA-based copolymers and PAMA--based polymers were prepared by SARA ATRP and ARGET ATRP, respectively, under eco-friendly conditions. The transfection ability of the copolymers was tested using COS-7 cell line. No transfection efficiency was observed for the PAMPTMA-based samples, which could be attributed to an inexistent interaction between the polyplex and the cell, an incapacity for the genetic material to be freed from the polyplex or even a high cytotoxicity of the polymer. Nonetheless, the PEG_{45}-*b*-PAMA samples showed promising results for gene delivery applications. Its transfection efficiencies, especially in the presence of serum, were higher than the gold standard (PEI) for several N/P ratios ($PAMA_{103}$ with serum: 5/1, 10/1, 25/1; PEG_{45}-*b*-$PAMA_{111}$ with serum: 50/1, 75/1, 100/1). From the comparison of the results between a PEGylated PAMA-based sample and a PAMA homopolymer, it was also possible to observe the advantage of incorporating PEG in the structure of a non-viral gene delivery vector.

2.2 INTRODUCTION

Designing an efficient gene delivery vector with low toxicity and high transfection efficiency is a puzzling task. A non-viral synthetic gene delivery vector has to have well-controlled properties and be as non-toxic, as biocompatible, as stable and as robust as possible [8]. Recent progress in RDRP techniques have provided essential tools for the synthesis of new polymeric gene vectors with tailor-made compositions, architectures and functionalities [78].

Several cationic monomers have already been used for gene delivery applications [78]. Likewise, different stimuli responsive monomers have been used in copolymers as non-viral gene delivery vectors [14, 18, 32]. Moreover, high levels of positive charge at the surface of a polyplex have been known to lead to non-specific interactions with several biological components (e.g., plasma proteins, fibrinogen, erythrocytes).

Therefore, a polymeric non-viral vector that is able to bind to DNA without requiring a high level of polycation could be advantageous. In order to stabilize the polyplex, macromolecules like PEG, transferrin and poly(*N*-[2--hydroxypropyl]methacrylamide) have been used [32]. The incorporation of hydrophobic chains have also been proven to increase transfection efficiency of cationic gene delivery vectors [79].

In this work, novel cationic copolymers PEG_{45}-*b*-PAMPTMA, PAMPTMA-*co*-PDPA, PAMPTMA-*co*-PNIPAAM and PAMPTMA-*co*-PMA were synthesized via SARA ATRP, as well as PEG_{45}-*b*-PAMA via ARGET ATRP.

2.3 EXPERIMENTAL

2.3.1 Materials

2,2'-Azobis(2-methylpropionitrile) (AIBN, 98%, Aldrich), AMA (≥ 95%, Polysciences), AMPTMA (solution 75 wt. % in H_2O, Aldrich), AscA (Sigma-Aldrich), copper(II) bromide (99.999%, Aldrich), copper (II) chloride (97%, Aldrich), D_2O (99.9%, Cambridge Isotope Laboratories), ethyl α-bromoisobutyrate (EBiB, 98%, Sigma Aldrich), ethyl α-bromophenyl acetate (EBPA, Alfa Aesar), ethyl 2-chloropropionate (ECP, 97%, Aldrich), EtOH (Panreac, 99.5%), isopropanol (Fisher Scientific), methanol (MeOH, Fisher Scientific), and water (HPLC grade, Fisher Scientific) were used as received.

MA (Acros, 99% stabilized), was passed through a sand/alumina (basic, Fisher Scientific), column before use in order to remove the radical inhibitor.

DPA (Aldrich, 97% stabilized), was passed over a sand/alumina column before use in order to remove the hydroquinone inhibitors.

Purified water (Milli-Q®, Millipore, resistivity >18 MΩ.cm) was obtained by reverse osmosis.

Metallic copper (Cu(0), *d* = 1 mm, Alfa Aesar) was washed with HCl in MeOH and subsequently rinsed with MeOH and dried under a stream of nitrogen following the literature procedures [80].

Me_6TREN [81] and TPMA [82] were synthesized as reported in the literature and their structures were confirmed by ^{1}H NMR (Appendix A, Figure A 3 and Figure A 4).

PEG-Br and Br-PEG-Br were synthesized and their structures confirmed by ^{1}H NMR (Appendix A, Figure A 1 and Figure A 2).

NIPAAM was recrystallized from hexane.

2.3.2 Techniques

Polymers number-average molecular weights (M_n^{SEC}) and dispersity ($Đ = M_w/M_n$) were determined by using a size exclusion chromatography (SEC) system equipped with an online degasser, a refractive index (RI) detector and a set of columns: Shodex OHpak SB-G guard column, OHpak SB-804HQ and OHpak SB-802.5HQ columns. The polymers were eluted at a flow rate of 0.5 mL/min with 0.1 M Na2SO4 (aq)/1 wt% acetic acid/0.02% NaN_3 at 40 °C. Before the injection, the samples were filtered through a polytetrafluoroethylene (PTFE) membrane with 0.45 µm pore. The system was calibrated with five narrow poly(ethylene glycol) standards and the polymers M_n^{SEC} and $Đ$ were determined by conventional calibration using the Clarity software version 2.8.2.648.400 MHz 1H NMR spectra of reaction mixture samples were recorded on a Bruker Avance III 400 MHz spectrometer, with a 5-mm TIX triple resonance detection probe, in D_2O. Conversion of monomers was determined by integration of monomer NMR signals obtained before and after the reaction as occurred using the MestRenova software version: 10.0.1-14719.

Fourier transform infrared attenuated total reflection (FTIR-ATR) spectroscopy was performed using a Jasco, model 4000 UK spectrometer. The samples were analyzed with 120 scans and 4 cm^{-1} resolution, between 600 and 4000 cm^{-1}.

Atomic absorption spectroscopy (AAS) was performed on a Perkin Elmer (Model 3300, USA) to evaluate the content of residual copper catalyst in the purified polymers.

All gene delivery essays were performed by Daniela Santo in *Center for Neuroscience and Cell Biology* (CNC). Procedures used to obtain the main results can be found in Appendix D.

2.3.3 Procedures

Procedure for the synthesis of PEG_{45}-Br macroinitiator

DMAP (1.83 g, 15.0 mmol, recrystallized in toluene) was dissolved in DCM (10 mL, distilled from CaH_2) in a vial. Upon dissolution, TEA (1.04 g, 10.0 mmol) was added to the vial. The reaction mixture was transferred to a 250 mL three-neck round-bottom flask equipped with a condenser dropping funnel, gas inlet/outlet and a magnetic stirrer bar. The mixture was cooled to 0 °C and BBiB (5.75 g, 25.0 mmol), dissolved in DCM (10 mL), was added, followed by a dropwise addition of a solution of PEO (20.0 g, 10.0 mmol, dried by azeotropic distillation) and DCM (50 mL) to the reaction mixture during 1h under N_2. The temperature was increased to room temperature and the reaction was allowed to proceed with stirring (600 rpm) for 18h. The filtered solution was concentrated under reduced pressure, precipitated in cold diethyl ether and dried under vacuum. The dried mixture was dissolved in absolute ethanol, stored overnight to recrystallize and the product was filtered, washed with cold diethyl ether and dried in vacuum.

The PEG_{45}-Br obtained was analyzed by aqueous SEC and ^1H RMN spectroscopy to evaluate the success of the functionalization (Appendix A, Figure A 1).

Procedure for the synthesis of Br-PEG_{3000}-Br macroinitiator

Previously freeze-dried OH-PEG_{3000}-OH (25 g, 8.3 mmol) and DCM (300 mL, distilled from CaH_2) were added to a three-neck round-bottom flask equipped with a magnetic stirrer bar. Upon dissolution, TEA (3.5 g, 33.3 mmol) was added to the flask and the reaction mixture was cooled to 0 °C and purged with nitrogen. BBiB (19.2 g, 83.3 mmol) was added dropwise to the reaction mixture during 1h. The temperature was increased to room temperature and the reaction was allowed to proceed with stirring (600 rpm) overnight. The filtered solution was concentrated under reduced pressure, precipitated in cold diethyl ether and dried under vacuum. The dried mixture was dissolved in water (pH 8-9) and extracted with DCM. The organic layer was collected and dried overnight over $MgSO_4$. The solution was filtered and the DCM was removed under

reduced pressure. The Br-PEG-Br was recovered by precipitation in cold diethyl ether and dried under vacuum.

The Br-PEG-Br obtained was analyzed by aqueous SEC and ^{1}H RMN spectroscopy to evaluate the success of the functionalization (Appendix A, Figure A 2).

Typical procedure for the synthesis of PEG_{45}-*b*-$PAMPTMA_{47}$ by SARA ATRP

PEG_{45}-Br (181.2 mg, 91 µmol) and water (2.2 mL) were added to a 10 mL round bottom Schlenk flask equipped with a magnetic stirrer bar. Upon dissolution, $CuCl_2$ (6.1 mg, 45 µmol), Me_6TREN (24.2 µL, 91 µmol) and AMPTMA (0.9 mL, 3.6 mmol) were added to the flask, followed by a Cu(0) wire (*l* = 10 cm; *d* = 1 mm). The Schlenk flask was then sealed with a glass stopper, deoxygenated with freeze-vacuum-thaw cycles and purged with nitrogen. The reaction was allowed to proceed under stirring (600 rpm) at room temperature (25 °C). Samples were collected after 50 min and analyzed by aqueous SEC to determine the molecular weights and dispersity, and by ^{1}H NMR spectroscopy to determine the monomer conversion. The reaction mixture was dialyzed (cut-off 3500) against deionized water for a minimum of 3 days. The pure copolymer was recovered by freeze-drying and the content of residual copper was determined by atomic absorption.

Kinetic studies were conducted using the same typical procedure, but samples were collected throughout the reaction, at predetermined reaction times.

Typical procedure for the SARA ATRP of AMPTMA

AMPTMA (2.0 mL, 7.26 mmol), a solution of $CuCl_2$ (2.9 mg, 22 µmol) and Me_6TREN (10 mg, 44 µmol) in water (2.4 mL) and a solution of ECP (9.9 mg, 73 µ µmol) in EtOH (2.0 mL) were added to a 10 mL Schlenk flask equipped with a magnetic stirrer bar. A Cu(0) wire (*l* = 10 cm; *d* = 1 mm) was added to the Schlenk flask, which was sealed with a glass stopper, deoxygenated with three freeze-vacuum-thaw cycles and purged with nitrogen. The reaction was allowed to proceed with stirring (ca. 700 rpm) at room temperature (25 °C). The reaction mixture samples collected were analyzed by ^{1}H NMR spectroscopy in order to determine the monomer conversion, and by aqueous SEC to determine the molecular weights and dispersity of the polymers. The final reaction

mixture was dialyzed (cut-off 3500) against deionized water. The pure copolymer was recovered by freeze-drying.

Typical procedure for the synthesis of PAMPTMA-*co*-PNIPAAM by SARA ATRP

ECP (6.8 µL, 53 µmol), water (1.3 mL) and EtOH (1.3 mL) were added to a 10 mL round bottom Schlenk flask equipped with a magnetic stirrer bar. Upon dissolution, $CuCl_2$ (3.6 mg, 27 µmol), Me_6TREN (14.2 µL, 53 µmol), AMPTMA (146 mg, 530 µmol) and NIPAAM (600 mg, 5.3mmol) were added to the flask, followed by a Cu(0) wire (*l* = 10 cm; *d* = 1 mm). The Schlenk flask was then sealed with a glass stopper, deoxygenated by freeze-vacuum-thaw cycles and purged with nitrogen. The reaction was carried out under stirring (600 rpm) at room temperature (25 °C). A sample was collected after 18h and analyzed by aqueous SEC to evaluate the molecular weights and dispersity, and by ^{1}H NMR spectroscopy to determine the monomer conversion. The reaction mixture was then dialyzed (cut-off 3500) against deionized water for a minimum of 3 days. The pure copolymer was recovered by freeze-drying. The copolymers were analyzed by ^{1}H NMR spectroscopy to determine degree of polymerization and molecular weight. The content of residual copper was determined by atomic absorption.

Similar procedures were followed for the synthesis of PAMPTMA-*co*-PDPA and PAMPTMA-*co*-PMA by SARA ATRP (Appendix A).

Typical procedure for the ARGET ATRP of AMA

AMA (0.5 g, 2.9 mmol), $CuBr_2$ (3.2 mg, 14 µmol), TPMA (16.6 mg, 57 µmol) and EBPA (7 mg, 29 µmol) were dissolved in water (1.43 mL). The mixture was added to a 10 mL round bottom Schlenck flask, equipped with a magnetic stirrer bar, and purged with nitrogen for 20 min. The flask was placed in a water bath at 35 °C and a deoxygenated AscA solution (43 mM) was continuously injected into the reaction medium using a syringe pump (KDS Scientific, Legato 101) at the rate of 1 µL/min. The reaction was stopped after 5.5 h and a sample was collected for ^{1}H NMR spectroscopy in order to determine the monomer conversion, and for aqueous SEC to determine the molecular weight and dispersity of the polymer. The final reaction mixture was dialyzed (cut-off 3500) against deionized water and the polymer was obtained after freeze-drying. A

sample of the pure polymer was then analyzed by ^{1}H NMR spectroscopy in order to determine polymer degree of polymerization, and by aqueous SEC to determine molecular weight and dispersity. The content of residual copper was determined by atomic absorption.

Typical procedure for the FRP of AMA

AMA (0.5 g, 2.9 mmol) was dissolved in water (1 mL) and IPA (0.4 mL). The mixture was added to a 10 mL round bottom flask, equipped with a magnetic stirrer bar, and purged with nitrogen for 20 min. AIBN (47.1 mg, 29 µmol) was added to the flask and the mixture was purged with nitrogen for another 5 min. The flask was placed in an oil bath at 60 °C and allowed to react overnight. The reaction mixture was analyzed by ^{1}H NMR spectroscopy in order to determine the monomer conversion, and by aqueous SEC to determine the molecular weight and dispersity of the polymer. The final reaction mixture was dialyzed (cut-off 3500) against deionized water and ethanol and the polymer was recovered by freeze-drying. A sample of the pure polymer was analyzed by ^{1}H NMR spectroscopy in order to determine the polymer degree of polymerization, and by aqueous SEC to determine the molecular weight and dispersity.

Typical procedure for the synthesis of PEG_{45}-*b*-$PAMA_{163}$ by ARGET ATRP

AMA (0.5 g, 2.9 mmol), $CuBr_2$ (2.1 mg, 10 µmol), TPMA (11.1 mg, 38 µmol) and PEG_{45}-Br (38.2 mg, 19 µmol) were dissolved in water (1.43 ml). The mixture was added to a 10 mL round bottom Schlenck flask, equipped with a magnetic stirrer bar, and purged with nitrogen for 20 min. The flask was placed in a water bath at 35 °C and a deoxygenated AscA solution (43 mM) was continuously injected into the reaction medium using a syringe pump (KDS Scientific, Legato 101) at the rate of 1 µL/min. The reaction was stopped after 5.5 h, and a sample was collected for ^{1}H NMR spectroscopy in order to determine the monomer conversion, and for aqueous SEC to determine the molecular weight and dispersity of the copolymer. The final reaction mixture was dialyzed (cut-off 3500) against deionized water and the copolymer was recovered by

freeze-drying. The content of residual copper was determined by atomic absorption. The chemical structure of the pure copolymer was confirmed by ^{1}H NMR spectroscopy.

Acid-base titration of PAMA-based samples

A 10 mg of polymer sample was dissolved using a magnetic stir bar in 10 mL of deionized water. The temperature was adjusted to either 25 °C or 37 °C using a water bath. The pH of the solution was adjusted to 2.6 using a 1% HCl solution (pH = 1). Then followed a stepwise addition of a 0.1M NaOH solution (pH = 12.8), 10 µL per addition, until a pH = 11 was reached. The pH was recorded to obtain a titration profile.

2.4 RESULTS AND DISCUSSION

2.4.1 PEG_{45}-*b*-PAMPTMA and PAMPTMA-*b*-PEG_{72}-*b*-PAMPTMA block copolymers

AMPTMA is a cationic hydrophilic monomer that has been used in combination with NIPAAM [43, 46, 47], having shown potential to be used as drug delivery systems [48], as microcarriers for cell proliferation [49] and as gene delivery vectors for the delivery os siRNA [43], showing promising results. In this work, new PEG_{45}-*b*-$PAMPTMA_n$ and $PAMPTMA_n$-*b*-PEG_{72}-*b*-$PAMPTMA_n$ block copolymers with different molecular weights were synthesized by SARA ATRP in aqueous medium at room temperature (Figure 6). The aim was to study the influence of the length of the cationic segment and the presence of PEG on the biological activity of the block copolymers. Bromine-terminated PEG (M_n^{NMR} = 2000; PEG_{45}-Br) was used as the macroinitiator (first block of the copolymer) for the SARA ATRP of AMPTMA.

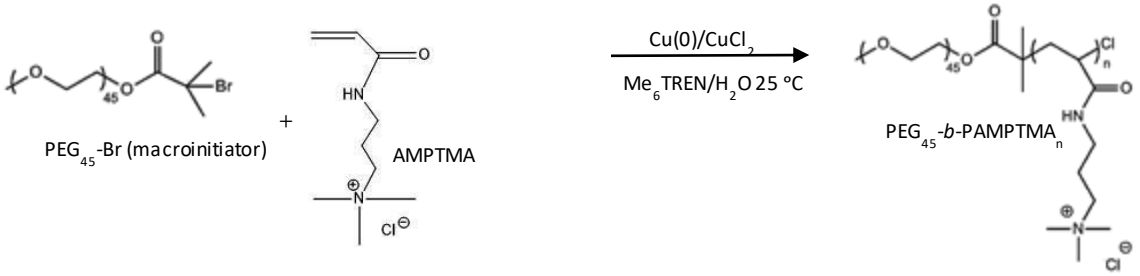

Figure 2 - Typical synthesis of PEG_{45}-*b*-$PAMPTMA_n$ via SARA ATRP.

Firstly, in order to understand the evolution of the molecular weight during the polymerization, kinetic studies were performed. Figure 7 shows the kinetic plots obtained for a typical chain extension of PEG_{45}-Br with AMPTMA.

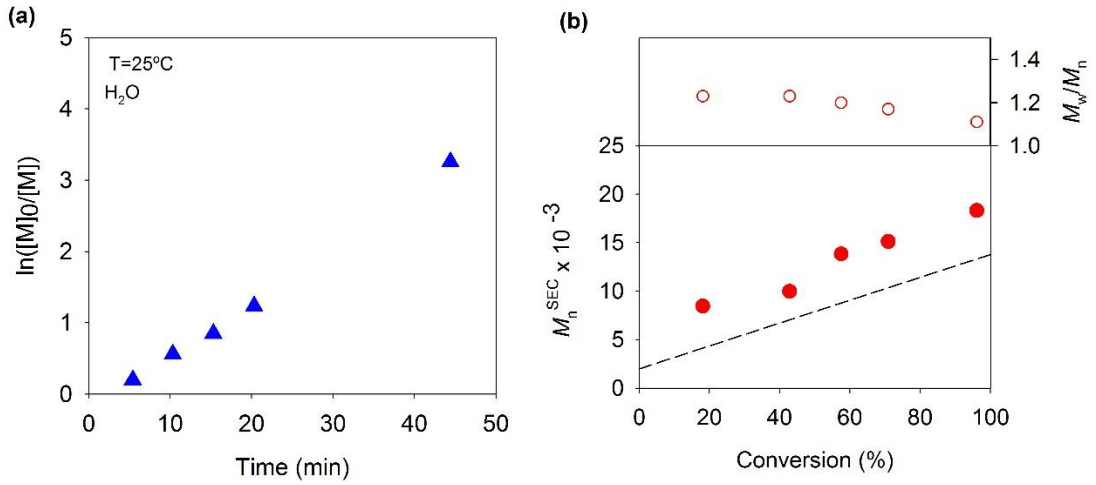

Figure 7 - **(a)** Kinetic plot of $\ln[M]_0/[M]$ *vs*. time (min) and **(b)** plot of number-average molecular weight (M_n^{SEC}) and Đ (M_w/M_n) *vs*. monomer conversion (the dashed line represents theoretical molecular weight at a given conversion) for the SARA ATRP of AMPTMA initiated by PEG_{45}-Br in water at 25°C. Reaction conditions: $[AMPTMA]_0/[PEG_{45}\text{-}Br]_0/[CuCl_2]_0/[Me_6TREN]_0$/Cu(0) wire = 57/1/0.5/1/Cu(0) wire: *l* = 10 cm; *d* = 1 mm; $V_{solvent}$ = 3.2 mL.

High monomer conversion was reached after 30 minutes (Figure 7 (a)). In addition, the experimental number-average molecular weights were in good agreement with the predicted values and the polymer presented low dispersity ($Đ \approx 1.2$) throughout the reaction. These results indicate that the SARA ATRP allowed a good control over the molecular weight of the block copolymers.

After the kinetic studies, different polymerizations were conducted, targeting different DP values of the AMPTMA segment. The reaction mixtures were purified by dialysis against water to remove traces of copper catalyst and the pure polymers were recovered by freeze-drying. Figure 8 presents a typical ^{1}H NMR spectrum of a PEG_{45}-*b*-$PAMPTMA_{47}$ block copolymer, which confirms the success of the reaction. The determination of the DP of the copolymer was possible due to the integration of a macroinitiator peak and a polymer peak in the ^{1}H NMR spectrum of the pure sample (in blue, Figure 8). The same procedure was used for all the block copolymers synthesized.

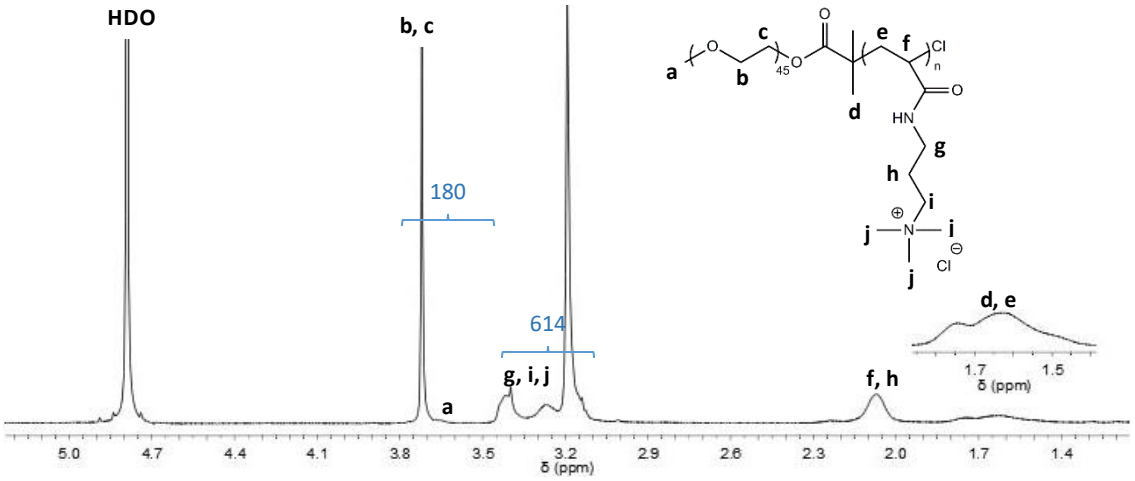

Figure 8 - 400 MHz ^{1}H NMR spectrum, in D_2O, of a pure PEG_{45}-*b*-$PAMPTMA_{47}$ sample (M_n^{SEC} = 15.9 x10^3; Đ = 1.10) obtained by SARA ATRP. Reaction conditions: $[AMPTMA]_0/[PEG_{45}\text{-}Br]_0/[CuCl_2]_0/[Me_6TREN]_0$/Cu(0) wire = 40/1/0.5/1/Cu(0) wire: l = 10 cm; d = 1 mm; $V_{solvent}$ = 3.2 mL

Table 1 presents different PEG_{45}-*b*-$PAMPTMA_n$ block copolymers synthesized, showing the success of the purification process, as judged by the very low concentration of copper present in the pure copolymers (given that, for example, for GD01 the initial amount of $CuCl_2$ is 12500 ppm, in respect to the monomer). This is a critical factor considering biomedical applications, due to the known toxicity of copper that could potentially reduce cell viability. Other PEG_{45}-*b*-$PAMPTMA_n$ samples were synthesized that were not tested in gene delivery assays due to either their general properties (Appendix B, Table B1) not being considered relevant in comparison to the ones presented in Table 1, or the synthesis not being successful.

Table 1 - General properties of the PEG_{45}-*b*-$PAMPTMA_n$ block copolymers.

Sample code	$DP_{PAMPTMA}$* (n)	M_n^{NMR} x 10^{-3}	M_n^{SEC} x 10^{-3}	Đ	[Cu] (ppm)	% charge (molar) **
GD01	47	11.8	15.9	1.10	9.7	51.1
GD02	31	8.3	12.6	1.11	8.0	40.8
GD03	15	5.0	9.6	1.10	9.5	25.0
GD18	54	13.1	19.6	1.10	7.6	54.5
GD20	100	22.6	27.3	1.10	10.5	69.0

* determined by ^{1}H NMR

** % charge (molar) = n / (n+45) x100

Aiming to study the influence of the PEG segment position in the copolymer chain, two PAMPTMA$_n$-*b*-PEG$_{72}$-*b*-PAMPTMA$_n$ block copolymers were synthesized in this work (Table 2).

Table 2 - General properties at 40 minutes of PAMPTMA$_n$-*b*-PEG$_{72}$-*b*-PAMPTMA$_n$ SARA ATRP reaction time.

Sample	Molar ratio	Monomer conversion (%)	M_n^{th}x10^{-3}
GD21	100:1	90	21.7
GD22	50:1	20	5.0

In gene delivery testing a control is needed for a correct understanding of the cellular response. The control samples used were a PAMPTMA$_{30}$ homopolymer (M_n^{th} = 6.0 x 10^3; [Cu] = 78.4 ppm) and the PEG-Br$_{45}$ (M_n^{RMN} = 2.0 x 10^3), which represent both polymeric segments present on the block copolymer. In the assays using COS-7 cells there was no transfection neither for the control samples, nor for the samples in Table 1. However, the results from the assays were not conclusive since there was high cell viability and all cationic block copolymers were able to form polyplexes. Presumably: (a) the polyplex was not able to enter in the cell and no interaction occurred; (b) deficient release of the gene cargo from the polyplex; (c) the polymer could be cytotoxic. From this, it could be potentially interesting to study whether the introduction of a more hydrophobic block to counteract the positive charges of the PAMPTMA block could improve the behavior of the PAMPTMA-based samples in gene delivery assays.

Due to the negative transfection results obtained for the PEG$_{45}$-*b*-PAMPTMA$_n$ samples the PAMPTMA$_n$-*b*-PEG$_{72}$-*b*-PAMPTMA$_n$ block copolymers were excluded from further testing.

2.4.2 PAMPTMA-based random copolymers

Aiming to test whether a more hydrophobic block was needed to counteract the positive charges of the PAMPTMA block, alternative PAMPTMA-based random copolymers were prepared using the same SARA ATRP system. The hydrophobic monomers used were NIPAAM, DPA and MA to prepare the following copolymers: PAMPTMA-*co*-PNIPAAM, PAMPTMA-*co*-PDPA and PAMPTMA-*co*-PMA.

Based on a previous report showing the success of PAMPTMA-*b*-PNIPAAM block copolymers for the *in vitro* transfection in HeLa cells [18], a different system was designed using the same monomers. The random copolymer was synthesized using SARA ATRP by starting the polymerization with both monomers present on the reaction mixture (Figure 9). NIPAAM is a well-known temperature-responsive polymer. It is water-solube at temperatures below its lower critical solution temperature (LCST), which is around 32 °C. Above its LCST, PNIPAAM colapses [46]. Hence, upon preparation of the polyplexes (r.t. - room temperature) the copolymer prepared should be soluble in the water solution, allowing the contact between the cationic segments and the DNA plasmid. After the polyplex formation, the copolymer should colapse when in contact with the cells at 37 °C, releasing the DNA plasmid from the copolymer.

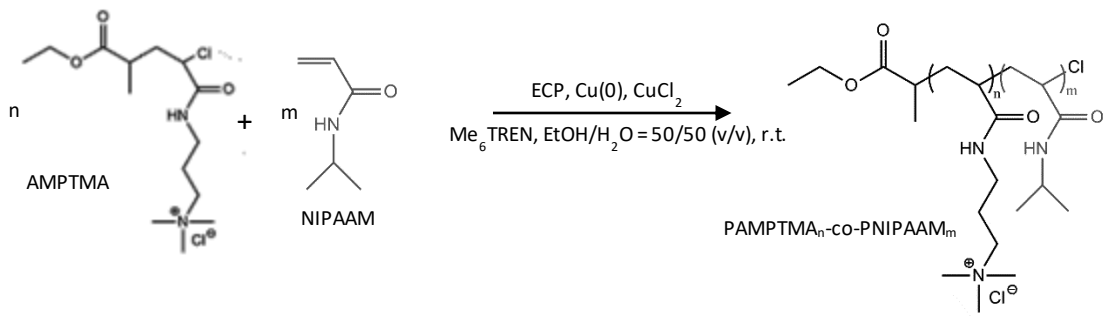

Figure 9 - Typical synthesis of $PAMPTMA_n$-*co*-$PNIPAAM_m$ by SARA ATRP.

PDPA is a well-known pH-responsive polymer with a pK_a around 6.2, that was also introduced in one copolymer aiming to provide a hydrophobic component in the non-viral PAMPTMA-based vector (Figure 10). PDPA has been studied as a co-monomer for the synthesis of folic acid-functionalized block copolymers by ATRP for gene delivery applications, showing good potential [41].

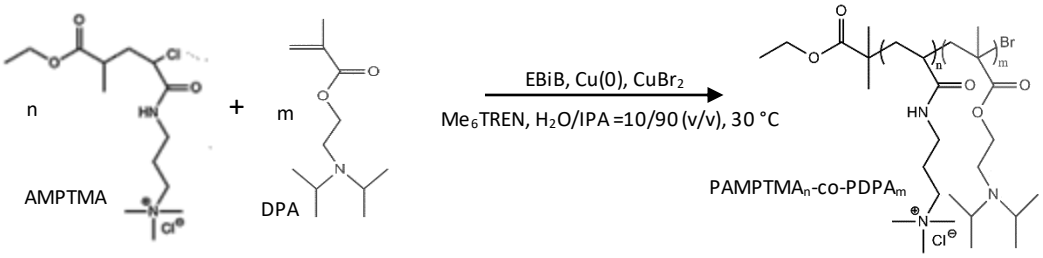

Figure 3 - Typical Synthesis of $PAMPTMA_n$-*co*-$PDPA_m$ by SARA ATRP.

PMA is a hydrophobic polymer often used as model compound for the development of ATRP systems. Recently a SARA ATRP method was developed for the preparation of star-shaped PMA-*b*-PAMPTMA in ethanol/water mixtures [83], for biomedical applications. Using that knowledge, and despite the very different nature of both PAMPTMA and PMA, in this work a linear random PAMPTMA-*co*-PMA copolymer was prepared (Figure 11).

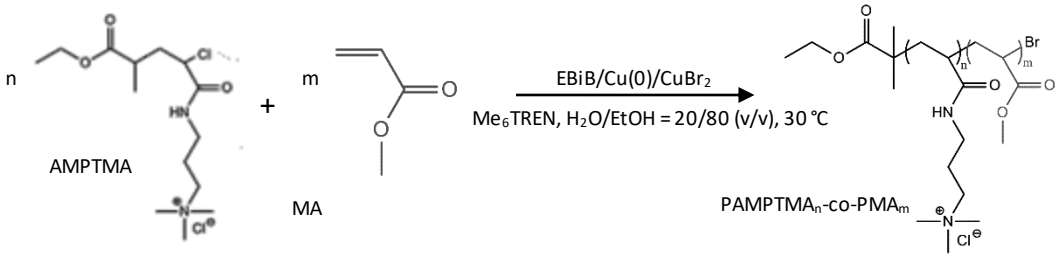

Figure 4 - Typical synthesis of $PAMPTMA_n$-*co*-PMA_m by SARA ATRP.

The general properties of the PAMPTMA-based random copolymers synthesized are summarized in Table 3.

Table 3 - Summary of $PAMPTMA_m$-*co*-$PNIPAAM_n$ (GD24), $PAMPTMA_m$-*co*-$PDPA_n$ (GD25) and $PAMPTMA_m$-*co*-PMA_n (GD26) general properties.

Sample	$DP_{PAMPTMA}$ (n)	$DP_{2nd\ monomer}$ (m)	M_n^{th} x 10^{-3}	M_n^{SEC} x 10^{-3}	Đ	% charge * (molar)	[Cu] (ppm)
$PAMPTMA_m$-*co*-$PNIPAAM_n$	11	101	1.9	--	--	6	57.4
$PAMPTMA_m$-*co*-$PDPA_n$	--	--	--	28.9	1.19	6	1.6
$PAMPTMA_m$-*co*-PMA_n	7	60	6.7	--	--	11	35.1

*% charge = (n / (n + m)) x 100

Several difficulties were faced during the characterization of the $PAMPTMA_{11}$-*co*-$PNIPAAM_{101}$. Firstly, it was not possible to determine the DP of both segments by NMR through the pure copolymer spectrum, since there were no isolated signals of the initiator (ECP) (Figure 12). The DP value was then determined from the monomer conversion. Despite being soluble in water, it was also not possible to fully characterize the pure sample in terms of molecular weight and dispersity, since it did not properly

elute in the SEC (aqueous). Several authors have also reported the same limitation when analyzing PAMPTMA-*b*-PNIPAAM by SEC using different eluents [3, 84].

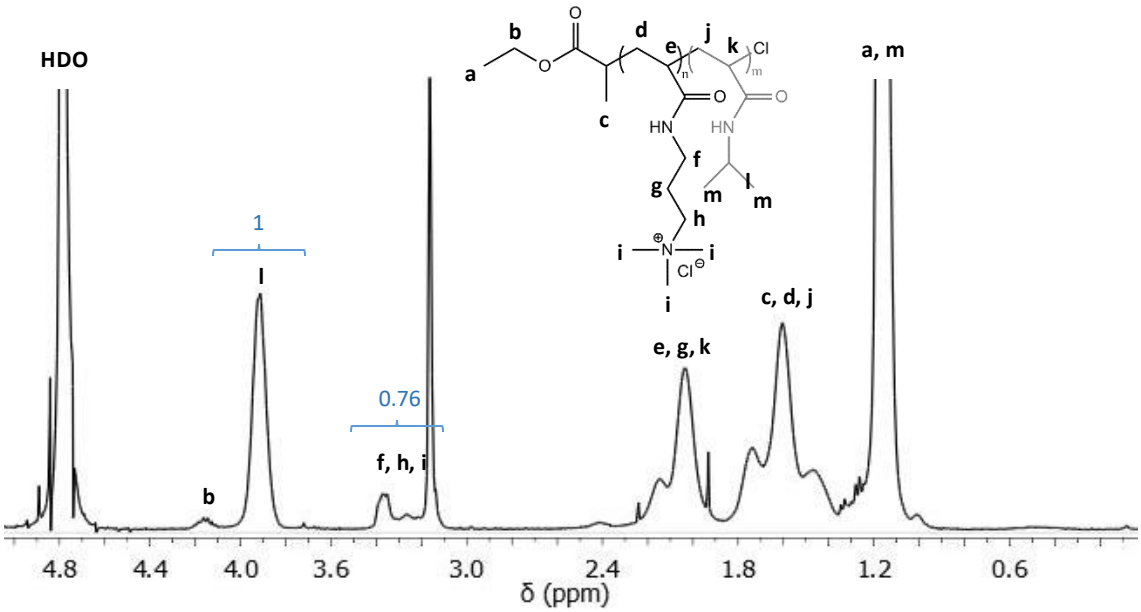

Figure 5 - 400 MHz ^{1}H NMR spectrum, in D_2O, of a pure PAMPTMA$_{11}$-*co*-PNIPAAM$_{101}$ sample (M_n^{th} = 1.9 x 10^3) obtained by SARA ATRP. Reaction conditions: [AMPTMA]$_0$/[NIPAAM]$_0$/[ECP]$_0$/[$CuCl_2$]$_0$/[Me_6TREN]$_0$/Cu(0) wire = 10/100/1/0.5/1/Cu(0) wire: *l* = 10 cm; *d* = 1 mm; $V_{solvent}$ = 3.2 mL

Another difficulty was that the percentage of cationic charge determined by the ratio of the DP of both AMPTMA and NIPAAM (DP determined by the monomer conversion; 10% cationic charge) did not match the one determined directly by the integration of the NMR signals (6% cationic charge) of both polymeric segments in the pure copolymer. It was considered as the most correct cationic charge the one determined using the ratio of the integral of the polymer peaks in the ^{1}H NMR spectrum of the pure polymer (Figure 12) since the it allows the correct identification of the signals.

The characterization of the PAMPTMA$_n$-*co*-PDPA$_m$ copolymer presented some difficulties as well, mainly due to the different solubility of both segments (PAMPTMA and PDPA). Firstly, since PDPA is not soluble in pure water, the determination of the monomer conversion was not possible, as there were no monomer peaks in the ^{1}H NMR spectrum in D_2O. The AMPTMA monomer conversion was also impossible to determine, since there were no isolated PAMPTMA peaks. However, after the purification of the

copolymer, the addition of diluted HCl to the D_2O was tested for the NMR analysis, since PDPA is soluble in water at low pH (≈ 3). Figure 13 shows the NMR spectrum of the random copolymer, whose charge density was estimated to be 6%, based on the ratio of the signals **n** and **f, h, i, m.**

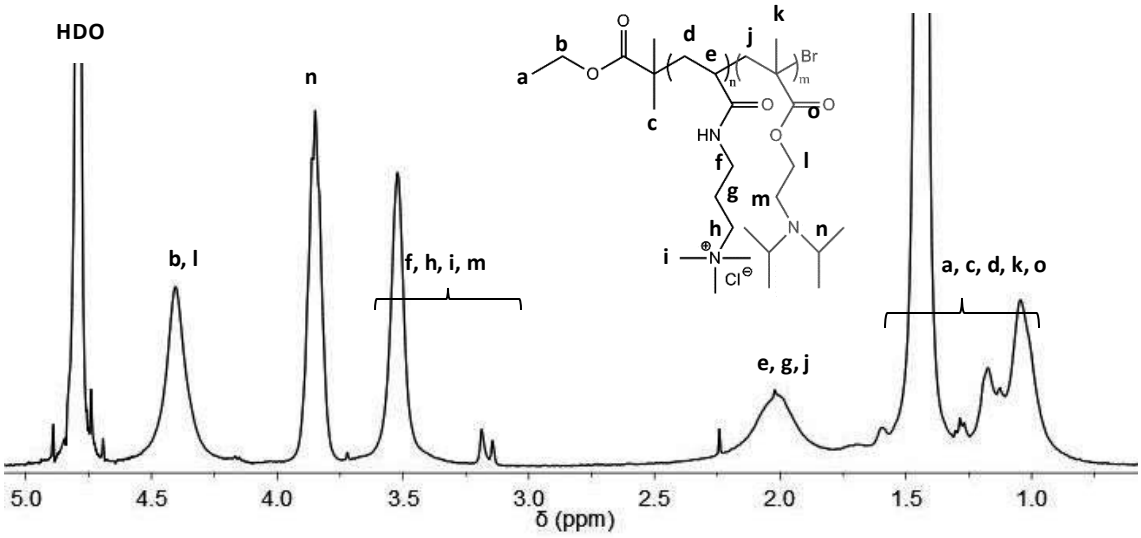

Figure 13 - 400 MHz ^{1}H NMR spectrum, in D_2O, of a pure PAMPTMA$_n$-*co*-PDPA$_m$ sample (M_n^{SEC} = 28.9 x 10^3, $Đ$ = 1.19) obtained by SARA ATRP. Reaction conditions: [AMPTMA]$_0$/[DPA]$_0$/[EBiB]$_0$/[$CuBr_2$]$_0$/[Me6TREN]$_0$/Cu(0) wire = 10/100/1/0.5/1/Cu(0) wire: *l* = 10 cm; *d* = 1 mm; H_2O/IPA = 10/90 (v/v) with DPA/solvent = 1.

The characterization of PAMPTMA$_7$-*co*-PMA$_{60}$ was also problematic. Taking into account that the preparation of the copolymer was done in a EtOH/H_2O = 80/20 (v/v) mixture, an attempt to prepare a similar NMR solvent was made, using D_2O and EtOD. Aiming for a better spectrum, another sample of the copolymer was analyzed by 1H NMR spectroscopy using a EtOH/D_2O = 80/20 (v/v) solvent mixture (Figure 14).

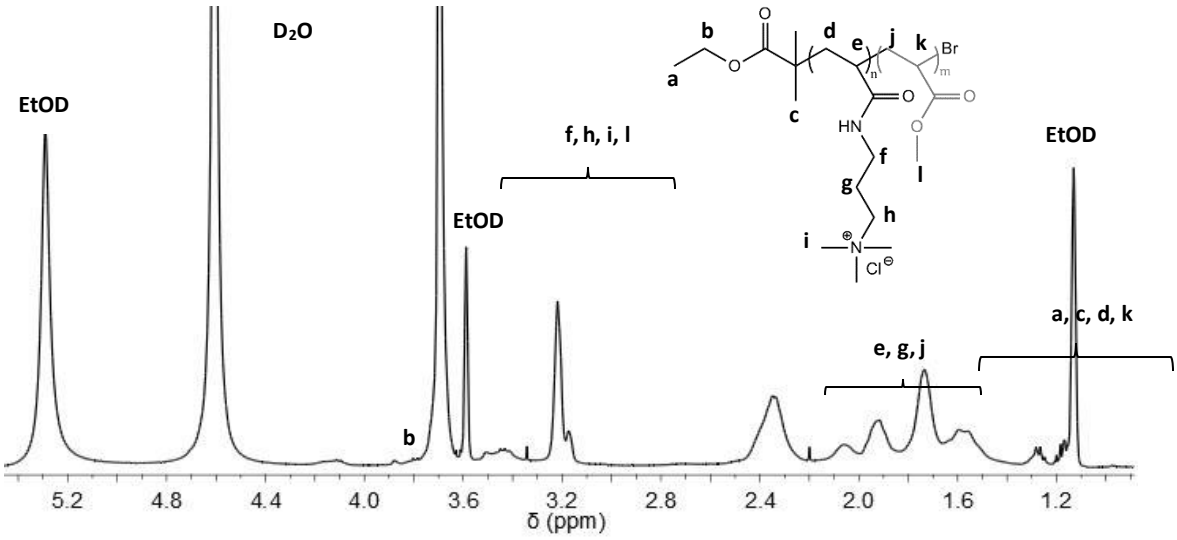

Figure 14 - 400 MHz ^{1}H NMR spectrum in 80/20 EtOD/D_2O of a pure PAMPTMA$_n$-*co*-PMA$_m$ sample (M_n^{th} = 6.7 x 10^3) obtained by SARA ATRP. Reaction conditions: $[AMPTMA]_0/[MA]_0/[EBiB]_0/[CuBr_2]_0/[Me6TREN]_0$/Cu(0) wire = 10/100/1/0.5/1/Cu(0) wire: *l* = 10 cm; *d* = 1 mm; H_2O/EtOH = 20/80 (v/v) with MA/solvent = 0.5

From the NMR of the reaction mixture, despite the poor solubility of PMA in water, it was possible to calculate both monomer conversions. From this data, as done for in PAMPTMA-*co*-PNIPAAM, it was possible to estimate DP of each monomer, the percentage of charge (% charge) and to calculate the theoretical molecular weight.

A FTIR of the PAMPTMA-*co*-PMA sample (Figure 15) showed that the copolymer had, indeed, both PAMPTMA and PMA segments.

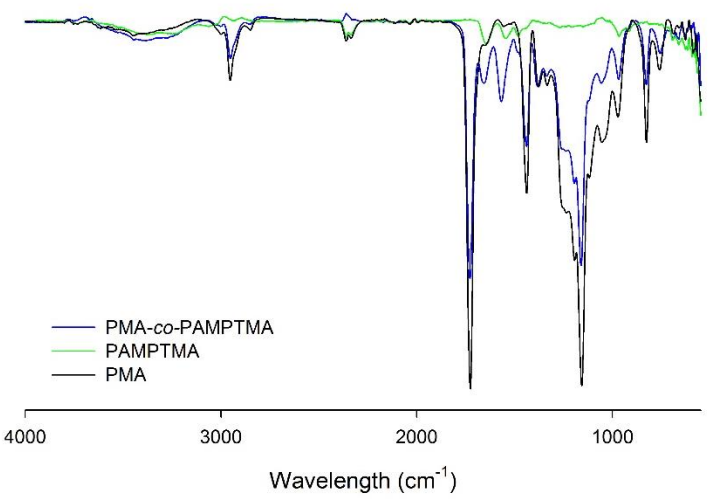

Figure 15 – FTIR spectra of PAMPTMA-*co*-PMA, PAMPTMA and PMA.

Despite the fact that DPA and NIPAAM have potentially interesting properties and were already used for gene delivery applications, all PAMPTMA-base random copolymer samples tested negatively for transfection in gene delivery assays. It is important to notice that the PAMPTMA-*b*-NIPAAM was reported [43] as a block copolymer and not a random copolymer (like the one synthesized in this work) for the siRNA release and not a DNA plasmid, as tested in this work. Also, the cell-line used was different (HT1080 instead of COS-7), which could radically change the results. Due to the poor performance of the PAMPTMA-based copolymers for the targeted application, new cationic copolymers were designed based on AMA.

2.4.3 PEG_{45}-*b*-$PAMA_n$ block copolymers

AMA is a pH-responsive monomer with a pK_a of 8.8 [50]. Due to the presence of primary amino groups, PAMA has a cationic behavior at physiological pH, being able to bind to negatively charged nucleic acids [51]. PAMA homopolymers synthesized via ARTP have been used as potential DNA vaccine to dendritic cells, pointing to the low cytotoxicity of the PAMA homopolymers and good transfection efficiency with or without serum [52]. PEGylated PAMA block copolymers synthesized via ATRP have been previously employed for the delivery of heparin [53], oligonucleotids (ONDs) [54], DNA in dendritic cells [51] and small interfering RNA (siRNA) [55] with promising results. AMA was also already used as a co-monomer with DMAEMA for gene delivery (DNA) in COS-1 cell lines [85]. The same co-monomers synthesized by RAFT were used in another study for the *in vitro* delivery of DNA plasmids to COS-7 cell lines [86]. The reported results revealed the high potential of PAMA-based polymeric vector for gene delivery applications. Recently, the synthesis of PAMA via ARGET ATRP under mild conditions was achieved [4]. The ARGET ATRP could be advantageous, since it allows the use of lower amount of metal catalyst to achieve control over the polymerization. The reducing agent used was AscA, which regenerates Cu(I) activator species *in situ* from oxidizable stable Cu(II) complexes. To the extent of the research made, PAMA-based polymers synthesized via ARGET ATRP have never been used in gene delivery to COS-7. In this work, PEG_{45}-*b*-$PAMA_n$ block copolymers were synthesized by ARGET ATRP (in aqueous medium, at 35°C with a slow feeding of AscA) with different DP target values of AMA

(Figure 16 (a)), in order to optimize the cellular transfection. $PAMA_n$ homopolymers were also synthesized to serve as control samples (Figure 16 (b)).

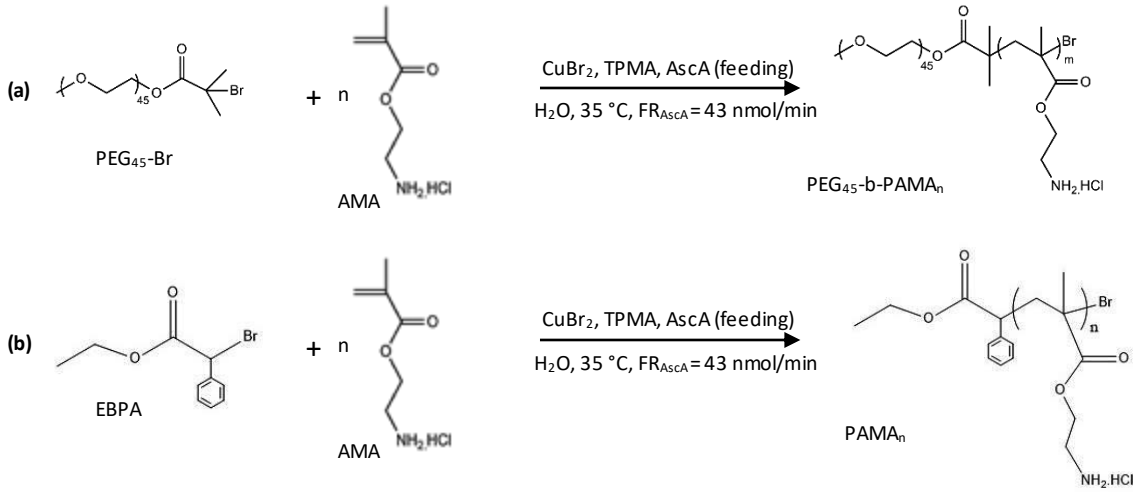

Figure 16 - Typical synthesis of **(a)** PEG_{45}-*b*-$PAMA_n$ and **(b)** of $PAMA_n$ by ARGET ATRP.

The characteristic properties of the polymers synthesized are summarized in Table 4.

Table 4 - General properties of the PAMA-based samples synthesized.

Entry	Sample	DP_{PAMA} (n)	DP_{PEG} (m)	M_n^{th} x 10^{-3}	M_n^{NMR} x 10^{-3}	M_n^{SEC} x 10^{-3}	Đ	$[Cu]_0$ (ppm) x 10^{-3}***	[Cu] (ppm)
1	GD29	163	45	24.7	28.9	34.9	1.14	3.3	2.7
2	GD27	111	45	18.0	20.4	20.6	1.09	5.0	0.9
3	GD28	63	45	10.6	124	24.4	1.09	10.0	17.6
4	GD31	40	45	7.2	8.6	13.7	1.18	16.7	7.3
5	GD30	103 *	--	17.4	--*	23.2	1.12	5.0	1.5
6	GD32	156**	--	--**	--**	26.0	1.15	--	--

*registered significant oscillations in the NMR spectrum; the initiator signals intensity was too small compared to the one of the polymer signal; DP estimated through monomer conversion.
**PAMA homopolymer synthesized by FRP; the average DP was estimated through the M_n^{SEC}.
*** $[Cu]_0$ (ppm) stands for the [Cu] in the reaction mixture. Note that this quantity could be minimized. However, a larger amount than required was used to ensure good control over the polymerization.

The molecular structure of the polymers was confirmed by ^{1}H NMR spectroscopy (Figure 17).

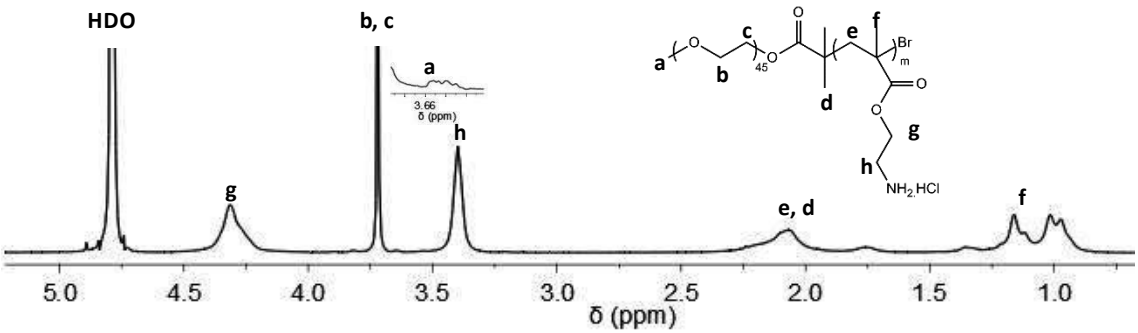

Figure 17 - 400 MHz ^{1}H NMR spectrum, in D_2O, of a pure PEG_{45}-*b*-$PAMA_{111}$ sample (M_n^{NMR} = 20.4 x 10^3; M_n^{SEC} = 20.6 x 10^3, Đ = 1.09) obtained by ARGET ATRP. Reaction conditions: $[AMA]_0/[PEG_{45}\text{-}Br]_0/[CuBr_2]_0/[TPMA]_0$ = 100/1/0.5/1/2; FR_{AscA} = 43 nmol/min; $V_{solvent}$ = 1.43 mL; T = 35°C.

As expected, the results indicated that the ARGET ATRP afforded a good control over the block copolymers and homopolymer (Table 4, entries 1 to 5), as jugged by the low dispersity values (Đ < 1.2) and by the agreement between the M_n^{RMN} and M_n^{th} values.

The reaction mixtures were purified by dialysis against water to remove traces of copper catalyst and the pure polymers were recovered by freeze-drying. The success of the purification process is confirmed by the low concentration of copper (determined by atomic absorption) in the pure polymers, which was significantly lower than the concentration of copper in the reaction mixture (Table 4). A FRP polymerization of AMA was also performed (metal-free sample), aiming to evaluate the influence of the copper content in the cell viability.

Since PAMA has a pH-dependent protonation, the pK_a of representative samples was determined. This was done through the acid-base titration method [87] at similar conditions to the ones used for the preparation of the polyplexes, using deionized water as the solvent, at room temperature (25°C) or at 37°C. Since the polyplexes are prepared at pH = 3, knowing the pK_a of the PAMA-based polymer used allows a more precise calculation of the percentage of protonation (% protonation or charge density - % charge). Representative samples including one homopolymer and two copolymers (one with the highest DP and another with the lowest DP), were tested at 37 °C. Another PAMA-based block copolymer with an intermediate DP was tested at room temperature.

From the analysis of the titration curve (Figure 18 (a)), it is possible to observe that there was a buffering effect at pH range around 4 – 9 for all the polymers and the different the conditions tested. In systems where the sample acts as a buffer, the pK_a can be found when the overall degree of protonation (α) is 0.5. The degree of protonation is the number of bound protons as a function of pH, and it ranges from 1 to 0, as the pH increases from the first inflection point of the titration curve to the second. The inflection points of each titration curve were determined from the maximum values of the first derivative of the titration curve [87]. According to the results of the titration curve in Figure19 (a), and considering $\mathrm{pH} = \mathrm{pK_a} + \log_{10}\left(\frac{1-\alpha}{\alpha}\right)$, the pK_a values were determined and the average degree of protonation (Figure19 (b)) was traced.

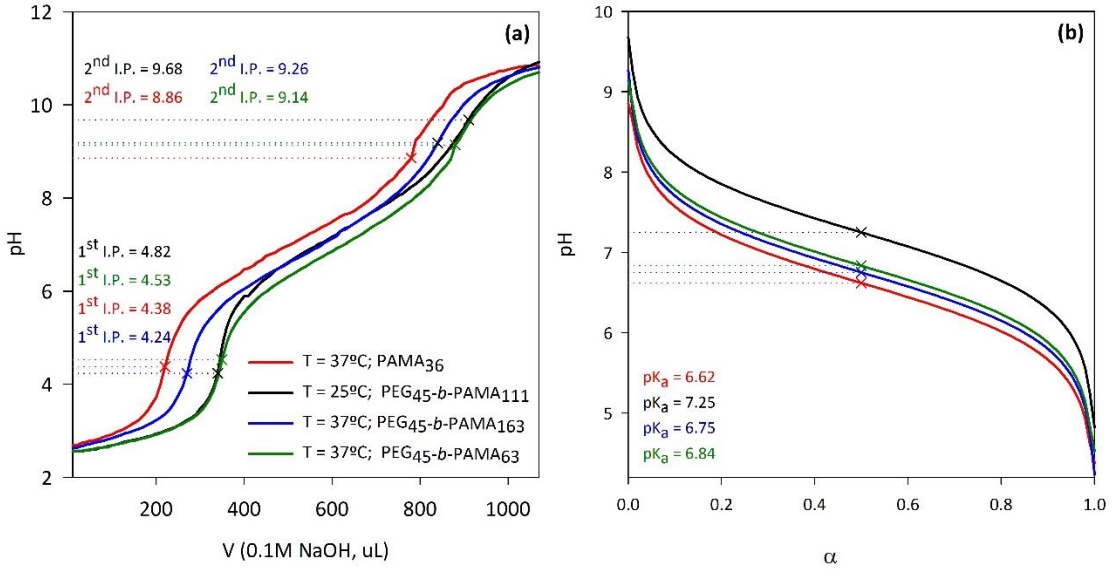

Figure 18 - **(a)** Titration curves of the PAMA-based samples tested; **(b)** same titration curves as in **(a)** with the x-axis expressed in terms of the average degree of protonation, α.

From Figure 18, it is possible to observe no significant differences between the polymers tested at 37 °C. An increase in the pK_a is, however, detectable with the decrease in temperature (black curves in Figure 19). From the Henderson-Hasselbalch equation, it is known that $\mathrm{pH} = \mathrm{pK_a} + \log_{10}(\frac{[\mathrm{A^-}]}{[\mathrm{AH}]})$, where A^- represents the non-protonated species, and AH the protonated species. From this equation, the ratio of non-protonated to protonated acid species allows the calculation of the percentage of ionization (% ionization): $\frac{[A^-]}{[AH]} = 10^{(pH-pK_a)}$. Similarly, the % charge can be calculated

through the proportion of acid A that is protonated, as being $\frac{[AH]}{[AH]+[A^-]} = \frac{1}{1+10^{(pH-pK_a)}}$. Hence, knowing the pK_a of the sample and the pH of its solution, the % charge can be determined. With this knowledge, and based on the results obtained, it can be expected that all the PAMA-based samples were fully protonated (< 99.9% protonation) when in a solution with pH = 3 (Appendix C, Table C 1).

2.4.4 Gene delivery results from PAMA-based polymers

The most promising gene delivery results from this work were the ones related to the PEG_{45}-*b*-$PAMA_n$ and $PAMA_n$ samples (Table 4, previous section). In this section the main results from the gene delivery assays are presented, as provided by Daniela Santo in *Center for Neuroscience and Cell Biology (CNC)*. The best results in gene delivery assays were obtained for samples PEG_{45}-*b*-$PAMA_{111}$ (GD27) and $PAMA_{103}$ (GD30), which are displayed in this section. Procedures can be found in Appendix D.

Figure 19 shows the comparison between the effect of the N/P ratio and composition of the polyplexes on the viability of COS-7 cells. Both samples tested showed better cell viability that PEI (gold standard) for different N/P ratios[3], both in the presence or the absence of serum. However, in the absence of serum the PEG_{45}-*b*-$PAMA_{111}$ block copolymer (Figure 19 (b)) showed better cell viability than the $PAMA_{103}$ homopolymer (Figure 19 (a)) for the same N/P ratios. Moreover, it is interesting to note that the higher the N/P ratio, the lower the cell viability without serum. However, the cell viability seems to be higher in the presence of serum in both samples, for the same N/P ratios.

[3] **N/P ratio:** the ratio between the positive charges of the cationic polymer (N - amine) and the negative charges from the nucleic acid (P – phosphate).

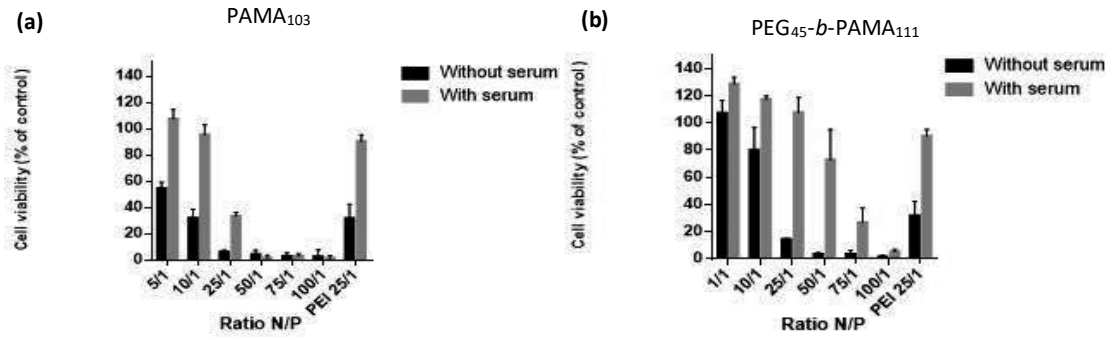

Figure 19 - Effect of the N/P ratio and composition of polyplexes on the viability of COS-7 cells using **(a)** $PAMA_{103}$ and **(b)** PEG_{45}-*b*-$PAMA_{111}$.

The effect of the N/P ratio and composition of the polyplexes in their transfection activity in COS-7 cell lines is presented on Figure 20. For one, $PAMA_{103}$ samples (Figure 20 (a)), although performing better than PEI in the presence of serum (for N/P ratios < 50/1), also performed better than the PEG_{45}-*b*-$PAMA_{111}$ samples (Figure 20 (b)) for N/P ratios < 25/1. It is also worth to note that while the $PAMA_{103}$ showed good transfection efficiency (similarly to PEI) in the absence of serum, no transfection is verified for higher N/P ratios (> 50/1). When comparing the results from Figure 20 (a) with the ones from Figure 20 (b), the PEG_{45}-*b*-$PAMA_{111}$ behaved better than the homopolymer, in the presence of serum and for higher N/P ratios (≥ 50/1), being the transfection activity in the absence of serum and form lower N/P ratios negligible. Hence, the comparison of the assays of the block copolymer and the homopolymer seems to suggest that the presence of PEG in the polymer structure can in fact increase the transfection activity in the presence of serum.

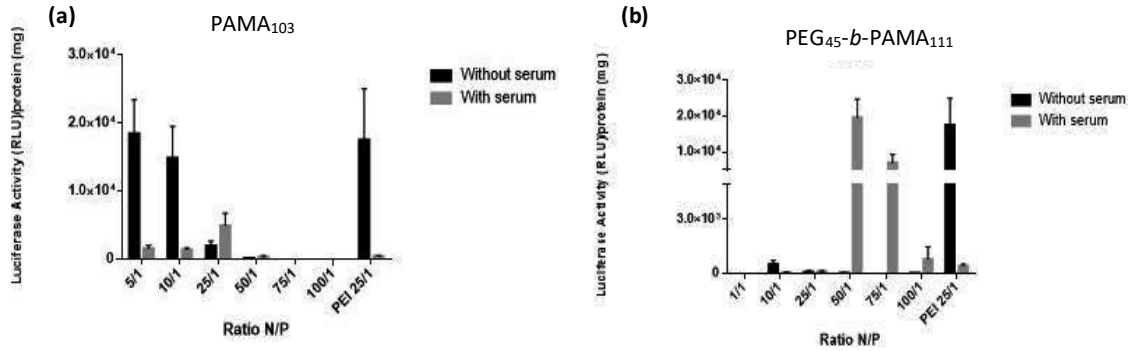

Figure 20 - Effect of the N/P ratio and composition of polyplexes on their transfection activity COS-7 cell lines using **(a)** $PAMA_{103}$ and **(b)** PEG_{45}-*b*-$PAMA_{111}$.

Ethidium bromide (EtBr) is used as a fluorescent probe for the detection of DNA. When bound to DNA molecules, the fluorescence emitted could be measured and quantified in order to determine the accessibility of DNA. In gene delivery assays, it is a measurement of DNA protection/binding to the polymer, meaning that the lower the EtBr access, the better the DNA is protected/bound in the polyplex. From Figure 21, it is clear that only in the homopolymer sample with N/P ratio 1/1 the DNA was sufficiently available to interact with the ethidium bromide (EtBr) probe, where in both PEG_{45}-*b*-$PAMA_n$ the DNA protection was high enough that no interaction occurred.

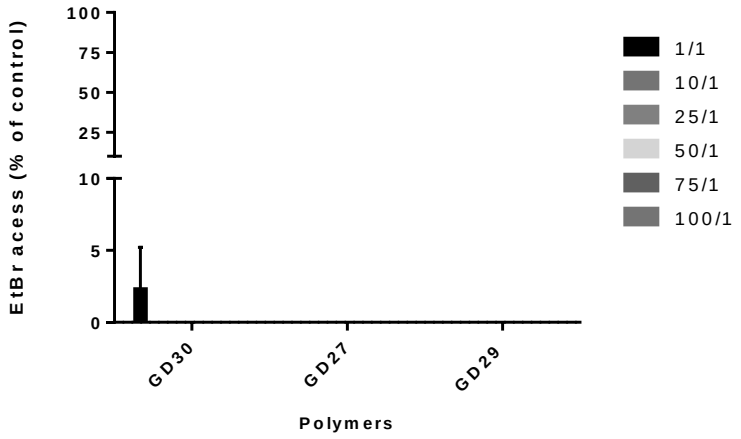

Figure 21 - Accessibility of ethidium bromide to DNA of the different polyplexes prepared at different N/P ratios.

All the results seem to suggest that PAMA-based samples have a good potential as gene delivery vectors. PAMA homopolymer and PEG-*b*-PAMA block copolymers have already been used for gene delivery [51, 52, 55].

PAMA homopolymers, synthesized by ATRP with well-defined chain length (DP = 45; 75; 150), showed good potential for DNA vaccine delivery to dendritic cells [52]. Moreover, the study from Weihang *et all* [52] reported a very low cytotoxicity of the PAMA homopolymers tested with efficient transfection in vitro either in the presence or the absence of serum. It is interesting to note that this study reported a dependence of the cellular uptake of the DNA plasmid (increases with longer polymer chain lengths) and intracellular release of the DNA plasmid (increases for shorter polymer chain lengths) with the polymer chain length [52]. Tang *et all* had previously studied the ability of a library of PEG_{45}-*b*-$PAMA_n$ block copolymers (M_n^{PEG} = 2000; DP_{PAMA} = 19; 39; 75), also

synthesized by ARTP, to condense and deliver DNA plasmids to DC 2.4 cells, where the influence of the cationic block length on the polyplex properties was also evident [51]. This study showed increasing stability of the polyplexes against electrostatic destabilization (by salt and heparin) and smaller average particle size with the increase of the cationic block chain length. The same correlation was found for *in vitro* transfection efficiency and cellular uptake: the longer the PAMA block chain length, the more efficient the transfection and the cellular uptake. Besides, cytotoxicity was also low, merely having a chain length dependent toxicity at high concentration (1 mg/mL). However, the presence of PEG in these block copolymers seemed to decrease the transfection efficiency [51] (when compared with the results from the homopolymer [52]), which is the opposite of what was found for the $PAMA_{103}$ and PEG_{45}-*b*-$PAMA_{111}$ polymers synthesized in this work (tested in the COS-7 cell line). In comparison with this work, despite using different cell lines, it is worth to notice that the synthesis of the PAMA-based polymers (by ARGET ATRP) was done in a far more ecofriendly reaction conditions, using water as a solvent; also the purification process was simpler and with fewer chemical waste.

More recently, the Cheng *et all* [55] reported the use of PEG_{113}-*b*-$PAMA_{98}$ (synthesized by ATRP) for the delivery of siRNA either *in vitro* (in HeLa-Luc cells) and *in vivo*. The results confirmed the potential of PAMA-based polymers to gene delivery applications [55]. Similarly, Dufrese *et al* [54] also reported a library of copolymers using both PEG and PAMA, but for the synthesis of oligonucleotide-based polyion complex micelles (ODN-based PCIMs). Although promising, these reported results are not comparable to the ones presented in this work, since the genetic material used is not DNA. Nonetheless, it can again be said that the PEG_{45}-*b*-$PAMA_n$ block copolymers here reported were synthesized using more ecofriendly reaction conditions.

2.5 CONCLUSIONS AND FUTURE WORK

Well-controlled PEG_{45}-*b*-$PAMPTMA_n$ and PEG_{45}-*b*-$PAMA_n$ block copolymers were synthesized under environmentally friendly conditions via SARA ATRP and ARGET ATRP, respectively, and characterized in terms of molecular weight, dispersity, pK_a and copper content. Samples of interest were sent to gene delivery assays in which the PEG_{45}-*b*-

$PAMA_{111}$ block copolymer produced the best transfection results, particularly in the presence of serum.

It would be interesting to further characterize the PEG_{45}-*b*-$PAMPTMA_n$ and PEG_{45}-*b*-$PAMA_n$ particles in terms of their zeta potential to better understand why they failed or succeeded in the cellular assays.

CHAPTER 3: INFLUENCE OF DIFFERENT "THF-LIKE" SOLVENTS ON THE PMA SYNTHESIS BY SARA ATRP

3 INFLUENCE OF DIFFERENT "THF-LIKE" SOLVENTS ON THE PMA SYNTHESIS BY SARA ATRP

3.1 ABSTRACT

The activity of metallic catalytic systems can be significantly affected by the polarity of the solvents. CPME and 2-MeTHF are two "THF-like" solvents that have been used to replace THF in more ecofriendly polymerization systems. The aim of this work was to study the differences in the reaction rate and control over the polymerization of MA by SARA ATRP, when using THF, 2-MeTHF or CPME in solvent mixtures containing water and EtOH. From the comparative results of the kinetic studies of the three systems designed, no significant differences between the reaction rates were found, regardless of the solvent mixture used. The theoretical molecular weights were in close agreement with the experimental values. However, there was an increase of the PMA dispersity for high monomer conversions when using either THF or 2-MeTHF in the solvent mixture. The "living" character of the PMA-Br samples obtained from each SARA ATRP system was confirmed by chain-extension experiments, which revealed the presence of unreacted macroinitiator chains in the extended polymers. The comproportionation of $CuBr_2$/Me_6TREN with Cu(0) in the different solvent mixtures investigated for the SARA ATRP was evaluated by UV-Vis spectroscopy. For all the systems studied, an unexpected increase in the maximum absorbance peak and a successive shift to smaller wavelengths was evident during the reaction time, suggesting the formation of different copper species. Further studies are required in order to clarify the interpretation of the results obtained.

3.2 INTRODUCTION

There has been an important tendency to reduce the chemical related impact whether in humans, or the environment. Since solvents are probably the biggest source of waste in chemical processes [5], the introduction of ecofriendly solvents could be the key to a more "Green Chemistry" [88]. A solvent-free chemical process would be ideal in order to minimize solvent waste; however, in many cases, this is not possible [5]. As

an alternative, water-based systems have been widely studied and proved effective for many different applications [89]. However, water-based systems cannot always be used (e.g., solubility issues) [5].

Tetrahydrofuran (THF) is a well-known and vastly used polar solvent, that is miscible with water and easily absorbed by all means of exposure. Despite having a relatively low toxicity, THF is corrosive to the eyes [90]. The general properties of THF are summarized in Table 5 [91, 92], showing less stability than the other two "THF-like" solvents, whose structures can be found in Figure 22 [91]. Extensive research was made on the impact of the usage of THF either in the environment or in human health and more information can be found in [90].

Cyclopentyl methyl ether (CPME) and 2-methyltetrahydrofuran (2-MeTHF) are two promising green solutions for the replacement of THF [5, 91]. With a "THF-like" structure (Figure 22), their general properties (Table 5) have attracted increasing interest and proved to be effective at both industrial [5] and laboratorial [6] scales.

Table 5 – Some general physical properties of the organic solvents: THF, 2-MeTHF and CPME.

Solvent	Boiling point (°C)	Density (at 25 °C, g/mL)	Solubility in water (g/100 g at 23°C)	Flashpoint (°C)	Viscosity (at 25 °C)	Dielectric constant (at 25 °C)
THF	65-67	0.89	∞	-17.2	0.46	7.52
2-MeTHF	78-80	0.86	14	-12.0	0.60	6.97
CPME	106	0.86	1.1	-1	0.55	4.76

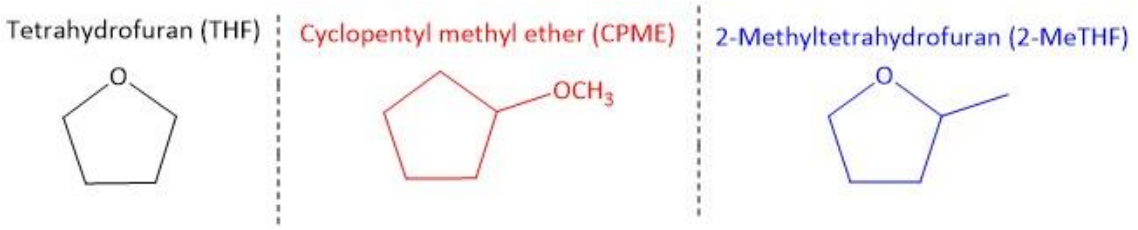

Figure 22 - Chemical structure of the "THF-like" solvents used in this work: THF, CPME and 2-MeTHF.

2-MeTHF is an aprotic polar solvent obtained from renewable resources (e.g., furfural or levulinic acid, from corncobs) that has an encouraging environmental footprint [5]. Moreover, 2-MeTHF is more stable than THF. Besides being an alternative

to THF, 2-MeTHF can also replace DCM in some cases. More information on this solvent can be found in the literature [5].

CPME is a green alternative to several organic solvents, including THF [91]. Amongst its several important features, it is important to highlight that it is more stable than THF and 2-MeTHF (resisting to peroxide formation), it is highly hydrophobic and it is relatively stable under acidic and basic conditions. It has a low vaporization energy and is less prone to explode than THF. More information on the solvent can be found in the literature [91].

A previous study showed the success of the use of CPME as a green alternative to other well-known solvents in the polymerization of MA, glycidyl methacrylate (GMA), styrene (Sty) and vinyl chloride (VC) by SARA ATRP using different SARA agents [6]. With this knowledge, the aim of this work was to investigate the eventual differences in the reaction rate and control over the polymerization of MA by SARA ATRP, when using THF, 2-MeTHF or CPME. To this end, three reaction systems were designed, in which only the main solvent was changed, and kinetic studies were performed.

3.3 EXPERIMENTAL

3.3.1 Materials

Copper(II) bromide (99.9%, Aldrich), $CDCl_3$(Euriso-top, +1%TMS), DMSO (Acros, 99.8+% extra pure), EBiB (98%, Sigma Aldrich), EtOH (Panreac, 99.5%), MeOH (Fisher Scientific), THF (Sigma-Aldrich, inhibitor-free, +99.9%), CPME (Sigma–Aldrich, inhibitor-free, anhydrous, +99.9%), 2-MeTHF (Sigma-Aldrich, inhibitor-free, anhydrous, +99.9%) were used as received.

MA (Acros, 99% stabilized), was passed through a sand/alumina (basic, Fisher Scientific), column before use in order to remove the radical inhibitor.

Purified water (Milli-Q®, Millipore, resistivity >18 MΩ.cm) was obtained by reverse osmosis.

THF (Panreac, HPLC grade) was filtered under reduced pressure before use.

Metallic copper (Cu(0), d = 1 mm, Alfa Aesar) was washed with HCl in MeOH and subsequently rinsed with MeOH and dried under a stream of nitrogen following the literature procedures [80].

Me_6TREN [81] was synthesized as reported in the literature and its structure was confirmed by ^{1}H NMR (Appendix A, Figure A 3).

3.3.2 Techniques

Polymers number-average molecular weights (M_n^{SEC}) and dispersity ($Đ = M_w/M_n$) were determined by using high performance size exclusion chromatography HPSEC, Viscotek (viscotek TDAmax) with a differential with a differential viscometer (DV), right-angle laser-light scattering (RALLS, Viscotek), low-angle laser-light scattering (LALLS, Viscotek); and refractive index (RI) detectors. The column set consisted of a Viscotek Tguard column (8 mm) followed by one Viscotek T2000 column (6 mm), one MIXED-E PLgel column (3 mm), and one MIXED-C PLgel column (5 mm). HPLC dual piston pump was set with a flow rate of 1 mL/min. The eluent (THF) was previously filtered through a 0.2 mm filter. The system was also equipped with an online degasser. The tests were done at 30 °C using an Elder CH-150 heater. Before the injection (100 mL), the samples were filtered through a polytetrafluoroethylene (PTFE) membrane with 0.2 mm pore. The system was calibrated with narrow PS standards. The dn/dc was determined as 0.063 mL/g for PMA, 0.105 mL/g for PVC, 0.087 mL/g for PGMA, and 0.185 mL/g for PS. M_n^{SEC} and Đ of the synthesized polymers were determined by multidetectors calibration using the OmniSEC software version: 4.6.1.354.

400 MHz 1H NMR spectra of reaction mixture samples were recorded on a Bruker Avance III 400 MHz spectrometer, with a 5-mm TIX triple resonance detection probe, in CDCl3 with tetramethylsilane (TMS) as an internal standard. Conversions of the monomer were determined by integration of monomer and polymer signals using MestRenova software version: 10.0.1-14719.

The ultraviolet-visible (UV-Vis) studies were performed with a Jasco V-530 spectrophotometer. The analyses were carried in the 350 – 1100 nm range at room temperature.

3.3.3 Procedures

Typical procedure for SARA ATRP of MA

Water (0.03 mL), EtOH (0.42 mL) and Cu(II)Br_2 (3.4 mg, 15 µmol) were added to a 10 mL Schlenk flask equipped with a magnetic stirrer bar. Upon dissolution, Me_6TREN (44.1 µL, 165 µmol), CPME (1.05 ml), EBiB (29.3 mg, 150 µmol) and MA (3.0 mL, 33.3 mmol) were added, and next a Cu(0) wire (l = 5 cm; d = 1 mm). The Schlenk flask was then sealed with a glass stopper, deoxygenated with five to seven freeze-vacuum-thaw cycles and purged with nitrogen. The reaction was carried out using at 30 °C. The kinetic study was done collecting samples for SEC and ^{1}H RMN at pre-determined time periods. THF SEC samples allowed the determination of the molecular weights and dispersity, and ^{1}H NMR spectroscopy was used to determine monomer conversion.

The same procedure was used for the other two reaction systems, replacing only CPME by either THF or 2-MeTHF in order to access the differences between the polymerization systems.

Typical procedure for chain extension of PMA-Br by SARA ATRP

A PMA-Br obtained from a typical SARA ATRP reaction was dissolved in THF and passed through an alumina column to remove copper traces. Then, the polymer was precipitated in water and dried under reduced pressure, until constant weight. The PMA-Br (M_n^{SEC} = 6.6 x 10^3, $Đ$ = 1.09; 366.5 mg, 56 µmol) was dissolved in DMSO (1.25 mL) in a 10 mL Schlenk flask equipped with a magnetic stirrer bar. Upon dissolution, Me_6TREN (16.3 µL, 61 µmol), $CuBr_2$ (1.2 mg, 6 µmol) and MA (2.5 mL, 27.8 mmol) were added. The Cu(0) wire (l = 5 cm; d = 1 mm) was then added to the reaction mixture. The Schlenk flask was sealed with a glass stopper, deoxygenated with five to seven freeze-vacuum-thaw cycles and purged with nitrogen. The reaction was carried out at 30 °C. SEC analyses allowed the determination of the molecular weights and dispersity, and ^{1}H NMR spectroscopy was used to determine monomer conversion.

The same procedure was used for the other two reaction systems, replacing only the PMA-Br obtained in CPME by either the one obtained in THF or in 2-MeTHF.

Typical UV-Vis spectroscopy study of Cu(II)Br_2 reduction

In a vial Me_6TREN (29.4 µL, 110 µmol) was added to $CuBr_2$ (2.2 mg, 10 µmol), followed by the addition of water (0.04 mL), EtOH (0.56 mL) and CPME (1.4 mL). A magnetic stirrer bar was added and the vial was sealed. After overnight stirring, the mixture was transferred to a UV-Vis cuvette, which was placed in the spectrometer for spectra acquisition. The mixture was again transferred to a vial, purged with N_2 for 15 min. A Cu(0) wire (l = 5 cm; d = 1 mm), a magnetic stirrer bar and the purged mixture were placed in the UV-Vis cuvette, which was sealed under nitrogen, isolated with parafilm and placed in the spectrometer for spectra acquisition. The absorbance was measured in different times (15, 30, 60, 90, 120, 180 and 240 min), being the mixture under stirring (600 rpm) in a 30 °C water bath in between each spectra acquisition.

The same procedure was used for the two other reaction systems, replacing only CPME by either THF or 2-MeTHF, in order to access differences in the comproportionation of $CuBr_2$/Me_6TREN with Cu(0) in the different solvent mixtures.

UV-Vis spectroscopy study of Cu(II)Br_2 reduction during the SARA ATRP of MA

Water (0.025 mL), EtOH (0.35 mL) and Cu(II)Br_2 (2.8 mg, 13 µmol) were added to a 10 mL tube Schlenk flask equipped with a magnetic stirrer bar. Upon dissolution, Me_6TREN (36.7 µL, 138 µmol), CPME (1.05 ml), EBiB (24.4 mg, 125 µmol) and MA (2.5 mL, 27.8 mmol) were added. The Schlenk flask was then sealed with a glass stopper, deoxygenated with five to seven freeze-vacuum-thaw cycles and purged with N_2.

To a round 10 mL Schlenck flask was added a magnetic stirrer bar and a Cu(0) wire (l = 5 cm; d = 1 mm). The round Schlenk flask was sealed with an adapted UV-Vis cuvette and purged with N_2 for 15 min. Under N_2 the reaction mixture was transferred to the Schlenk flask sealed with the UV-Vis cuvette, which was placed in the spectrometer for spectra acquisition. The absorbance was measured in different times (15, 30, 60, 90,

120, 180 and 240 min), being the polymerization allowed to proceed under stirring (600 rpm) in a water bath (30 °C) in between each spectra acquisition.

3.4 RESULTS AND DISCUSSION

Aiming to access differences in the polymerization rate between the SARA ATRP systems using solvents similar to THF, and based on a previously reported system showing the success of a SARA ATRP of MA using a solvent mixture of CPME/EtOH/H_2O = 70/28/2 (v/v/v) [6], kinetic studies were performed. In these studies, the influence of CPME was compared to THF and 2-MeTHF. The resultant kinetic plots can be found in Figure 23.

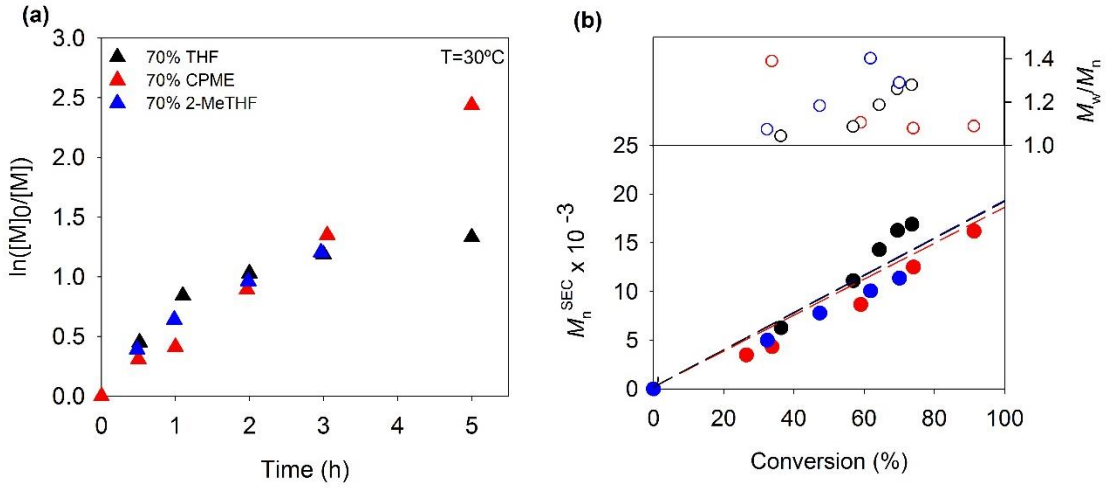

Figure 23 – **(a)** Kinetic plots of conversion and ln[M]$_0$/[M] *vs.* time (h) and **(b)** plot of number-average molecular weights (M_n^{SEC}) and *Đ vs.* monomer conversion (the dashed lines represent theoretical molecular weight at a given conversion) for the SARA ATRP of MA in CPME/EtOH/H_2O = 70/28/2 (v/v/v) (red), THF/EtOH/H_2O = 70/28/2 (v/v/v) (black) and 2-MeTHF/EtOH/H_2O = 70/28/2 (v/v/v) (blue) at 30°C. Reaction conditions: [MA]$_0$/[EBiB]$_0$/[$CuBr_2$]$_0$/[Me_6TREN]$_0$/Cu(0) wire = 222/1/0.1/1.1/Cu(0) wire: *l* = 5 cm; *d* = 1 mm; $V_{solvent}$ = 2 mL.

The kinetic plots from Figure 23 show that there were no significant differences between the reaction rates obtained, regardless of the solvent mixture used. In this case, it is not possible to ensure that the "THF-like" solvents can afford the same polymerizations with different rates, since there was also EtOH and H_2O in the solvent mixture. It is known that water increases the reaction rate o ATRP reactions, due to high catalytic activity of Cu(I) in this solvent [74, 93]. However, it was not possible to compare the "THF-like" solvents as pure in the polymerization solvents, since CPME does not dissolve the deactivator catalytic system ($CuBr_2$/Me_6TREN) [6]. Despite the similar reaction rates, the systems with 70 % THF and 70 % 2-MeTHF showed increasing values

of their dispersity (*Đ*) during the polymerization, in opposition to what was reported for the case of CPME [6]. Besides the loss of control throughout the reactions for the solvent mixtures containing 2-MeTHF and THF, Figure 23 (b) shows that the theoretical molecular weights were in close agreement with the experimental values (with only small deviation for the high monomer conversion in the case of THF). The increase on the dispersity of the PMA-Br could indicate the loss of chain-end functionality for high monomer conversions. Also, it is interesting to note that the maximum monomer conversion achieved for the systems containing THF and 2-MeTHF was lower than the one obtained using CPME (Figure 23 (a)). To confirm the hypothesis of the presence of dead chains, chain extension reactions were designed using as macro-initiator purified samples of PMA-Br obtained from each SARA ATRP system investigated. The molecular structure and chain-end functionality of each macro-initiator was accessed by ^{1}H NMR spectroscopy (Figure 24; Appendix E, Figure E 1 and Figure E 2).

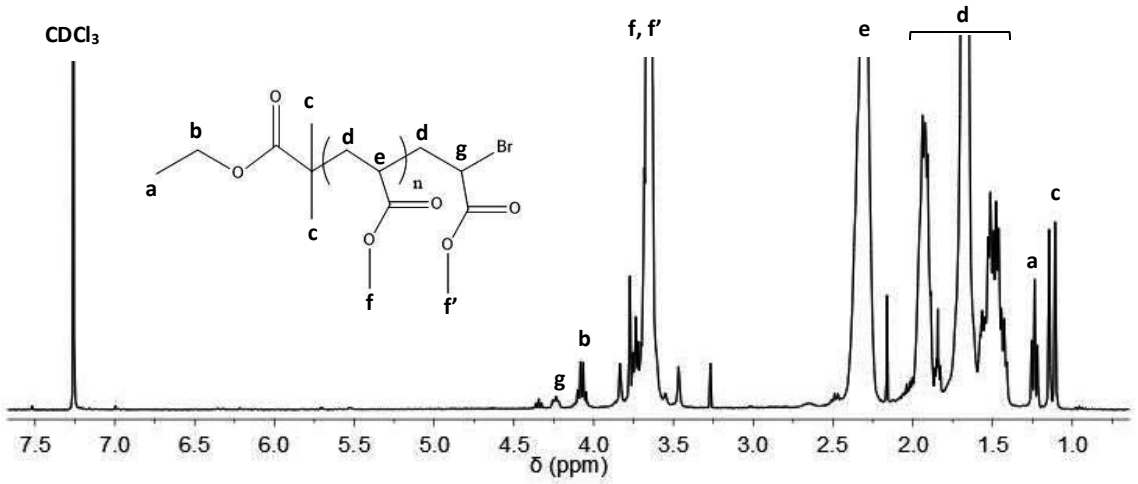

Figure 24 - 400 MHz ^{1}H NMR spectrum, in $CDCl_3$, of a purified PMA_{65} sample (M_n^{RMN} = 5.8 x 10^3; M_n^{sec} = 6.6 x 10^3; Đ = 1.09, monomer conversion = 84 %) obtained by SARA ATRP. Reaction conditions: $[MA]_0/[solvent]$ = 2/1 (v/v); CPME/EtOH/H_2O = 70/28/2 (v/v/v); $[MA]_0/[EBiB]_0/[CuBr_2]_0/[Me_6TREN]_0$/Cu(0) wire = 70/1/0.1/1.1/Cu(0) wire: *l* = 5 cm; *d* = 1 mm; $V_{solvent}$ = 2 mL; T = 30 °C.

All PMA-Br macroinitiators were obtained at around 80% of monomer conversion (Table 6), since the kinetic studies suggested that the loss of control was significant at around this value. Additionally, it is known that for very high monomer conversions (> 90%), it is expected an increase of the percentage of dead chain-ends [93, 94]. In that case, probably it would not be possible to observe the difference between the systems.

In Table 6 are summarized the general properties of each PMA-Br macroinitiator synthesized. DP and percentage of functionalization (% functionalization) were determined by the integration of ^{1}H NMR signals.

Table 6 - General properties of the PMA_n-Br polymers used as macroinitiators in the chain extensions.

Entry	Sample	"THF-like" solvent	Monomer conversion (%)	DP** (n)	M_n^{th} x 10^{-3}	M_n^{NMR} x 10^{-3}	M_n^{SEC} x 10^{-3}	Đ	% Funct. ***
1	ML T12	CPME	84	65	5.4	5.8	6.6	1.09	79
2	ML T13	THF	77*	66	4.8*	5.8	7.3	1.05	84
3	ML T14	2-MeTHF	85*	60	5.3*	5.3	6.0	1.08	71

*The ^{1}H NMR spectrum of the reaction mixture was contaminated, values presented are estimates;
The DP was determined by the integration of the ^{1}H RMN signal **c and **e** of the pure macroinitiator samples;
***The % of functionality was determined by the integration of the ^{1}H RMN signal **c** and **g** of the pure macroinitiator samples.

The differences between the determination of the % functionalization (active chain-ends) using different initiators NMR signals was accessed. The signal **c** (Figure 24) was chosen, since it was less affected than the signal **a** by the influence of the polymer signal, and more intense than signal **b**. The presence of the signal **g** in the NMR spectrum confirms the "living" character of the polymer. The same was verified for the remaining two PMA-Br macroinitiators obtained by either the THF-containing or the 2-MeTHF-containing SARA ATRP systems (Appendix E, Figure E 1 and Figure E2).

The NMR results (Table 6) suggested that the system based on 2-MeTHF afforded PMA-Br with the lowest percentage of chain-end functionality, for similar monomer conversions. However, it is important to analyze the results with caution, since the determination of the % of functionality by NMR could be affected by errors due to the very low intensity of the initiator signal, in comparison to the signal of the polymer (even for low M_w polymers, as in this case). Therefore, chain extension experiments were performed to confirm the "living" character of the PMA-Br samples synthesized. It is worth to mention that all PMA-Br macroinitiators were extended in the same conditions, using dimethyl sulfoxide (DMSO) as the SARA ATRP solvent, to ensure that the results could be comparable.

For all cases, a shift of the SEC trace was observed. However, a small shoulder corresponding to the macroinitiator in the PMA-Br extended SEC trace was also observed (Figure 25), which points to the presence of some dead chains in the PMA-Br macroinitiator. Similar results were found for all macroinitiators synthesized (Appendix E, Figure E 3 and Figure E 4).

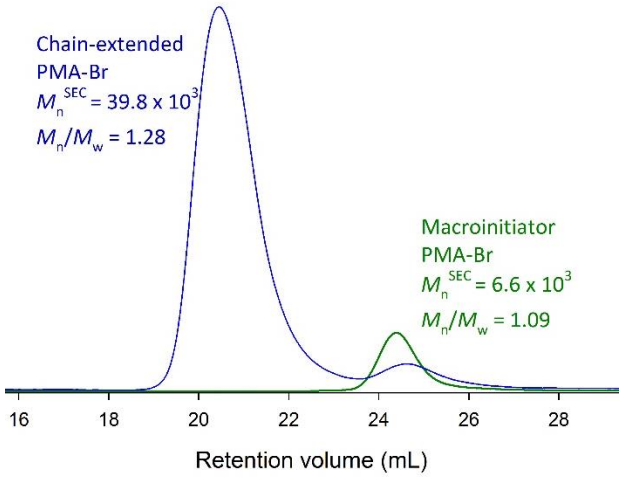

Figure 25 - SEC traces of PMA-Br before and after chain extension with MA: macroinitiator obtained at 84% of monomer conversion (green line) and extended polymer at 75% monomer conversion (blue line); macroinitiator - $[MA]_0/[solvent]$ = 2/1 (v/v) in CPME/EtOH/H_2O = 70/28/2 (v/v/v), with $[MA]_0/[EBiB]_0/[CuBr_2]_0/[Me_6TREN]_0$/Cu(0) wire = 70/1/0.1/1.1/Cu(0) wire: *l* = 5 cm; *d* = 1 mm at 30 °C; chain extension by SARA ATRP in DMSO with $[MA]_0/[solvent]$ = 2/1 (v/v), $[MA]_0/[PMA\text{-}Br]_0/[CuBr_2]_0/[Me_6TREN]_0$/Cu(0) wire = 500/1/0.1/1.1/Cu(0) wire: *l* = 5 cm; *d* = 1 mm at 30 °C, $V_{solvent}$ = 1.25 mL.

The general properties of the chain-extended PMA-Br polymers are summarized in Table 7. To exclude the hypothesis that the apparent presence of dead chains could be derived from an insufficient dissolution of the PMA-Br macroinitiator before the chain extension, rather than due to the low % of functionality, a control reaction was performed. In this chain-extension the macroinitiator was allowed to dissolved overnight in a double amount of DMSO ($[MA]_0/[DMSO]$ = 1/1 (v/v), V_{DMSO} = 2.5 mL) to ensure complete dissolution. Figure E 4 (Appendix E) shows that a similar shoulder on the extended PMA-Br SEC trace, confirming that the dead chains are created during the SARA ATRP of MA (macroinitiator for synthesis).

Table 7 – General properties of the PMA-Br extended polymers.

Entry	Macroinitiator *	% dead chain (expected)**	% dead chain ***	% dead chain ****	M_n^{SEC} x 10^{-3}	$Đ$
1	ML T12 (CPME)	21	6.1	8.3	39.8	1.28
2	ML T13 (THF)	16	13.8	16.4	33.5	1.34
3	ML T14 (2-MeTHF)	29	8.5	10.4	26.9	1.72
4	ML T14 (2-MeTHF)	29	6.9	8.0	27.2	1.95

*See Table 6;
**From the NMR results (see Table 6);
*** The % of dead chains was obtained through the areas of the SEC traces;
****The % of dead chain estimated trough SEC traces data treatment in MatLab.

The percentage of dead chains was estimated through the areas under the SEC peaks of each extended polymer and the respective macroinitiator shoulder. Since there were significant differences between the percentage of dead chains expected according to the percentage of functionalization of each macroinitiator (Table 6) and the percentage of dead chains determined from the SEC traces of the extended polymers (Table 7), a MatLab data treatment was done to the SEC traces, in order to separate the two distributions. From the normalization and integration of each peak in MatLab, no significant differences were found between the percentage of dead chains (% dead chains) obtained directly from the SEC traces integration (using the OmniSEC software) and the one determined via MatLab data treatment. With this, considering the noise in the ^{1}H NMR spectra of the macroinitiators, it is possible that the % functionalization was underestimated, due to the reasons previously pointed. Nonetheless, the presence of dead chains was undeniable for all the macroinitiators synthesized. However, the values were in the same range and in agreement to what is expected from a SARA ATRP process [94].

UV spectroscopy is a helpful tool for the characterization of metallic catalytic systems used in ATRP reaction, since it provides information about the speciation of the metals (different oxidation states are characterized by the different absorbance spectra). Therefore, in order to study the comproportionation of $CuBr_2$/Me_6TREN with

Cu(0) in the different solvent mixtures investigated for the SARA ATRP, UV spectroscopy was used. In the CPME/H_2O/EtOH = 70/2/28 (v/v/v) system (Figure 26) an increase in the absorbance and a successive shift of the absorbance peaks to smaller wavelengths was evident during the reaction time. This experiment was repeated 3 times in order to exclude malpractice errors, since the results were unexpected.

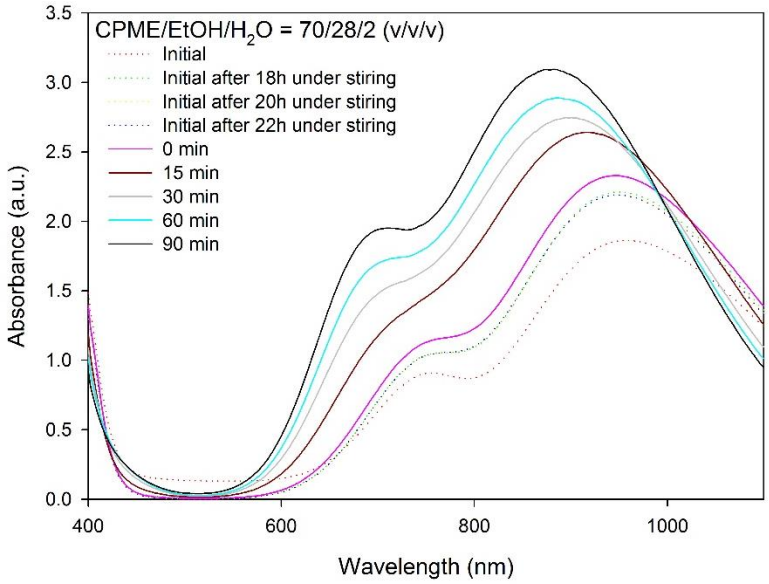

Figure 26 - Comproportionation of $CuBr_2$/Me_6TREN with Cu(0) in CPME/EtOH/H_2O = 70/28/2 (v/v/v) in the presence of ligand excess, $[CuBr_2]_0/[Me_6TREN]_0$/Cu(0) wire = 0.1/1.1/Cu(0) wire: *l* = 5 cm; *d* = 1 mm, with $[CuBr_2]$ = 0.005 mmol/mL, at 30°C.

In Figure 26, the red dotted trace represents the spectrum measured with Cu(II)Br_2, solvent mixture and Me_6TREN prior to oxygen removal or addition of Cu(0) wire, in which the maximum absorbance was registered at 958 nm with a value of 1.86 a. u. After the spectrum measurement, the reaction mixture was left to stir overnight, in order to verify whether or not the issue was a poor dissolution of the catalytic complex. The green dotted line (Figure 26), with a maximum of absorbance of 2.21 a. u. at 950 nm, clearly shows that at the time of the first spectrum measurement, the Cu(II)Br_2 was not completely dissolved in the reaction mixture. Aiming to verify if the increase of absorbance previously registered was due to solvent evaporation (and consequent concentration of the reaction mixture), two more spectrums were measured within a 2-hour interval in between (yellow and blue dotted lines), during which the stirring was maintained at 30 °C. Since the green, yellow and blue dotted lines were virtually indistinguishable, it was possible to assume that the system afforded no

significant solvent losses while the reaction mixture was inside the cuvette and isolated with safe amounts of parafilm. With this information, the reaction mixture was purged with N_2 and the activated Cu(0) coil was added, resulting in the pink trace in Figure 26. Since the absorbance curve increased (from a maximum of 2.19 a. u. to one of 2.33 a. u., still at 948 nm), it was safe to reason that during the N_2 purge a significant amount of solvent was lost. However, as expected, a deviation of the wavelength for the maximum absorbance peak was observed. The reaction was kept under stirring at 30°C and after 15 min another spectrum was measured (brown trace) in which a significant deviation to lower wavelength values of the maximum absorbance point was registered, from 948 nm (2.33 a. u.) to 916 nm (2.64 a. u.). This increase in the absorbance and the shift in the wavelength continued as the reaction proceeded.

These results were, as previously mentioned, unexpected since, usually, $CuBr_2$ is reduced by Cu(0). Therefore, a decrease in the absorbance spectrum, maintaining the same wavelength for the maximum absorption, was expected. In order to have an additional confirmation that the procedure was done correctly, the reproduction of the comproportionation of $CuBr_2$ in DMSO was performed. The results obtained (Appendix E, Figure E 5) were in agreement with those reported [84], confirming that the experimental procedure was being correctly performed. Therefore, comproportionation studies were also done for the THF and 2-MeTHF-based systems.

Both systems, THF/H_2O/EtOH = 70/2/28 (v/v/v) and the 2-MeTHF/H_2O/EtOH = 70/2/28 (v/v/v), have also evidenced wavelength shifts and unexpected increases in the maximum absorbance peak (Figure 27).

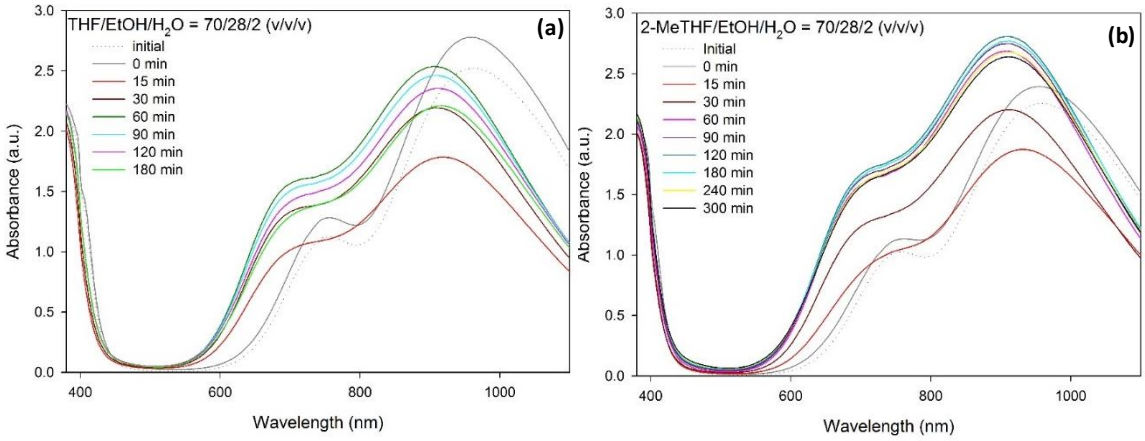

Figure 27 - Comproportionation of $CuBr_2$/Me_6TREN with Cu(0) in **(a)** THF/EtOH/H_2O = 70/28/2 (v/v/v) and **(b)** 2-MeTHF/EtOH/H_2O = 70/28/2 (v/v/v) in the presence of ligand excess, $[CuBr_2]_0/[Me_6TREN]_0$/Cu(0) wire = 0.1/1.1/Cu(0) wire: *l* = 5 cm; *d* = 1 mm, with $[CuBr_2]$ = 0.005 mmol/mL, at 30°C.

However, for these systems, at a certain time of reaction, the maximum absorbance started to decrease, suggesting a reduction of copper (see example on Figure 27 (a) – lines light blue, pink and light green).

These shifts in the maximum absorbance point could be explained by the presence of unidentified copper species in the mixture. Aiming to exclude the possibility of the presence of CuCl species due to the interaction of the copper wire with a possible contamination by the Cu(0) wire activation solution (HCl/MeOH = 30/70 (v/v)), the system in Figure 26 was re-tested with mechanical activation of the copper wire, instead of a chemical activation. The results obtained (Appendix E, Figure E 6) were similar to the ones obtained with the chemical activation of Cu(0), suggesting that there was no contamination of the solvent mixture in the original experiment (Figure 26).

A study of the comproportionation of $CuBr_2$/Me_6TREN with Cu(0) in the presence of MA and using EBiB as the initiator of the SARA ATRP was also performed with the CPME/H_2O/EtOH = 70/2/28 (v/v/v) solvent mixture (Figure 28) (real polymerization conditions).

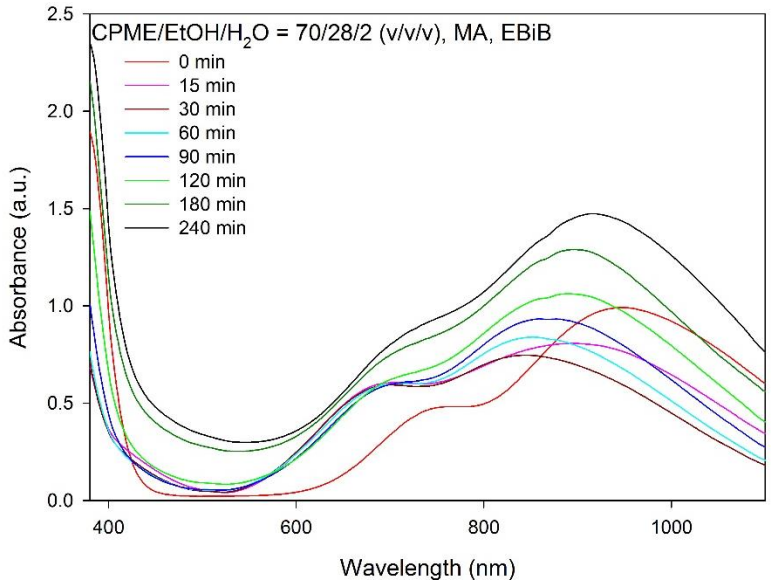

Figure 28 - Comproportionation of $CuBr_2$/Me_6TREN with Cu(0) in CPME/EtOH/H_2O = 70/28/2 (v/v/v) in the presence of ligand excess, reaction conditions: $[MA]_0$/[solvent] = 2/1 (v/v); CPME/EtOH/H_2O = 70/28/2 (v/v/v); $[MA]_0/[EBiB]_0/[CuBr_2]_0/[Me_6TREN]_0$/Cu(0) wire = 222/1/0.1/1.1/Cu(0) wire: l = 5 cm; d = 1 mm; $V_{solvent}$ = 1.25 mL, with $[CuBr_2]$ = 0.005 mmol/mL, at 30°C.

As Figure 28 clearly shows, even in polymerization conditions the behavior of the system was similar to the one in Figure 26. To the extent of the research done, there were no similar reported systems that could explain these results. Therefore, further testing is required.

3.5 CONCLUSIONS AND FUTURE WORK

The three systems studied (THF, CPME and 2-MeTHF) presented similar characteristics and polymerization rates on the SARA ATRP of MA, suggesting that both CMPE and 2-MeTHF could be good substitutes of THF. In fact, CPME-based showed the best results in terms of M_w control ($Đ \approx 1.1$) amongst the solvent mixtures investigated. Comproportionation studies followed by UV-Vis spectroscopy revealed the formation of, so far, unknown copper-based species, instead of a reduction of $CuBr_2$ by Cu(0), which is characteristic of SARA ATRP systems. Further testing is then necessary.

The UV-Vis study of the comproportionation of Cu(II)Br_2 in other volume ratios and in the polymerization of MA using the THF/EtOH/H_2O and 2-MeTHF/EtOH/H_2O system could potentially be interesting to better understand these results, as well as the polymerization of a different monomer using the same three solvent systems in order

get monomer insights about the speciation of the metal catalyst during the polymerization.

REFERENCES

1. Braunecker, W.A. and K. Matyjaszewski, *Controlled/living radical polymerization: Features, developments, and perspectives.* Progress in Polymer Science, 2007. **32**(1): p. 93-146.
2. Matyjaszewski, K. and J. Xia, *Atom Transfer Radical Polymerization.* Chemical Reviews, 2001. **101**(9): p. 2921-2990.
3. Mendonca, P.V., et al., *Synthesis of cationic poly((3-acrylamidopropyl)trimethylammonium chloride) by SARA ATRP in ecofriendly solvent mixtures.* Polymer Chemistry, 2014. **5**(19): p. 5829-5836.
4. Mendonça, P.V., et al., *Straightforward ARGET ATRP for the Synthesis of Primary Amine Polymethacrylate with Improved Chain-End Functionality under Mild Reaction Conditions.* Macromolecules, 2014. **47**(14): p. 4615-4621.
5. Pace, V., et al., *2-Methyltetrahydrofuran (2-MeTHF): A Biomass-Derived Solvent with Broad Application in Organic Chemistry.* ChemSusChem, 2012. **5**(8): p. 1369-1379.
6. Maximiano, P., Mendes, J. P., Mendonça, P. V., Abreu, C. M. R., Guliashvili, T., Serra, A. C. and Coelho, J. F. J., *Cyclopentyl methyl ether: A new green co-solvent for supplemental activator and reducing agent atom transfer radical polymerization.* J. Polym. Sci. Part A: Polym. Chem., 2015. **53**(23): p. 2722-2729.
7. Mountain, A., *Gene therapy: the first decade.* Trends in Biotechnology, 2000. **18**(3): p. 119-128.
8. Pack, D.W., et al., *Design and development of polymers for gene delivery.* Nat Rev Drug Discov, 2005. **4**(7): p. 581-593.
9. Stone, D., *Novel Viral Vector Systems for Gene Therapy.* Viruses, 2010. **2**(4): p. 1002-1007.
10. Blaese, R.M., et al., *T Lymphocyte-Directed Gene Therapy for ADA− SCID: Initial Trial Results After 4 Years.* Science, 1995. **270**(5235): p. 475-480.
11. gsk, *Strimvelis™ receives European marketing authorisation to treat very rare disease, ADA-SCID.* http://www.gsk.com/en-gb/media/press-releases/2016/strimvelistm-receives-european-marketing-authorisation-to-treat-very-rare-disease-ada-scid/, 26 May 2016.
12. Nayerossadat, N., T. Maedeh, and P.A. Ali, *Viral and nonviral delivery systems for gene delivery.* Adv Biomed Res, 2012. **1**.
13. Collins, M. and A. Thrasher, *Gene therapy: progress and predictions.* Proceedings of the Royal Society B: Biological Sciences, 2015. **282**(1821): p. 20143003.
14. York, A.W., S.E. Kirkland, and C.L. McCormick, *Advances in the synthesis of amphiphilic block copolymers via RAFT polymerization: Stimuli-responsive drug and gene delivery*. Advanced Drug Delivery Reviews, 2008. **60**(9): p. 1018-1036.
15. Kurisawa, M., M. Yokoyama, and T. Okano, *Transfection efficiency increases by incorporating hydrophobic monomer units into polymeric gene carriers.* Journal of Controlled Release, 2000. **68**(1): p. 1-8.
16. Xiaoli, S. and Z. Na, *Cationic Polymer Optimization for Efficient Gene Delivery.* Mini-Reviews in Medicinal Chemistry, 2010. **10**(2): p. 108-125.
17. Yue, Y. and C. Wu, *Progress and perspectives in developing polymeric vectors for in vitro gene delivery.* Biomaterials Science, 2013. **1**(2): p. 152-170.
18. Calejo, M.T., et al., *Temperature-responsive cationic block copolymers as nanocarriers for gene delivery.* International Journal of Pharmaceutics, 2013. **448**(1): p. 105-114.

19. Cordeiro, R.A., et al., *Novel Cationic Triblock Copolymer of Poly[2-(dimethylamino)ethyl methacrylate]-block-poly(β-amino ester)-block-poly[2-(dimethylamino)ethyl methacrylate]: A Promising Non-Viral Gene Delivery System.* Macromolecular Bioscience, 2015. **15**(2): p. 215-228.
20. Kakizawa, Y. and K. Kataoka, *Block copolymer micelles for delivery of gene and related compounds.* Advanced Drug Delivery Reviews, 2002. **54**(2): p. 203-222.
21. Wolfert, M.A., et al., *Polyelectrolyte Vectors for Gene Delivery: Influence of Cationic Polymer on Biophysical Properties of Complexes Formed with DNA.* Bioconjugate Chemistry, 1999. **10**(6): p. 993-1004.
22. Wu, G.Y.W.a.C.H., *Receptor-mediated in vitro gene transformation by a soluble DNA carrier system.* J. Biol. Chem., 1987(262): p. 4429-.
23. Mintzer, M.A. and E.E. Simanek, *Nonviral Vectors for Gene Delivery.* Chemical Reviews, 2009. **109**(2): p. 259-302.
24. Godbey, W.T., K.K. Wu, and A.G. Mikos, *Poly(ethylenimine)-mediated gene delivery affects endothelial cell function and viability.* Biomaterials, 2001. **22**(5): p. 471-480.
25. Lv, H., et al., *Toxicity of cationic lipids and cationic polymers in gene delivery.* Journal of Controlled Release, 2006. **114**(1): p. 100-109.
26. Benjaminsen, R.V., et al., *The Possible "Proton Sponge" Effect of Polyethylenimine (PEI) Does Not Include Change in Lysosomal pH.* Molecular Therapy, 2013. **21**(1): p. 149-157.
27. Boussif, O., et al., *A versatile vector for gene and oligonucleotide transfer into cells in culture and in vivo: polyethylenimine.* Proceedings of the National Academy of Sciences of the United States of America, 1995. **92**(16): p. 7297-7301.
28. Godbey, W.T., K.K. Wu, and A.G. Mikos, *Poly(ethylenimine) and its role in gene delivery.* Journal of Controlled Release, 1999. **60**(2–3): p. 149-160.
29. Männistö, M., et al., *Structure–activity relationships of poly(l-lysines): effects of pegylation and molecular shape on physicochemical and biological properties in gene delivery.* Journal of Controlled Release, 2002. **83**(1): p. 169-182.
30. Cherng, J.-Y., et al., *Effect of Size and Serum Proteins on Transfection Efficiency of Poly ((2-dimethylamino)ethyl Methacrylate)-Plasmid Nanoparticles.* Pharmaceutical Research, 1996. **13**(7): p. 1038-1042.
31. van de Wetering, P., et al., *Structure–Activity Relationships of Water-Soluble Cationic Methacrylate/Methacrylamide Polymers for Nonviral Gene Delivery.* Bioconjugate Chemistry, 1999. **10**(4): p. 589-597.
32. Alexander, C., *Temperature- and pH-responsive smart polymers for gene delivery.* Expert Opinion on Drug Delivery, 2006. **3**(5): p. 573-581.
33. van de Wetering, P., et al., *Relation between transfection efficiency and cytotoxicity of poly(2-(dimethylamino)ethyl methacrylate)/plasmid complexes.* Journal of Controlled Release, 1997. **49**(1): p. 59-69.
34. Plamper, F.A., et al., *Synthesis and Characterization of Star-Shaped Poly(N,N-dimethylaminoethyl methacrylate) and Its Quaternized Ammonium Salts.* Macromolecules, 2007. **40**(16): p. 5689-5697.
35. Cordeiro, R.A., et al., *Synthesis of well-defined poly(2-(dimethylamino)ethyl methacrylate) under mild conditions and its co-polymers with cholesterol and PEG using Fe(0)/Cu(ii) based SARA ATRP.* Polymer Chemistry, 2013. **4**(10): p. 3088-3097.
36. Venkataraman, S., et al., *The role of PEG architecture and molecular weight in the gene transfection performance of PEGylated poly(dimethylaminoethyl methacrylate) based cationic polymers.* Biomaterials, 2011. **32**(9): p. 2369-2378.
37. Kurinomaru, T. and K. Shiraki, *Noncovalent PEGylation of L-Asparaginase Using PEGylated Polyelectrolyte.* Journal of Pharmaceutical Sciences, 2014. **104**(2): p. 587-592.
38. Rungsardthong, U., et al., *Copolymers of amine methacrylate with poly(ethylene glycol) as vectors for gene therapy.* Journal of Controlled Release, 2001. **73**(2–3): p. 359-380.

39. Cheung, C.Y., et al., *A pH-Sensitive Polymer That Enhances Cationic Lipid-Mediated Gene Transfer.* Bioconjugate Chemistry, 2001. **12**(6): p. 906-910.
40. Gois, J.R., et al., *Synthesis of well-defined functionalized poly(2-(diisopropylamino)ethyl methacrylate) using ATRP with sodium dithionite as a SARA agent.* Polymer Chemistry, 2014. **5**(12): p. 3919-3928.
41. Licciardi, M., et al., *Synthesis of Novel Folic Acid-Functionalized Biocompatible Block Copolymers by Atom Transfer Radical Polymerization for Gene Delivery and Encapsulation of Hydrophobic Drugs.* Biomacromolecules, 2005. **6**(2): p. 1085-1096.
42. Schild, H.G., *Poly(N-isopropylacrylamide): experiment, theory and application.* Progress in Polymer Science, 1992. **17**(2): p. 163-249.
43. Cardoso, A.M., et al., *Application of Thermoresponsive PNIPAAM-b-PAMPTMA Diblock Copolymers in siRNA Delivery.* Molecular Pharmaceutics, 2014. **11**(3): p. 819-827.
44. Pamies, R., et al., *Thermal response of low molecular weight poly-(N-isopropylacrylamide) polymers in aqueous solution.* Polymer Bulletin, 2009. **62**(4): p. 487-502.
45. Sahiner, N., *Colloidal nanocomposite hydrogel particles.* Colloid and Polymer Science, 2007. **285**(4): p. 413-421.
46. Bayati, S., et al., *Effects of Temperature and Salt Addition on the Association Behavior of Charged Amphiphilic Diblock Copolymers in Aqueous Solution.* The Journal of Physical Chemistry B, 2012. **116**(36): p. 11386-11395.
47. Shovsky, A., et al., *Cationic Poly(N-isopropylacrylamide) Block Copolymer Adsorption Investigated by Dual Polarization Interferometry and Lattice Mean–Field Theory.* Langmuir, 2012. **28**(39): p. 14028-14038.
48. Oddo, L., et al., *Novel thermosensitive calcium alginate microspheres: Physico-chemical characterization and delivery properties.* Acta Biomaterialia, 2010. **6**(9): p. 3657-3664.
49. Tamura, A., et al., *Simultaneous Enhancement of Cell Proliferation and Thermally Induced Harvest Efficiency Based on Temperature-Responsive Cationic Copolymer-Grafted Microcarriers.* Biomacromolecules, 2012. **13**(6): p. 1765-1773.
50. Thompson, K.L., E.S. Read, and S.P. Armes, *Chemical degradation of poly(2-aminoethyl methacrylate).* Polymer Degradation and Stability, 2008. **93**(8): p. 1460-1466.
51. Tang, R., et al., *Well-defined block copolymers for gene delivery to dendritic cells: Probing the effect of polycation chain-length.* Journal of Controlled Release, 2010. **142**(2): p. 229-237.
52. Ji, W., et al., *Poly(2-aminoethyl methacrylate) with Well-Defined Chain Length for DNA Vaccine Delivery to Dendritic Cells.* Biomacromolecules, 2011. **12**(12): p. 4373-4385.
53. Dufresne, M.-H. and J.-C. Leroux, *Study of the Micellization Behavior of Different Order Amino Block Copolymers with Heparin.* Pharmaceutical Research, 2004. **21**(1): p. 160-169.
54. Dufresne, M.-H., M. Elsabahy, and J.-C. Leroux, *Characterization of Polyion Complex Micelles Designed to Address the Challenges of Oligonucleotide Delivery.* Pharmaceutical Research, 2008. **25**(9): p. 2083-2093.
55. Cheng, Q., et al., *The effect of guanidinylation of PEGylated poly(2-aminoethyl methacrylate) on the systemic delivery of siRNA.* Biomaterials, 2013. **34**(12): p. 3120-3131.
56. Li, X., et al., *Progress in reactor engineering of controlled radical polymerization: a comprehensive review.* Reaction Chemistry & Engineering, 2016. **1**(1): p. 23-59.
57. Uhrig, D. and J. Mays, *Synthesis of well-defined multigraft copolymers.* Polymer Chemistry, 2011. **2**(1): p. 69-76.
58. Konkolewicz, D., et al., *SARA ATRP or SET-LRP. End of controversy?* Polymer Chemistry, 2014. **5**(15): p. 4396-4417.

59. Matyjaszewski, K., et al., *Diminishing catalyst concentration in atom transfer radical polymerization with reducing agents.* Proceedings of the National Academy of Sciences, 2006. **103**(42): p. 15309-15314.
60. Jakubowski, W. and K. Matyjaszewski, *Activators Regenerated by Electron Transfer for Atom-Transfer Radical Polymerization of (Meth)acrylates and Related Block Copolymers.* Angewandte Chemie International Edition, 2006. **45**(27): p. 4482-4486.
61. Mendonça, P.V., et al., *Ambient temperature rapid ATRP of methyl acrylate, methyl methacrylate and styrene in polar solvents with mixed transition metal catalyst system.* European Polymer Journal, 2011. **47**(7): p. 1460-1466.
62. Zhang, Y., Y. Wang, and K. Matyjaszewski, *ATRP of Methyl Acrylate with Metallic Zinc, Magnesium, and Iron as Reducing Agents and Supplemental Activators.* Macromolecules, 2011. **44**(4): p. 683-685.
63. Magenau, A.J.D., et al., *Investigation of Electrochemically Mediated Atom Transfer Radical Polymerization.* Macromolecules, 2013. **46**(11): p. 4346-4353.
64. Magenau, A.J.D., et al., *Electrochemically Mediated Atom Transfer Radical Polymerization.* Science, 2011. **332**(6025): p. 81-84.
65. Treat, N.J., et al., *Metal-Free Atom Transfer Radical Polymerization.* Journal of the American Chemical Society, 2014. **136**(45): p. 16096-16101.
66. Pan, X., et al., *Mechanism of Photoinduced Metal-Free Atom Transfer Radical Polymerization: Experimental and Computational Studies.* Journal of the American Chemical Society, 2016. **138**(7): p. 2411-2425.
67. Grimaud, T. and K. Matyjaszewski, *Controlled/"Living" Radical Polymerization of Methyl Methacrylate by Atom Transfer Radical Polymerization.* Macromolecules, 1997. **30**(7): p. 2216-2218.
68. Rocha, N., et al., *Facile Synthesis of Well-Defined Telechelic Alkyne-Terminated Polystyrene in Polar Media Using ATRP With Mixed Fe/Cu Transition Metal Catalyst.* Macromolecular Chemistry and Physics, 2013. **214**(1): p. 76-84.
69. Percec, V., et al., *Ultrafast Synthesis of Ultrahigh Molar Mass Polymers by Metal-Catalyzed Living Radical Polymerization of Acrylates, Methacrylates, and Vinyl Chloride Mediated by SET at 25 °C.* Journal of the American Chemical Society, 2006. **128**(43): p. 14156-14165.
70. Ye, J. and R. Narain, *Water-Assisted Atom Transfer Radical Polymerization of N-Isopropylacrylamide: Nature of Solvent and Temperature.* The Journal of Physical Chemistry B, 2009. **113**(3): p. 676-681.
71. Simakova, A., et al., *Aqueous ARGET ATRP.* Macromolecules, 2012. **45**(16): p. 6371-6379.
72. Konkolewicz, D., et al., *Aqueous RDRP in the Presence of Cu0: The Exceptional Activity of CuI Confirms the SARA ATRP Mechanism.* Macromolecules, 2014. **47**(2): p. 560-570.
73. Konkolewicz, D., et al., *ICAR ATRP with ppm Cu Catalyst in Water.* Macromolecules, 2012. **45**(11): p. 4461-4468.
74. Abreu, C.M.R., et al., *Accelerated Ambient-Temperature ATRP of Methyl Acrylate in Alcohol–Water Solutions with a Mixed Transition-Metal Catalyst System.* Macromolecular Chemistry and Physics, 2012. **213**(16): p. 1677-1687.
75. Abreu, C.M.R., et al., *Inorganic Sulfites: Efficient Reducing Agents and Supplemental Activators for Atom Transfer Radical Polymerization.* ACS Macro Letters, 2012. **1**(11): p. 1308-1311.
76. Guliashvili, T., et al., *Copper-Mediated Controlled/"Living" Radical Polymerization in Polar Solvents: Insights into Some Relevant Mechanistic Aspects.* Chemistry – A European Journal, 2012. **18**(15): p. 4607-4612.
77. Jakubowski, W., K. Min, and K. Matyjaszewski, *Activators Regenerated by Electron Transfer for Atom Transfer Radical Polymerization of Styrene.* Macromolecules, 2006. **39**(1): p. 39-45.

78. Xu, F.J. and W.T. Yang, *Polymer vectors via controlled/living radical polymerization for gene delivery.* Progress in Polymer Science, 2011. **36**(9): p. 1099-1131.
79. Liu, Z., et al., *Hydrophobic modifications of cationic polymers for gene delivery.* Progress in Polymer Science, 2010. **35**(9): p. 1144-1162.
80. Zhang, Y., et al., *Copper-Mediated CRP of Methyl Acrylate in the Presence of Metallic Copper: Effect of Ligand Structure on Reaction Kinetics.* Macromolecules, 2012. **45**(1): p. 78-86.
81. Ciampolini, M. and N. Nardi, *Five-Coordinated High-Spin Complexes of Bivalent Cobalt, Nickel, andCopper with Tris(2-dimethylaminoethyl)amine.* Inorganic Chemistry, 1966. **5**(1): p. 41-44.
82. Britovsek, G.J.P., J. England, and A.J.P. White, *Non-heme Iron(II) Complexes Containing Tripodal Tetradentate Nitrogen Ligands and Their Application in Alkane Oxidation Catalysis.* Inorganic Chemistry, 2005. **44**(22): p. 8125-8134.
83. Mendonca, P.V., et al., *Synthesis of tailor-made bile acid sequestrants by supplemental activator and reducing agent atom transfer radical polymerization.* RSC Advances, 2016. **6**(57): p. 52143-52153.
84. Mendonça, P.V., *Metal-catalyzed reversible deactivation radical polymerization: mechanistic studies and application on the design of polymer drugs*, in *Chemical Engineering Department*. 2015, University of Coimbra.
85. Dubruel, P., et al., *Buffering Properties of Cationic Polymethacrylates Are Not the Only Key to Successful Gene Delivery.* Biomacromolecules, 2004. **5**(2): p. 379-388.
86. Zhu, C., et al., *Cationic methacrylate copolymers containing primary and tertiary amino side groups: Controlled synthesis via RAFT polymerization, DNA condensation, and in vitro gene transfection.* Journal of Polymer Science Part A: Polymer Chemistry, 2010. **48**(13): p. 2869-2877.
87. Jianxun, D., et al., *Facile preparation of a cationic poly(amino acid) vesicle for potential drug and gene co-delivery.* Nanotechnology, 2011. **22**(49): p. 494012.
88. Anastas, P. and N. Eghbali, *Green Chemistry: Principles and Practice.* Chemical Society Reviews, 2010. **39**(1): p. 301-312.
89. Li, C.-J. and L. Chen, *Organic chemistry in water.* Chemical Society Reviews, 2006. **35**(1): p. 68-82.
90. Fowles, J., et al., *A review of the toxicological and environmental hazards and risks of tetrahydrofuran.* Critical Reviews in Toxicology, 2013. **43**(10): p. 811-828.
91. Watanabe, K., N. Yamagiwa, and Y. Torisawa, *Cyclopentyl Methyl Ether as a New and Alternative Process Solvent.* Organic Process Research & Development, 2007. **11**(2): p. 251-258.
92. Sigma-Aldrich. *2-Methyltetrahydrofuran - An alternative to Tetrahydrofuran and Dichloromethane*. [cited 2016 12/08/2016]; Available from: http://www.sigmaaldrich.com/chemistry/solvents/learning-center/methyltetrahydrofuran.html.
93. Wang, Y., et al., *Reversible-Deactivation Radical Polymerization in the Presence of Metallic Copper. Comproportionation–Disproportionation Equilibria and Kinetics.* Macromolecules, 2013. **46**(10): p. 3793-3802.
94. Zhong, M., et al., *Reversible-Deactivation Radical Polymerization in the Presence of Metallic Copper. Kinetic Simulation.* Macromolecules, 2013. **46**(10): p. 3816-3827.

APPENDICES

APPENDIX A

SUPPORTING INFORMATION FOR THE SYNTHESIZED MACROINITIATORS AND LIGANDS AND FOR THE PROCEDURES USED IN CHAPTER 2: PEG_{45}-BR ^{1}H NMR SPECTRUM; BR-PEG_{72}-BR ^{1}H NMR SPECTRUM; ME_6TREN ^{1}H NMR SPECTRUM; TPMA ^{1}H NMR SPECTRUM; TYPICAL PROCEDURE FOR THE SYNTHESIS OF PAMPTMA-*CO*-PDPA AND PAMPTMA-*CO*-PMA BY SARA ATRP

Omega-bromo poly(ethylene glycol) (PEG-Br) was obtained through functionalization of PEG-OH (M_n = 2000). The structure was confirmed by ^{1}H NMR spectroscopy (Figure A 1). The PEG-Br obtained did not elute in the aqueous SEC, despite the fact that its precursor did.

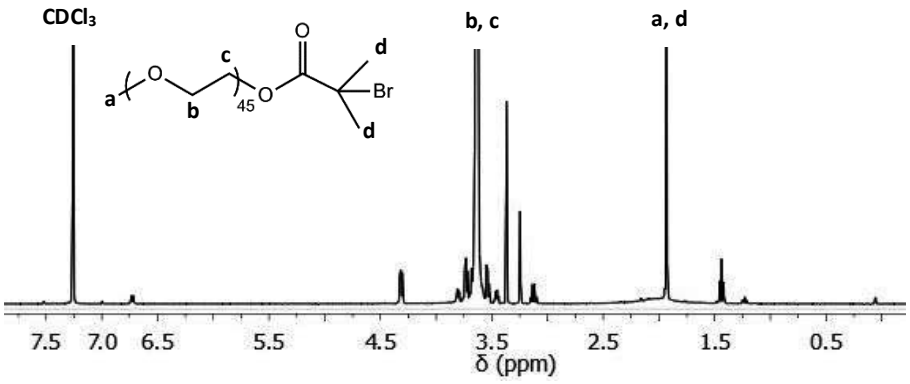

Figure A 1 - 400 MHz 1H NMR spectrum, in $CDCl_3$ of a purified PEG_{45}-Br (M_n = 2000).

Alpha-omega-bis-bromo poly(ethylene glycol) (Br-PEG-Br) was obtained through bi-functionalization of OH-PEG-OH (M_n = 3000), which had a monomodal M_w, evaluated by aqueous SEC. Two bi-functionalizations were performed, ML02 and ML03. The structure was confirmed by ^{1}H NMR spectroscopy (Figure A 2). Neither one of the Br-PEG-Br samples obtained eluted in the aqueous SEC, despite the fact that their precursor did.

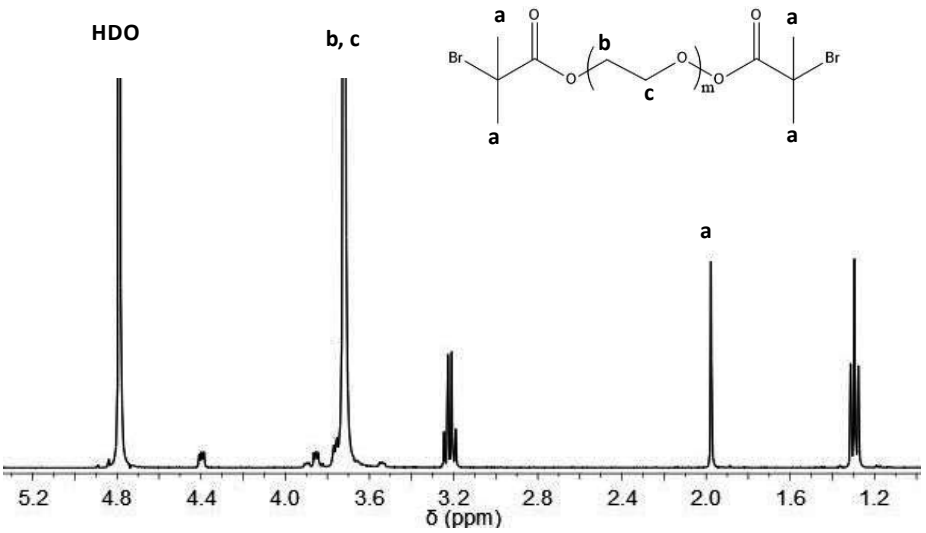

Figure A 2 - 400 MHz ^{1}H NMR spectrum, in D_2O of a purified Br-PEG_{72}-Br (M_n = 3000).

Me_6TREN [81] and TPMA [82] were synthesized according to the literature and the structures were confirmed by ^{1}H NMR spectroscopy (Figure A 3 and Figure A 4).

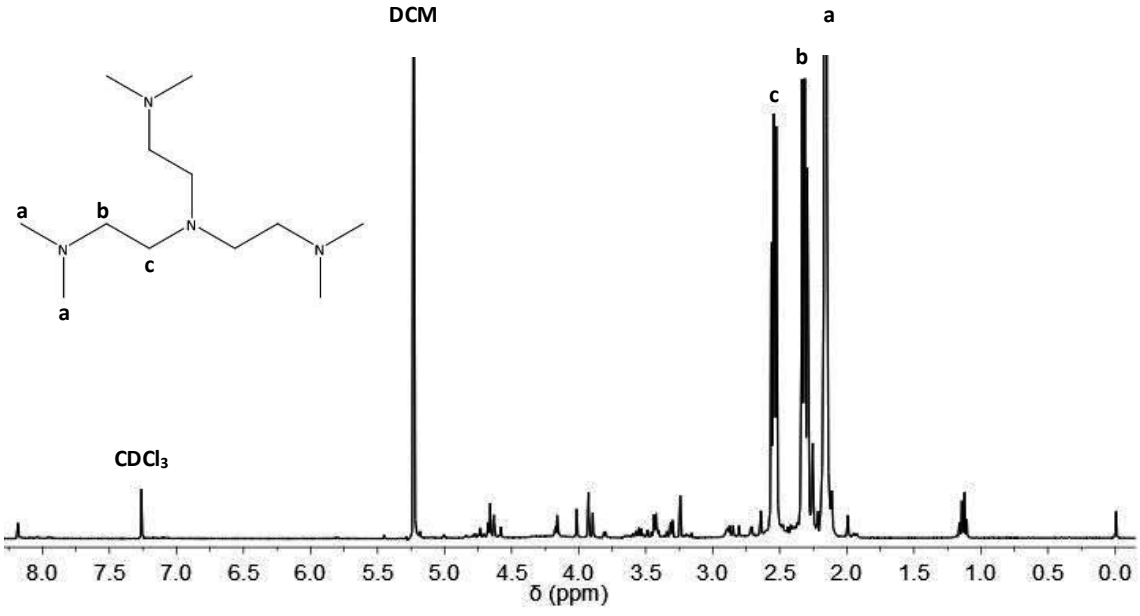

Figure A 3 - 400 MHz ^{1}H NMR spectrum, in $CDCl_3$ of a purified Me_6TREN sample.

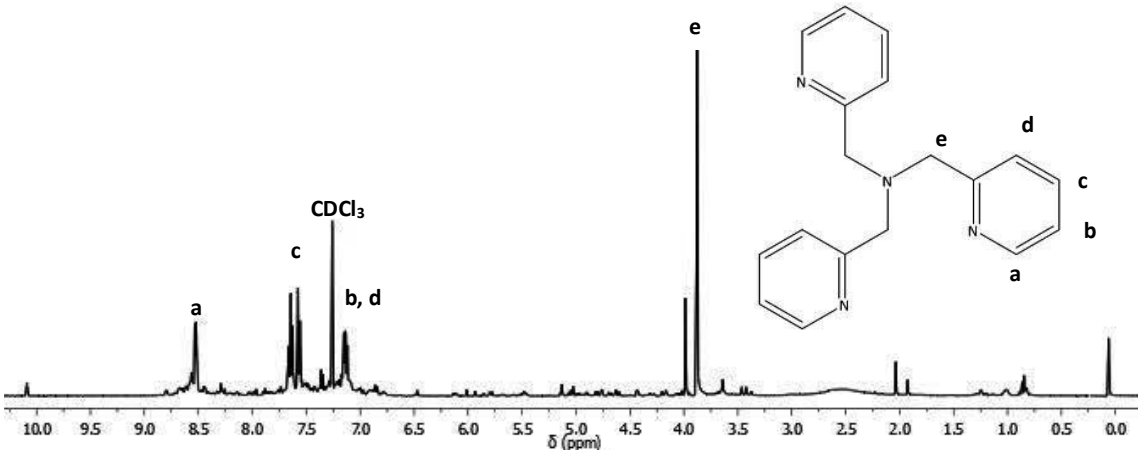

Figure A 4 – 400 MHz ^{1}H NMR spectrum, in $CDCl_3$ of a purified TPMA sample.

Typical procedure for the synthesis of PAMPTMA-*co*-PDPA by SARA ATRP

EBiB (12.4 µL, 84 µmol), water (0.15 mL) and IPA (1.8 mL) were added to a 10 mL round bottom Schlenk flask equipped with a magnetic stirrer bar. Upon dissolution, $CuBr_2$ (9.4 mg, 42 µmol), Me_6TREN (22.5 µL, 84 µmol), AMPTMA (233 mg, 844 µmol) and DPA (2 mL, 8.4 mmol) were added to the flask, followed by a Cu(0) wire (*l* = 10 cm; *d* = 1 mm). The Schlenk flask was then sealed with a glass stopper, deoxygenated by freeze--vacuum-thaw cycles and purged with nitrogen. The reaction was carried out under stirring (600 rpm) at 30 °C. A sample was collected after 16 h and analyzed by aqueous SEC to evaluate the molecular weights and dispersity and by ^{1}H NMR spectroscopy to determine the monomer conversion. The reaction mixture was dialyzed (cut-off 3500) against deionized water for a minimum of 3 days. The copolymer was recovered by freeze-drying. Purified copolymer samples were analyzed by ^{1}H NMR spectroscopy to determine the degree of polymerization and molecular weight. The content of residual copper was determined by atomic absorption.

Typical procedure for the synthesis of PAMPTMA-*co*-PMA by SARA ATRP

EBiB (32.6 µL, 222 µmol), water (0.26 mL) and EtOH (1.6 mL) were added to a 10 mL round bottom Schlenk flask equipped with a magnetic stirrer bar. Upon dissolution, $CuBr_2$ (24.8 mg, 111 µmol), Me_6TREN (59.3 µL, 222 µmol), AMPTMA (612 mg, 2.2 mmol)

and MA (2 mL, 22.2 mmol) were added to the flask, followed by a Cu(0) wire (l = 10 cm; d = 1 mm). The Schlenk flask was then sealed with a glass stopper, deoxygenated by freeze-vacuum-thaw cycles and purged with nitrogen. The reaction was carried out under stirring (600 rpm) at 30 °C. A sample was collected after 16h and analyzed by aqueous SEC to determine the molecular weights and dispersity and by ^{1}H NMR spectroscopy to determine the monomer conversion. The reaction mixture was dialyzed (cut-off 3500) against deionized water for a minimum of 3 days. The copolymer was recovered by freeze-drying. The pure copolymer samples were analyzed by ^{1}H NMR spectroscopy to determine the degree of polymerization and molecular weight. The content of residual copper was determined by atomic absorption.

APPENDIX B

SUPPORTING INFORMATION FOR CHAPTER 2, SECTION 2.4.1. PEG_{45}-*B*-$PAMPTMA_N$ AND $PAMPTMA_N$-*B*-PEG_{72}-*B*-$PAMPTMA_N$ BLOCK COPOLYMERS.

In Table B 1 are summarized the general properties of all the PAMPTMA-based copolymers synthesized in this work that were not tested in gene delivery essays, either due to high M_w shoulder in SEC traces, low monomer conversions or the properties of the copolymer were unsuited (e.g., if DP was not significantly different). Samples GD07 to GD13 were kinetic studies.

Table B 1 - General properties of the copolymers untested in gene delivery assays.

Entry	Sample	Target DP / $DP_{PAMPTMA}$ (n)	Macroinitiator	Monomer conversion (%)	M_n^{th} x 10^{-3}	M_n^{NMR} x 10^{-3}	M_n^{SEC} x 10^{-3}	Đ
1	GD04*	40/--	Br-PEG_{135}-Br**	67.3	11.6	--	--	--
2	GD05*	25/--	Br-PEG_{135}-Br**	--	--	--	--	--
3	GD06*	15/--	Br-PEG_{135}-Br**	--	--	--	--	--
4	GD14	36/18	PEG_{45}-Br	49.7	5.7	5.8	10.0	1.19
5	GD15*	22/--	PEG_{45}-Br	14.2	2.6	--	--	--
6	GD16	57/17	PEG_{45}-Br	22.6	4.7	5.6	8.0	1.21
7	GD17*	150/--	PEG_{45}-Br	21.2	8.6	--	9.7	1.24
8	GD19	150/--***	PEG_{45}-Br	87.1	29.0	--***	--***	--***

*unpurified sample;
**bimodal SEC distribution due to the macroinitiator; experiments failed, no further characterization was made;
***poor purification process; no further characterization was made.

APPENDIX C

SUPPORTING INFORMATION FOR CHAPTER 2, SECTION 2.4.3. PEG_{45}-*B*-$PAMA_N$ BLOCK COPOLYMERS

Table C 1 - Percentage of charge for each of the PAMA-based sample tested.

Entry	Sample	Temperature (°C)	pK_a	pH *	*% charge* **
1	PEG_{45}-*b*-$PAMA_{111}$	25	7.25	3 / 4	99.99 / 99.94
2	$PAMA_{36}$	37	6.62	3 / 4	99.98 / 99.76
3	PEG_{45}-*b*-$PAMA_{63}$	37	6.84	3 / 4	99.98 / 99.85
4	PEG_{45}-*b*-$PAMA_{163}$	37	6.75	3 / 4	99.98 / 99.82

*hypothetical pH of the solution containing the polymeric sample

** % charge = $(\frac{[AH]}{[AH]+[A^-]}) \times 100 = (\frac{1}{1+10^{(pH-pK_a)}}) \times 100$

APPENDIX D

SUPPORTING INFORMATION FOR CHAPTER 2, SECTION 2.4.4. GENE DELIVERY RESULTS FROM PAMA-BASED POLYMERS. GENE DELIVERY ASSAYS PROCEDURES.

Effect of the N/P ratio and composition of polyplexes on the viability of COS-7 cells.

GD27 polymer and bPEI were complexed with 1µg of pCMV-Luc at the indicated N/P ratios. Cells were covered with 0.3 ml of serum-free medium or medium containing 10% FBS and the polyplexes were added. After an incubation for 4 h, the medium was replaced with DMEM-HG containing 10% FBS and the cells were further incubated for 48 h. Cell viability was measured by an Alamar blue and it is expressed as a percentage of untreated control cells. The results are representative of at least three independent experiments.

The same procedure was followed for GD30 samples.

Effect of the N/P ratio and composition of polyplexes on their transfection activity COS-7 cell lines.

GD27 polymer and bPEI were complexed with 1µg of pCMV-Luc at the indicated N/P ratios. The data is expressed as RLU of luciferase per mg of total cell protein (mean_SD, obtained from triplicates). The results are representative of at least three independent experiments.

The same procedure was followed for GD30 samples.

Accessibility of ethidium bromide to DNA of the different polyplexes prepared at different N/P ratios.

Polyplexes prepared with GD27, GD29, GD30 and containing 1µg of DNA, were incubated with EtBr. The amount of DNA available to interact with the probe was calculated by subtracting the values of residual fluorescence from those obtained for the samples and expressed as the percentage of the control. Control corresponds to free DNA in the same amount as that associated with the polyplexes (100% of EtBr accessibility). The data is expressed as EtBr access (% of control) (mean ± SEM, obtained from triplicates). The results are representative of at least three independent experiments.

APPENDIX E

SUPPORTING INFORMATION FOR CHAPTER 3. INFLUENCE OF DIFFERENT "THF-LIKE" SOLVENTS ON THE PMA SYNTHESIS BY SARA ATRP

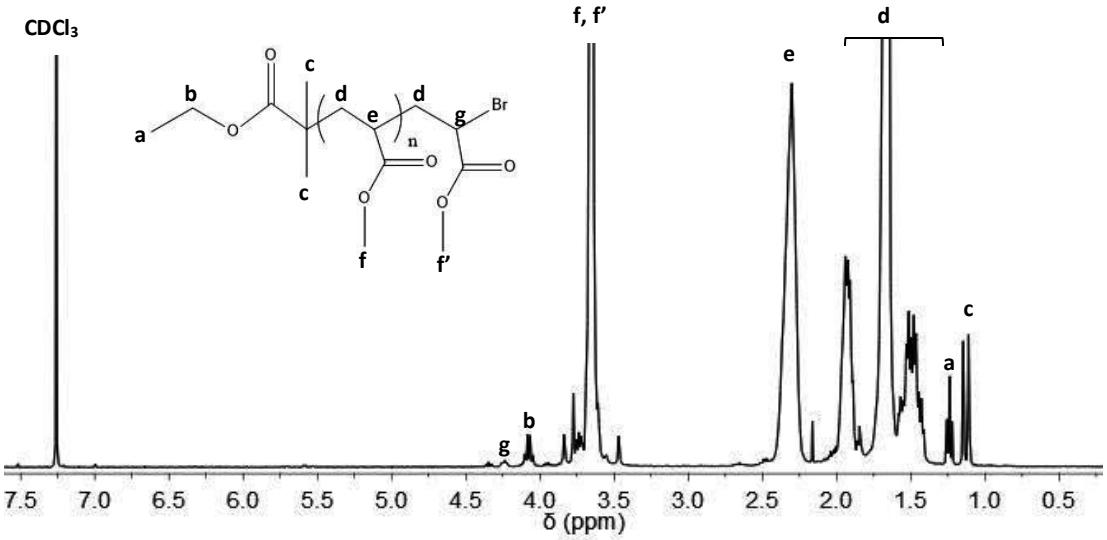

Figure E 1 - 400 MHz ^{1}H NMR spectrum, in $CDCl_3$, of a purified PMA_{66} sample (M_n^{RMN} = 5.8 x 10^3 M_n^{sec} = 7.3 x 10^3; Đ = 1.05) obtained by SARA ATRP. Reaction conditions: $[MA]_0$/ [solvent] = 2/1 (v/v); THF/EtOH/H_2O = 70/28/2 (v/v/v); $[MA]_0/[EBiB]_0/[CuBr_2]_0/[Me_6TREN]_0$/Cu(0) wire = 70/1/0.1/1.1/Cu(0) wire: *l* = 5 cm; *d* = 1 mm; $V_{solvent}$ = 2 mL; T = 30 °C.

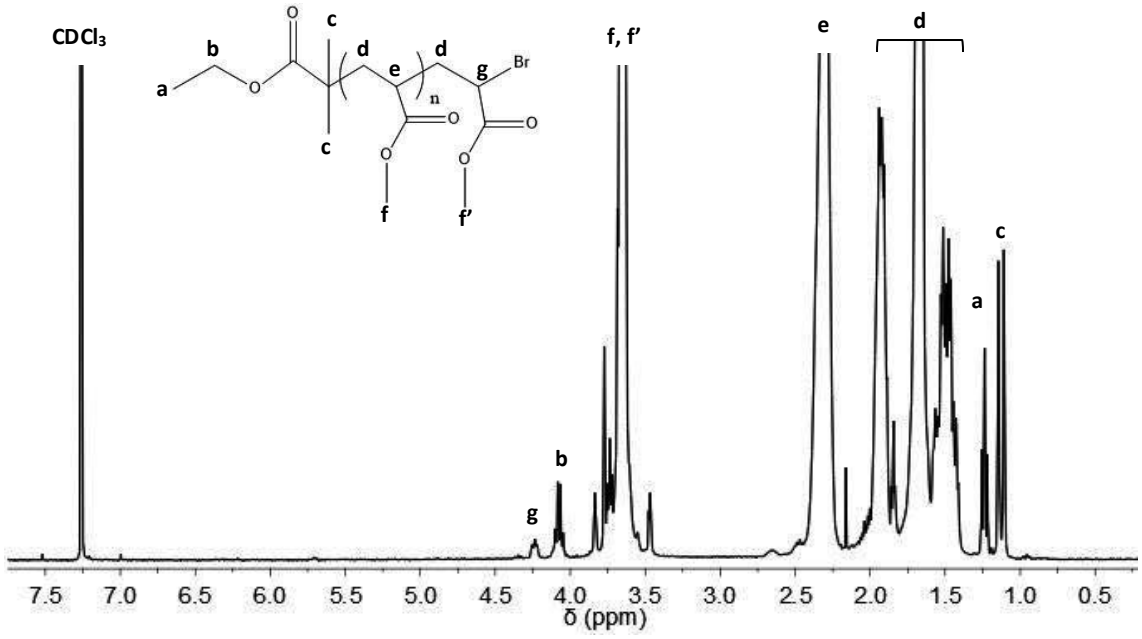

Figure E 2 - 400 MHz ^{1}H NMR spectrum, in $CDCl_3$, of a purified PMA_{60} sample (M_n^{RMN} = 5.3 x 10^3 M_n^{SEC} = 6.0 x 10^3; Đ = 1.08) obtained by SARA ATRP. Reaction conditions: $[MA]_0$/ [solvent] = 2/1 (v/v); 2-MeTHF/EtOH/H_2O = 70/28/2 (v/v/v); $[MA]_0/[EBiB]_0/[CuBr_2]_0/[Me_6TREN]_0$/Cu(0) wire = 70/1/0.1/1.1/Cu(0) wire: l = 5 cm; d = 1 mm; $V_{solvent}$ = 2 mL; T = 30 °C.

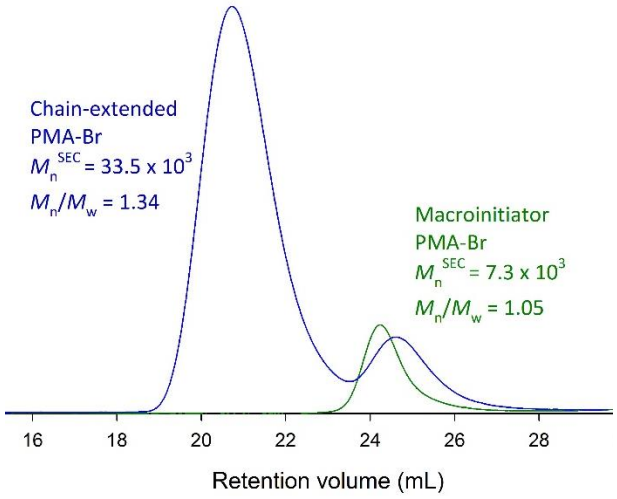

Figure E 3 - SEC traces of PMA-Br before and after the extension with MA: macroinitiator obtained with M_n^{SEC} x 10^{-3} = 7.3 (green line) and extended polymer with M_n^{SEC} x 10^{-3} = 33.5 (blue line); macroinitiator - $[MA]_0$/ [solvent] = 2/1 (v/v) in THF/EtOH/H_2O = 70/28/2 (v/v/v), with $[MA]_0/[EBiB]_0/[CuBr_2]_0/[Me_6TREN]_0$/Cu(0) wire = 70/1/0.1/1.1/Cu(0) wire: *l* = 5 cm; *d* = 1 mm at 30 °C; chain extension by SARA ATRP in DMSO with $[MA]_0$/[solvent] = 2/1 (v/v), $[MA]_0/[PMA\text{-}Br]_0/[CuBr_2]_0/[Me_6TREN]_0$/Cu(0) wire = 500/1/0.1/1.1/Cu(0) wire: *l* = 5 cm; *d* = 1 mm at 30 °C, $V_{solvent}$ = 1.25 mL.

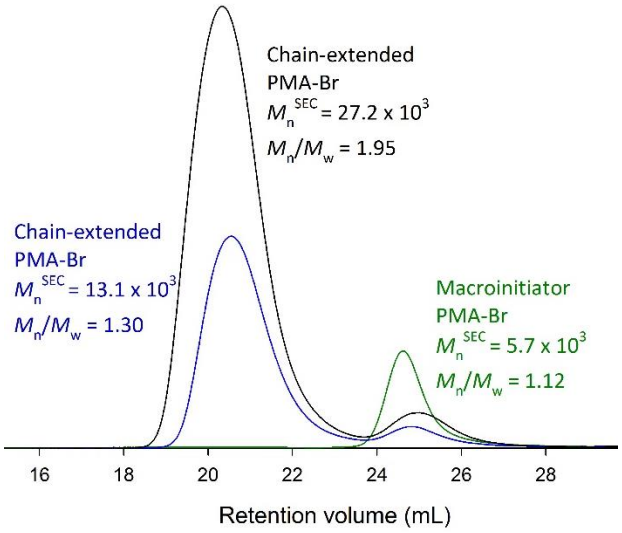

Figure E 4 - SEC traces of PMA-Br before and after the extension with MA: macroinitiator obtained with M_n^{SEC} x 10^{-3} = 5.7 (green line), extended polymer with M_n^{SEC} x 10^{-3} = 13.1 (blue line) and extended polymer with overnight stirring of the macroinitiator in DMSO with M_n^{SEC} x 10^{-3} = 27.2 (black line); macroinitiator - $[MA]_0$/ [solvent] = 2/1 (v/v) in 2-MeTHF/EtOH/H_2O = 70/28/2 (v/v/v), with $[MA]_0/[EBiB]_0/[CuBr_2]_0/[Me_6TREN]_0$/Cu(0) wire = 70/1/0.1/1.1/Cu(0) wire: *l* = 5 cm; *d* = 1 mm at 30 °C; chain extension by SARA ATRP in DMSO with $[MA]_0/[PMA\text{-}Br]_0/[CuBr_2]_0/[Me_6TREN]_0$/Cu(0) wire = 500/1/0.1/1.1/Cu(0) wire: *l* = 5 cm; *d* = 1 mm at 30 °C, blue trace had $[MA]_0$/[solvent] = 2/1 (v/v), $V_{solvent}$ = 1.25 mL and black trace $[MA]_0$/[solvent] = 1/1 (v/v), $V_{solvent}$ = 2.5 mL.

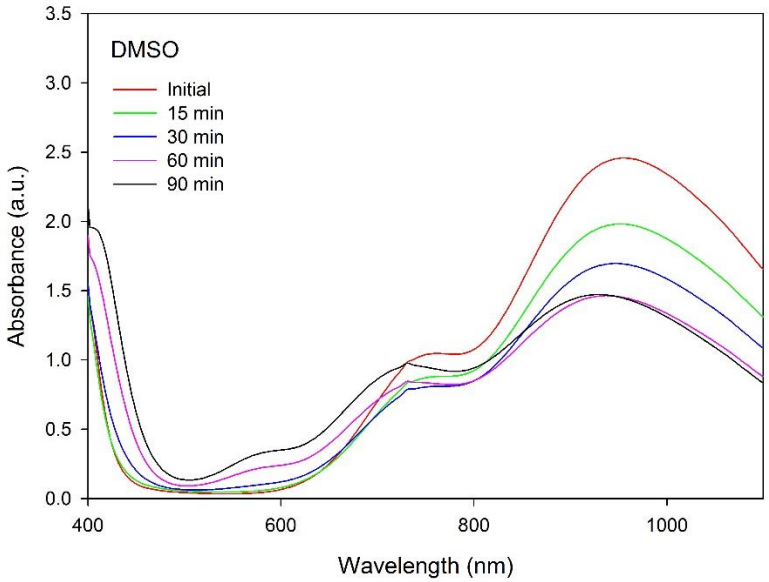

Figure E 5 - Comproportionation of $CuBr_2$/Me_6TREN with Cu(0) in DMSO in the presence of ligand excess, $[CuBr_2]_0$/$[Me_6TREN]_0$/Cu(0) wire = 0.1/1.1/Cu(0) wire: *l* = 5 cm; *d* = 1 mm, with $[CuBr_2]$ = 0.005 mmol/mL, at 30°C.

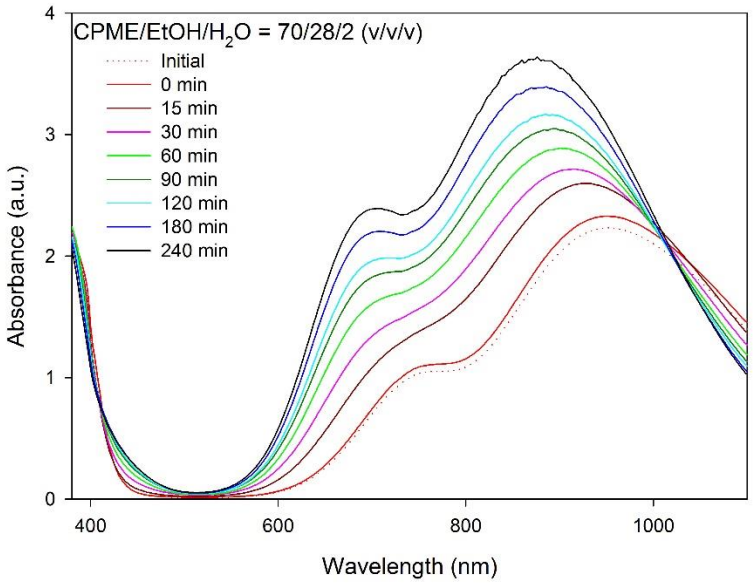

Figure E 6 - Comproportionation of $CuBr_2$/Me_6TREN with Cu(0) CPME/EtOH/H_2O = 70/28/2 (v/v/v) in the presence of ligand excess, $[CuBr_2]_0$/$[Me_6TREN]_0$/Cu(0) wire = 0.1/1.1/Cu(0) wire: *l* = 5 cm; *d* = 1 mm, with $[CuBr_2]$ = 0.005 mmol/mL, at 30°C, with mechanical activation of the Cu(0) wire.